

SIMULATING OCCUPANT RESPONSE TO EMERGENCY SITUATIONS

by

Michelle Lynn Isenhour
A Dissertation
Submitted to the
Graduate Faculty
of
George Mason University
in Partial Fulfillment of
The Requirements for the Degree
of
Doctor of Philosophy
Computational Sciences and Informatics

Committee:

_____ Dr. Rainald Löhner, Dissertation Director
_____ Dr. Fernando Camelli, Committee Member
_____ Dr. Juan Cebral, Committee Member
_____ Dr. Timothy Sauer, Committee Member
_____ Dr. Kevin Curtin, Acting Department Chair
_____ Dr. Donna M. Fox, Associate Dean, Office
of Student Affairs & Special Programs,
College of Science
_____ Dr. Peggy Agouris, Dean, College of
Science

Date: _____ Spring Semester 2016
George Mason University
Fairfax, VA

Simulating Occupant Response to Emergency Situations

A Dissertation submitted in partial fulfillment of the requirements for the degree of
Doctor of Philosophy at George Mason University

by

Michelle Lynn Isenhour
Master of Science
Western Michigan University, 2004
Bachelor of Science
United States Military Academy, 1994

Director: Rainald Löhner, Professor
Department of Computational Sciences and Informatics

Spring Semester 2016
George Mason University
Fairfax, VA



This work is licensed under a [creative commons attribution-noncommercial 3.0 unported license](https://creativecommons.org/licenses/by-nc/3.0/).

DEDICATION

I dedicate this dissertation to my husband, Steven, and my boys, Forrest and Miles. Without your sacrifice, support, and encouragement, this would not have been achievable.

ACKNOWLEDGEMENTS

There are several people who I need to thank for their significant influence, support, and encouragement as an Army professional, doctoral student, and aspiring educator. First and foremost, I need to thank my family. To my husband, Steven, who sacrificed so much to ensure I could complete my PhD and chase my dream to return to West Point – you are my rock. To my boys, who grew up way too fast and sacrificed far too much as the children of a dual-military couple. To my father and mother, Kirk and Cheryl, who taught me my work ethic, instilled the value of education, and assisted in the completion of my PhD by continually asking, “Are you done yet?” Without the support, encouragement, and persistence of my family, the completion of this dissertation would not have been possible.

Next, I would like to thank the contingent of professionals at George Mason University who made this project feasible. To my advisor, Dr. Rainald Löhner, who taught me the ways of pedestrian science, willingly shared his passion with me, and spent countless hours reading and revising this dissertation. To George Mason University’s Director of Safety and Emergency Management, Mr. David Farris; the Fire Safety Coordinator, Mr. Gregg Black; and the Director of the Public Safety Division, Mr. James McCarthy, all of whom were extremely supportive of this project and willingly assisted my data collection efforts at the Johnson Center. To my fellow doctoral students, Dr. John Keady and Muhammad Baqui, who were always available to share ideas, review literature and provide counsel.

Lastly, I would be remiss if I did not take the time to thank my Army colleagues. First, a huge thank you to the West Point Math Department for the opportunity to attend George Mason University and earn my PhD. To the former commander of the Big Red One, General Vincent Brooks, who understood my desire to return to West Point and supported me before, during, and after my time at George Mason. And to all of my brothers and sisters-in-arms, thank you for keeping the country safe while I attended graduate school, I am forever indebted to you.

TABLE OF CONTENTS

	Page
List of Tables	ix
List of Figures	x
List of Equations	xiv
List of Abbreviations	xvii
Abstract	xviii
1 Introduction	1
1.1 Motivation and Research Objectives	4
1.2 Organization of the Dissertation	6
2 Literature Survey I: The Mathematical Models Behind Pedestrian Science.....	9
2.1 Pedestrian Literature: Microscopic Models	9
2.1.1 Social Force Model.....	10
2.1.2 Cellular Automata Model	15
2.1.3 Agent-based Microscopic Model	24
2.2 Pedestrian Literature: Macroscopic Models	31
2.2.1 Gas-Kinetic Macroscopic Model.....	31
2.2.2 Fluid-dynamic Macroscopic Model	35
2.2.3 Advantages and Disadvantages of Macroscopic Models	40
2.3 Pedestrian Literature: Mesoscopic Models	40
2.3.1 Gas-Kinetic Mesoscopic Model	41
2.3.2 Fluid-dynamic Mesoscopic Model	43
2.3.3 Agent-based Mesoscopic Model	46
2.4 Pedestrian Literature: Combined Models	47
3 Literature Survey II: Evacuation Dynamics	49
3.1 Evacuation Modeling Software Reviews.....	49
3.2 Pre-Evacuation Phase: Modeling Using Distributions	53
3.3 Pre-Evacuation Phase: Modeling Using Decision Models	58

4	Evacuation Decision Model Single Alarm Implementation.....	61
4.1	Basic Model	61
4.2	Prior Knowledge	67
4.3	Social Influence	72
4.4	Complete EDM (Single Alarm).....	78
4.5	Discussion.....	82
5	Literature Survey III: Evacuation Data Collection Efforts.....	84
5.1	Literature Survey: Evacuation Dynamics and Data Collection	85
5.2	Evacuation Delay: Psychological Factors and Empirical Data.....	88
5.3	Route-to-Exit Choices: Psychological Factors and Empirical Data	94
6	PEDFLOW	98
6.1	Model Considerations	98
6.2	Mathematical Model Formulation	100
6.2.1	Internal Will Force	102
6.2.2	Other Internal Forces.....	103
6.2.3	Neighbor Avoidance Force: Intermediate-Range.....	104
6.2.4	Neighbor Avoidance Force: Close-Range.....	106
6.2.5	Wall Avoidance Force.....	108
6.2.6	Virtual Fence Avoidance Force.....	108
6.2.7	Elevator Avoidance Force	110
6.2.8	Contact Forces.....	110
6.2.9	Pedestrian-Pedestrian Contact Forces	111
6.2.10	Pedestrian-Wall Contact Force.....	113
6.3	Advancing the Pedestrians.....	114
6.4	Evaluation of PEDFLOW as an Evacuation Model	116
7	Verification of PEDFLOW.....	118
7.1	Description of NIST Verification Tests.....	119
7.2	Existing Capabilities	120
7.2.1	NIST Verification Test 2.1: Speed in a Corridor	121
7.2.2	NIST Verification Test 2.3: Movement around a Corner.....	121
7.2.3	NIST Verification Test 2.7: Elevator Usage	122
7.2.4	NIST Verification Test 2.9: Group Behaviors	123

7.2.5	NIST Verification Test 3.1: Exit Route Allocation.....	125
7.2.6	NIST Verification Test 4.1: Dynamic Availability of Exit	126
7.2.7	NIST Verification Test 5.1: Congestion.....	127
7.3	Modified Capabilities.....	128
7.3.1	NIST Verification Test 2.2: Speed on Stairs	128
7.3.2	NIST Verification Test 2.4: Assigned Occupant Demographics ...	132
7.3.3	NIST Verification Test 2.8: Horizontal Counterflows.....	133
7.3.4	NIST Verification Test 2.10: People with Movement Disabilities.....	135
7.3.5	NIST Verification Test 5.2: Maximum Flow Rates	136
7.4	Added Capabilities.....	137
7.4.1	NIST Verification Test 1.1: Pre-evacuation Delay Times	137
7.4.2	NIST Verification Tests 2.5 & 2.6: Reduced Visibility vs. Walking Speed & Occupant Incapacitation	139
7.4.3	NIST Verification Tests 3.2 & 3.3: Social Influence & Affiliation	141
7.5	Suggested Improvements to Recommended Test Cases.....	142
7.6	Conclusion	143
8	Pedestrian Speed On Stairs: A Mathematical Model Based on Empirical Analysis for use in Computer Simulations.....	146
8.1	Mathematical Model	147
8.2	Empirical Analysis.....	150
8.3	Verification of Model	153
8.4	Johnson Center Validation.....	154
8.5	Conclusion	158
9	Validation of PEDFLOW	160
9.1	Description of NIST Stairwell Data.....	161
9.2	Geometric and Pedestrian Definitions	165
9.3	Comparison of Actual and Simulated Values.....	166
9.4	Conclusion	169
10	Building Evacuation Study – Spring 2015	171
10.1	Johnson Center.....	171
10.2	Video Analysis.....	174

10.2.1	Overall Evacuation Times	175
10.2.2	Occupant Initial Locations and Activities	176
10.2.3	Evacuation Delay.....	182
10.2.4	Occupant Route-to-Exit Selection.....	184
10.3	PEDFLOW Simulation	190
10.4	Conclusion	193
11	Conclusion.....	195
11.1	Contributions.....	196
11.2	Future Work.....	198
	References.....	200

LIST OF TABLES

Table		Page
Table 1	CA Model Bi-directional Rule Set (extracted from [24]).....	18
Table 2	Basic Implementation Algorithm of a CA Model with Floor Field Interactions.....	20
Table 3	Initial Evaluation of PEDFLOW According to Main Features [55]....	116
Table 4	Initial Evaluation of PEDFLOW According to Special Features [55].....	117
Table 5	Summary of NIST Verification Tests as Applied to PEDFLOW	119
Table 6	Room 1 to Room 2 Traversal Time Statistics after 30 PEDFLOW Simulation Runs.....	134
Table 7	Room Exit Time Statistics after 30 PEDFLOW Simulation Runs	136
Table 8	Post-verification Evaluation of PEDFLOW According to Main Features [55]	144
Table 9	Post-verification Evaluation of PEDFLOW According to Special Features [55]	145
Table 10	Frequency and Step Size Correction Factors for Pedestrians Ascending a Flight of Stairs.....	152
Table 11	Frequency and Step Size Correction Factors for Pedestrians Descending a Flight of Stairs.....	152
Table 12	Stair Descent Statistics as Recorded from Security Camera Footage.....	157
Table 13	Average Stair Descent Times after 20 PEDFLOW Simulation Runs	158
Table 14	Initial Occupant Activities	182
Table 15	Occupant Evacuation Route Described by Initial Location, Stair, and Exit Choice.....	189

LIST OF FIGURES

Figure		Page
Figure 1	Predtechenskii and Milinskii Fundamental Diagram (extracted from [2]).....	2
Figure 2	Pedestrian and Evacuation Dynamics Conference Growth 2001-2014 [4]–[10].....	4
Figure 3	Weidmann Velocity vs Density Fundamental Diagram (extracted from [21]).....	14
Figure 4	Most Common CA Pedestrian Grids – Square Lattice (left) and Hexagonal Lattice (right).....	16
Figure 5	Pedestrian Movement Directions Allowed using a Von Neumann Neighborhood on a Square Lattice	16
Figure 6	Pedestrian Movement Directions allowed using a Moore Neighborhood on a Square Lattice (left) and Hexagonal Lattice (right).....	17
Figure 7	Multi-Agent Navigation Incorporating PLE (extracted from [38]).....	27
Figure 8	FSM and RVO Coupling (extracted from [41]).....	30
Figure 9	Example Fundamental Diagrams derived from Density-Velocity Models (extracted from [46]).....	37
Figure 10	Example Discretized Grid Used to Compute Density Field (extracted from [51]).....	44
Figure 11	Evacuation Models (circa 1999) Classified According to Methodology (extracted from [53]).....	50
Figure 12	Evacuation Models (circa 2005) Classified According to Main Features (extracted from [54]).....	51
Figure 13	Evacuation Models (circa 2010) Classified According to Main Features (extracted from [55]).....	52
Figure 14	Accident Sequence Model (extracted from [57])	54
Figure 15	Evacuation Models (circa 2010) Classified According to Special Features (extracted from [55]).....	55
Figure 16	Description of Pre-evacuation Times Performance Component (extracted from [58]).....	56
Figure 17	Distribution of Office Building Pre-evacuation Times (extracted from [59]).....	57
Figure 18	Distribution of Apartment Building Pre-evacuation Times (extracted from [59]).....	57
Figure 19	Risk Perception Curve (Single Pedestrian).....	63

Figure 20	Pedestrian Initial Locations and Activities within Room	64
Figure 21	Risk Perception Curves for Pedestrians with Normal Awareness.....	65
Figure 22	Risk Perception Curves for Pedestrians with Increased Awareness.....	65
Figure 23	Effect of Knowledge Cue Value on Risk Perception Level (Single Pedestrian)	69
Figure 24	Impact of Prior Knowledge Values on Transition Times	70
Figure 25	Risk Perception Curves for Pedestrians with Prior Knowledge and Normal Awareness.....	70
Figure 26	Risk Perception Curves for Pedestrians with Prior Knowledge and Increased Urgency	71
Figure 27	Effect of $N_{N,i}$ (Observed Neighbors in Normal State) on Pedestrian i	75
Figure 28	Example Risk Perception Curves for Pedestrian i when $N_{N,i} \geq N_{O,i}$ and $N_{I,i} = 1$	76
Figure 29	Risk Perception Curves for Pedestrians with Social Influence and Normal Awareness.....	77
Figure 30	Risk Perception Curves for Pedestrians with Social Influence and Increased Awareness.....	77
Figure 31	Complete EDM Simulation with Normal Awareness.....	79
Figure 32	Positive Effect of Social Influence on the Risk Perception Curve	80
Figure 33	Complete EDM Simulation with Increased Awareness	81
Figure 34	Negative Effect of Social Influence on the Risk Perception Curve.....	81
Figure 35	Empirical Data Classifications (extracted from [14]).....	86
Figure 36	Evacuation Delay Times from Four Mid-Rise Apartment Buildings [73].....	91
Figure 37	Pre-evacuation Times (extracted from [74]).....	93
Figure 38	Creation of the Force Vector in PEDFLOW	101
Figure 39	Velocity Adjustment Routines Available in PEDFLOW	115
Figure 40	Geometric Definition and Initial Pedestrian Placement for Verification Test 2.1	121
Figure 41	Geometric Definition, Pedestrian Initialization, and Qualitative Verification for Verification Test 2.3	122
Figure 42	Verification of Elevator Usage in PEDFLOW (Verification Test 2.7).....	123
Figure 43	Geometric Definition, Pedestrian Initialization, and Group Cohesion through Exit for Verification Test 2.9	124
Figure 44	Geometric Definition, Initial Pedestrian Locations, and Qualitative Verification of Exit Selection for Verification Test 3.1	125
Figure 45	Building Exit Time Distribution after 30 Simulation Runs.....	126
Figure 46	Geometric Definition and Initial Pedestrian Placement for Verification Test 4.1	127
Figure 47	Comparison of Velocity in both the Upward (left) and Downward (right) Directions for Verification Test 5.1 (notice lack of congestion at the top of the stairs)	128

Figure 48	Geometric Definition and Initial Pedestrian Placement for Verification Test 2.2	129
Figure 49	Recommended Additional Verification Test (Speed on Ramps).....	129
Figure 50	Empirical Stair Data (extracted from [90]).....	131
Figure 51	Improved PEDFLOW Velocity Curves when Traveling Up (left) and Down (right) a 30° Staircase.....	132
Figure 52	Assignment of Pedestrian Characteristics within PEDFLOW	133
Figure 53	Geometric Definition, Initial Pedestrian Positions, and Horizontal Counterflow with “Cultural Behavior”	134
Figure 54	Geometric Definition and Initial Pedestrian Placement for Verification Test 2.10	135
Figure 55	Geometric Definition and Initial Pedestrian Placement for Verification Test 5.2	137
Figure 56	Geometric Definition, Initial Pedestrian Placement for Verification Test 1.1.....	138
Figure 57	Pre-evacuation Delay Distribution after 10 runs (Verification Test 1.1).....	139
Figure 58	Geometric Definition and Initial Pedestrian Placement for Verification Test 2.5	140
Figure 59	Geometric Definition and Initial Pedestrian Placement for Verification Test 2.6	140
Figure 60	Ascent and Descent Velocity as a Function of Stair Angle.....	149
Figure 61	PEDFLOW Velocity Curves when Traveling Up (left) and Down (right) a 32.7° Staircase	154
Figure 62	Johnson Center Floor Plans (Stairs Highlighted in Green).....	155
Figure 63	Occupant Evacuation Route Described by Initial Location, Stair, and Exit Choice.....	156
Figure 64	Example Comparison of PEDFLOW Stair Descent Times with Empirical Data Obtained from Video	158
Figure 65	Evacuee Total Evacuation Times from a 10-story Building [97].....	163
Figure 66	Evacuee Initial Floor Locations in a 10-story Building [97].....	164
Figure 67	Evacuee Pre-observation Delay Times in a 10-story Building [97]....	165
Figure 68	Evacuee Initial Positions and Geometric Description of a 10-story Building with 2 Stairwells	165
Figure 69	Average Velocity during Descent from 10 th Floor	167
Figure 70	Comparison of Experimental (red line) versus Simulation-obtained Values for Pre-Evacuation Delay (left) and Building Exit Times (right) for Gaussian Distribution of Pre-evacuation Delay.....	168
Figure 71	Comparison of Experimental (red line) versus Simulation-obtained Values for Pre-evacuation Delay (left) and Building Exit Times (right) with Video-extracted Pre-evacuation Delay.....	169
Figure 72	Johnson Center Floor Plans (Stairs Highlighted in Green).....	172
Figure 73	Johnson Center Exits (Stairs Highlighted in Green).....	173
Figure 74	Johnson Center Exterior Doors.....	174

Figure 75	Representative Images from Exterior Security Cameras (Left: West Door, Center: Northwest Door, Right: East Door).....	175
Figure 76	Johnson Center Occupant Evacuation Time (Grouped by Exit Door).....	176
Figure 77	Johnson Center Occupant Evacuation Times (Aggregate).....	176
Figure 78	Representative Images from Interior Security Cameras Demonstrating Progressive Identification of Initial Locations.....	178
Figure 79	Initial Occupant Locations – Johnson Center Ground Floor	179
Figure 80	Initial Occupant Locations – Johnson Center 1st Floor.....	180
Figure 81	Initial Occupant Locations – Johnson Center 2 nd (top) and 3 rd (bottom) Floors	181
Figure 82	Johnson Center Occupant Evacuation Delay (Aggregate)	183
Figure 83	Johnson Center Occupant Evacuation Delay (Grouped by Occupant Type).....	184
Figure 84	Occupant Route-to-Exit Choices (Ground Floor).....	185
Figure 85	Occupant Route-to-Exit Choices (First Floor).....	186
Figure 86	Occupant Route-to-Exit Choices (Second Floor)	187
Figure 87	Occupant Route-to-Exit Choices (Third Floor).....	188
Figure 88	Occupant Evacuation Times (Empirical Data vs PEDFLOW).....	190
Figure 89	Johnson Center Simulation Inputs used with PEDFLOW (*Derived from Spring 2015 Fire Drill)	191
Figure 90	Occupant Desired Velocity Assignments for 5 Randomized PEDFLOW Trials	192
Figure 91	Occupant Evacuation Delay Time Assignments (based on a table of probabilities) for 5 PEDFLOW Trials.....	192
Figure 92	Overall Evacuation Exit Times for 5 Randomized PEDFLOW Trials	193

LIST OF EQUATIONS

Equation		Page
Equation 1	Social Force Model [17]	10
Equation 2	HMFV Social Force Model [18].....	11
Equation 3	Modified HMFV Social Force Model [20].....	13
Equation 4	Dynamic Floor Field Diffusion and Decay Model	19
Equation 5	Generalized Transition Probability for CA Model with Floor Field Interactions.....	19
Equation 6	Transition Probability During Evacuations for CA Model with Floor Field Interactions [28].....	21
Equation 7	Probability Pedestrian i Selects Exit E for F.A.S.T Model [29]–[31].....	22
Equation 8	Probability Pedestrian i Selects Destination Cell (x, y) for F.A.S.T Model [29]–[31].....	22
Equation 9	PLE Objective Function [38].....	26
Equation 10	Physiological Constraint due to Natural Stride Length	28
Equation 11	Psychological Constraint due to Desired Privacy Space	28
Equation 12	Physiological Constraint due to Natural Stride Length (corrected).....	28
Equation 13	Space Required for Specified Speed v	29
Equation 14	Natural Speed for Available Space S	29
Equation 15	Probability Density Function for Velocity (x-component) [42]	32
Equation 16	Probability Density Function for Velocity (y-component) [42]	32
Equation 17	Probability Density Function for Velocity (resultant) [42]	32
Equation 18	Probability Density Function for Speed [42].....	33
Equation 19	Henderson’s Conservation Equations [43]	33
Equation 20	Henderson’s Equation of State [43].....	34
Equation 21	Henderson’s Conservation Equations – Interactive Speed Modes and Density Phases [43].....	34
Equation 22	Governing Equations for Crowd Flow [45].....	36
Equation 23	Mass Conservation.....	36
Equation 24	Momentum Conservation	37
Equation 25	Example Density-Velocity Models [46].....	37
Equation 26	One-Dimensional Payne-Whitham (PW) Model.....	38
Equation 27	One-Dimensional Aw and Rascle (AR) Model	39
Equation 28	One-Dimensional Zhang Model	39
Equation 29	Pedestrian Gas-Kinetic Equation.....	42
Equation 30	Derivation of the Acceleration Term A in Equation 29.....	42

Equation 31	Density Contribution Equations for Pedestrian i	45
Equation 32	Path Objective Function.....	45
Equation 33	Path Objective Function w/Unit Cost Field C	45
Equation 34	Basic Risk Perception Model.....	59
Equation 35	Complete Risk Perception Model.....	60
Equation 36	Basic Risk Perception Model (Single Continuous Alarm)	62
Equation 37	Maximum Value of $\Delta t_{E,i}$ for Pedestrian i	64
Equation 38	Prior Knowledge Cue Value.....	67
Equation 39	Modified Risk Perception Model (Single Continuous Alarm with Prior Knowledge Cue).....	68
Equation 40	Social Influence Cue.....	73
Equation 41	Modified Risk Perception Model (Single Continuous Alarm with Social Influence Cue).....	73
Equation 42	Complete Risk Perception Model (Single Continuous Alarm)	78
Equation 43	Newton's Equations of Motion.....	100
Equation 44	Will Force	102
Equation 45	Initial Value Problem (IVP).....	102
Equation 46	Solution to the IVP given in Equation 45.....	103
Equation 47	Objective Function to Find Δt that Minimizes the Distance between Two Moving Pedestrians.....	104
Equation 48	Tangential and Normal Directions for Vector \mathbf{v}	105
Equation 49	Normalized Distance δ Between two Pedestrians in PEDFLOW	105
Equation 50	Tangential and Normal Components of the Normalized Distance δ ...	105
Equation 51	Pedestrian-Pedestrian Intermediate-Range Forces	106
Equation 52	Normalized Distance δ between Two Close-Range Pedestrians in PEDFLOW.....	107
Equation 53	Pedestrian-Pedestrian Close-Range Forces	107
Equation 54	Pedestrian-Wall Collision Avoidance Force.....	108
Equation 55	Pedestrian-Fence Avoidance Force	110
Equation 56	Pedestrian-Elevator Avoidance Force	110
Equation 57	Normalized Distance δ_{ij} Between two Pedestrians in PEDFLOW	111
Equation 58	Pedestrian-Pedestrian Contact Forces.....	112
Equation 59	Pedestrian-Wall Contact Force	114
Equation 60	Velocity Update	114
Equation 61	Position Update.....	115
Equation 62	Velocity Reduction Coefficient for Conditions of Limited Visibility	141
Equation 63	Corrected Velocity for Conditions of Limited Visibility.....	141
Equation 64	Basic Velocity Correction Formula Used for Travel on Stairs.....	147
Equation 65	Velocity Reduction Coefficient for Stair Ascension	148
Equation 66	Velocity Reduction Coefficient for Stair Decent.....	149
Equation 67	Individual Step Frequency.....	149
Equation 68	Step Frequency Formula Used for Travel on Stairs to Find Steps Per Second	150

Equation 69	Corrected Step Size for Travel on Stairs	151
Equation 70	Velocity Correction Formula Used for Travel on Stairs.....	153

LIST OF ABBREVIATIONS

ABM	Agent-Based Model
AR	Aw and Rascole Model
CA	Cellular Automata
CASA	Centre for Advanced Spatial Analysis
EDM	Evacuation Decision Model
F.A.S.T.	Floor field- and Agent-based Simulation Tool
FSM	Finite State Machine
GMU	George Mason University
HMFV	Helbing- Molnár-Farkas-Vicsek Model
IMO	International Maritime Organization
ISO	International Standards Organization
LCA	Local Collision Avoidance
NIST	National Institute for Standards and Technology, United States of America
ORCA	Optimal Reciprocal Collision Avoidance
PED	Pedestrian and Evacuation Dynamics Conference
PEDFLOW	Pedestrian Flow Simulation Tool (by Löhner)
PGS	Preferred Gap Size
PLE	Principle of Least Effort
P-PSD	Pedestrian Phase-Space Density
PSM	Personal Space Measure
PPPM	Particle-Particle Particle-Mesh
PW	Payne-Whitham Model
RiMEA	Richtlinie für Mikroskopische Entfluchtungs-Analysen
RVO	Reciprocal Velocity Obstacle
SFM	Social Force Model
VO	Velocity Obstacles

ABSTRACT

SIMULATING OCCUPANT RESPONSE TO EMERGENCY SITUATIONS

Michelle Lynn Isenhour, Ph.D.

George Mason University, 2016

Dissertation Director: Dr. Rainald Löhner

When evaluating building evacuation processes, the inclusion of occupant response to emergency situations is essential in the overall assessment of the evacuation plan.

Simulations which model the movement of people within buildings aid in the study of evacuation processes and are most often used to validate evacuation plans, optimize evacuation time, and identify any potential safety hazards. The accurate prediction of movement during a building evacuation depends greatly upon the actions and decisions individuals make at the start of the emergency. This dissertation employs a mathematical formulation which accounts for occupant behaviors during this pre-movement phase and implements a computational model to account for the situation dependent dynamic processes which determine the selection of route and exit from a building. The overall effect of these decisions and choices on the evacuation from a student center located at George Mason University (GMU) is presented.

This dissertation begins with a comprehensive review of the mathematical models most often used in computer simulations to model evacuation processes at the micro-, macro-, and mesoscopic levels of pedestrian science. The second literature survey reviews evacuation dynamics; namely, the study of occupant response to emergency situations. Evacuation dynamics encompasses a multitude of research areas and disciplines, most often seen at the intersection of psychology and sociology, mechanics and kinematics, mathematical modeling and analysis, numerical methods, parallel computing, visualization, and data collection. A final literature review highlights psychological factors commonly seen in emergency situations and summarizes evacuation data collection efforts. To better understand the physical, social, and psychological factors involved in the decision to evacuate, a continuous alarm implementation of Reneke's Evacuation Decision Model (EDM) is implemented as a sub-model to a microscopic cellular automata (CA) model.

A pedestrian flow simulation tool (PEDFLOW) is described, verified, validated, and evaluated throughout this dissertation. PEDFLOW has been in development at GMU over the past decade to numerically model the motion of pedestrians and uses a microscopic model where each pedestrian is treated individually and motion is influenced by Newtonian dynamics. As PEDFLOW was not designed specifically for evacuation, when this project began PEDFLOW did not have any pre-evacuation capabilities, nor did it contain modules to account for physiological, sociological, or psychological factors seen during evacuation. PEDFLOW now contains modules which account for pedestrian discomfort, exhaustion, social influence, and affiliative behaviors such as familiar route

and exit choice. This work not only incorporated pre-movement behaviors described in literature into PEDFLOW, but also included behaviors observed during the pre-movement phase of routine fire drills on the campus of GMU. This observational study captured the activities of building occupants prior to and immediately after a routine fire drill in a student center on the campus of GMU and resulted in a very thorough newly collected set of empirical data for use by researchers in the validation of computer simulation models. The data compiled was used as input for PEDFLOW and the results obtained were compared to the field data. Furthermore, a series of trials with randomized distribution of behaviors was conducted in order to assess variability and statistical significance.

1 INTRODUCTION

Empirical studies of crowd dynamics and pedestrian motion dates back more than fifty years. The 1950's and 1960's saw a substantial increase in the various modes of transportation (plane, train, and automobile) which not only enabled individuals to travel more frequently, but also increased the need for pedestrian safety on the city streets and inside rail stations and airport terminals. In 1958, as claimed in one of the earliest published empirical studies, the Chief Civil Engineer for London Transport asked the company's operational research section to develop "logically founded theory" on how to measure subway capacity and determine appropriate facility widths [1]. The researchers agreed to "study the flow of passengers in subways including the effect of constrictions such as stairs and corners in order to assist in the design of new facilities." Finding existing information on the topic lacking, the researchers attempted to collect real-time pedestrian flow data via direct observation of various subway stations and, after realizing the complexity involved, opted to conduct controlled experiments utilizing participants at a boys' school in southern England. More than a half-century later, their objectives, research methods, and even the challenges they encountered remain an area of active pedestrian research.

With the increase in mass transportation systems and rapid growth of urban environments, large-scale crowd gatherings became increasingly more common. In the

late 1960s and early 1970s, researchers continued empirically studying crowd dynamics, published techniques and guidelines to improve efficiency while ensuring pedestrian and crowd safety, and introduced basic pedestrian modeling and simulation guidelines in urban environments. From an engineering standpoint, pedestrian science includes theoretical principles and flow calculations, elements of design, level of service standards, and other general pedestrian planning guidelines. The development of these standards began with Predtechenskii and Milinskii's 1969 publication, *Planning for Foot Traffic Flow in Buildings* [2], and Fruin's 1971 *Pedestrian Planning and Design* thesis publication [3]. One of the most frequently referenced items from Predtechenskii and Milinskii's book are the fundamental diagrams, graphs that typically describe speed of movement (or flux) as a function of density for various situations. Figure 1 is one such fundamental diagram reproduced from the book [2] and shows speed of movement along horizontal paths as a function of density under comfortable (relaxed), normal, and emergency conditions.

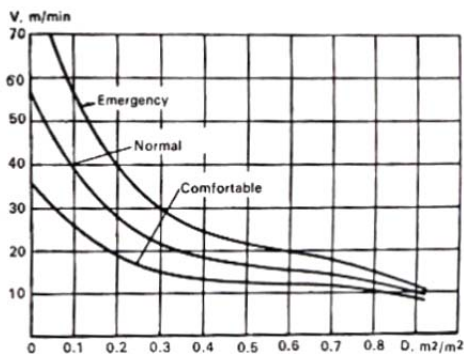


Fig. 22. Speed of movement along horizontal paths as function of flow density for normal, emergency and comfortable conditions.

Figure 1 Predtechenskii and Milinskii Fundamental Diagram (extracted from [2])

Since the publication of these two foundational books on the subject, there has been a plethora of subsequent research efforts over the next five-plus decades. Ramping up in the 1990s, the turn of the century saw an exponential increase in pedestrian research activities. The now biennial International Pedestrian and Evacuation Dynamics conference (PED) fuels the current research efforts. The inaugural 2001 conference, held in Duisburg, Germany, had more than one hundred participants from twelve countries and resulted in thirty published papers grouped according to three topics: pedestrian dynamics, evacuation simulation, and ship evacuation [4]. In comparison, the seventh international conference held in 2014 in Delft, The Netherlands, had one hundred and forty-eight participants from twenty countries (personal communication from W. Daamen, 2015 Oct 11; unreferenced). In all, researchers submitted one hundred and forty-three abstracts from which only one hundred and twenty-three were accepted, resulting in one hundred and ten published papers – two of those papers are included as chapters within this dissertation [5]. Topics covered during the conference included multiple aspects of pedestrian science: empirical data collection; microscopic and macroscopic models; decision models and behavior; operations and management of pedestrians; calibration and validation; laboratory studies using animals; and evacuation. The growth in published papers (Figure 2), as well as the significant increase in research categories, between 2001 and 2014 illustrates the importance and relevance of pedestrian science as an area of active research.

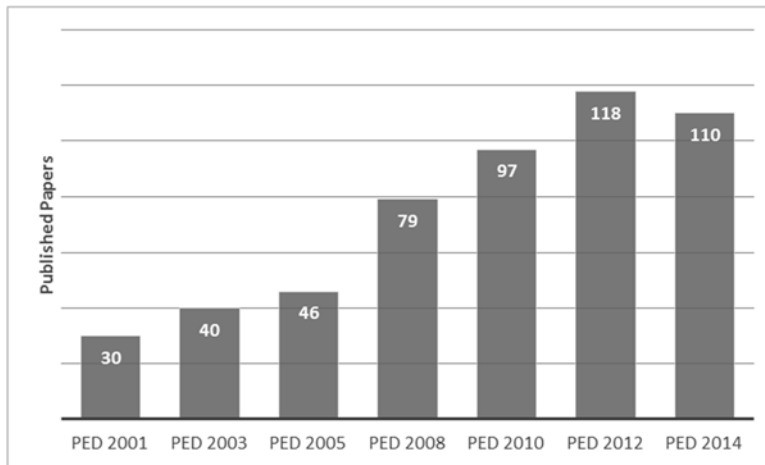


Figure 2 Pedestrian and Evacuation Dynamics Conference Growth 2001-2014 [4]–[10]

1.1 Motivation and Research Objectives

The attack on and subsequent collapse of the World Trade Center buildings in New York City on September 11, 2001 sparked a personal interest in emergency evacuation procedures. According to Amanda Ripley’s 2009 book, *The unthinkable: who survives when disaster strikes - and why* [11], those who were able to evacuate the buildings took, on average, about one minute per floor which was “twice as long as the standard engineering codes had predicted.” Inspired by her research, the main objective of this dissertation was to implement a model which goes beyond the standards established by the engineering codes and employs a mathematical formulation which incorporates pre-movement pedestrian behaviors such as event recognition, denial, response, and/or deliberation into a pre-existing pedestrian simulation tool.

In 2008, Fang et al. [12] stated that the evacuation process consists of two main phases, pre-movement and movement, with the pre-movement phase divided between two sub-phases, recognition and response. When developing his crowd dynamics model,

Fang ignores the pre-movement phase and focuses solely on pedestrian actions during the movement phase. Other evacuation researchers such as Klüpfel et al. [13], acknowledge the pre-movement phase, but then simplify the model by assuming that this reaction time simply increases the overall evacuation time and therefore can be added post-movement. This dissertation presupposes the opposing view – the pre-movement activities of an individual (event recognition, deliberation about what to do, etc.) affect the movement phase and should not be neglected nor modeled as a simple addition to total time. The application of the pre-movement behaviors to evacuation simulations leads to more accurate building clearance predictions and may also lead to adjusted building capacities and/or modified building design elements since the delay in pedestrian movement may cause significant changes to pedestrian self-organizing behaviors during evacuations. The need to incorporate pre-movement activities into existing evacuation simulations leads directly to the first objective of this work:

Objective One: Implement a mathematical formulation which accounts for individual pre-movement behaviors and show the effect of these behaviors on subsequent movement patterns and processes during facility evacuations.

In her book, *The Unthinkable*, Amanda Ripley [11] describes the pre-movement and movement process described by Fang and others as “The Survival Arc”, a three phase, often cyclical, process of denial, deliberation, and decisive action. In its purest form, the denial and deliberation processes occur during the aforementioned pre-movement phase and the decisive action process corresponds to the movement phase. However, in contrast to the sequential nature of the first objective, Ripley describes the

process as a “looping roller coaster, doubling up and back upon itself” and indicates throughout her book that survival typically requires a visit to each stage at least once, but more often than not, requires repeat visits as individuals reassess their situation. Understanding that decisions during the movement phase must, therefore, be dynamic leads to the second objective of this dissertation:

Objective Two: Implement a computational model to account for the situation-dependent dynamic processes which determine the selection of route and exit from a building and show the effect of these choices on the overall evacuation.

As will be demonstrated in the subsequent chapters, this work accomplishes both of these objectives. This dissertation employs a mathematical formulation which accounts for occupant behaviors during this pre-movement phase and also implements a computational model to account for the situation dependent dynamic processes which determine the selection of route and exit from a building. The overall effect of these decisions and choices on a simulated evacuation is compared with field data obtained through an observational study of building occupants prior to and immediately after a routine fire drill in a student center on the campus of George Mason University (GMU).

1.2 Organization of the Dissertation

This dissertation is organized into 11 chapters, including this introductory chapter and the concluding chapter. Chapter 2 contains a comprehensive review of the mathematical models most often used in computer simulations to model pedestrian motion at the micro-, macro-, and mesoscopic levels of pedestrian science. In Chapter 3, a second literature survey reviews evacuation dynamics – the study of occupant response

to emergency situations. Evacuation dynamics encompasses a multitude of research areas and disciplines, most often seen at the intersection of psychology and sociology, mechanics and kinematics, mathematical modeling and analysis, numerical methods, parallel computing, visualization, and data collection. To better understand the physical, social, and psychological factors involved in the decision to evacuate, Chapter 4 contains a continuous alarm implementation of Reneke's Evacuation Decision Model (EDM), implemented as a sub-model to a basic microscopic cellular automata (CA) model. A final literature review in Chapter 5 highlights psychological factors commonly seen in emergency situations and summarizes the state of current evacuation data collection efforts.

In Chapter 6, a pedestrian flow simulation tool (PEDFLOW) is described and evaluated. PEDFLOW has been in development at GMU over the past decade to numerically model the motion of pedestrians and uses a microscopic model where each pedestrian is treated individually and motion is influenced by Newtonian dynamics. PEDFLOW is taken through a series of verification tests in Chapter 7 which resulted in the identification of capability shortfalls, as well as the discovery of several errors and anomalies. During these tests, one such anomaly was discovered for pedestrians traveling on stairs and the newly developed mathematical model is described in Chapter 8.

Chapter 9 contains a PEDFLOW validation study of several core behavioral components needed for evacuation simulations such as the assignment of the pre-evacuation time distributions and speed on stairs. This validation study demonstrated the importance of selecting the correct pre-evacuation distribution and confirms that pre-

movement times affect the movement phase and should not be neglected nor modeled as a simple addition to total evacuation time. The validation study also revealed that getting sufficient structural and occupant data for entire buildings is difficult. Therefore, Chapter 10 contains an observational study designed to capture the activities of building occupants prior to and immediately after a routine fire drill in a student center on the campus of GMU and resulted in a very thorough newly collected set of empirical data for use by researchers in the validation of computer simulation models. The data compiled was used as input for PEDFLOW and the results obtained were compared to the field data. Furthermore, a series of trials with randomized distribution of behaviors was conducted in order to assess variability and statistical significance.

When this research began, the pedestrian simulation tool used in this study, PEDFLOW, did not have any pre-evacuation capabilities, nor did it contain modules to account for physiological, sociological, or psychological factors seen during evacuations such as discomfort, exhaustion, social influence, or affiliation. The direct result of this work is a much more robust version of PEDFLOW.

2 LITERATURE SURVEY I: THE MATHEMATICAL MODELS BEHIND PEDESTRIAN SCIENCE

One of the most influential and foundational books in pedestrian science is Predtechenskii and Milinskii's 1969 publication, *Planning for Foot Traffic Flow in Buildings* [2]. This book, translated to English from Russian in 1978, along with Fruin's 1971 publication, *Pedestrian Planning and Design* [3], formalized pedestrian science topics such as design elements, level of service standards, and planning guidance for engineers. Now midway through the fifth decade, pedestrian research activities, including experimentation and simulation, continue to grow at an exponential rate. New researchers will find an extremely current collection of scholarly articles, experimental data, and animated simulations readily available at the micro-, macro-, and mesoscopic levels of pedestrian science. Additional comprehensive reviews of the mathematics behind the modeling of pedestrians were provided most recently in articles published by Schadschneider et al. in 2008 [14] and Bellomo and Dogbe in 2011 [15].

2.1 Pedestrian Literature: Microscopic Models

Pedestrian science at the microscopic level concerns the study of pedestrian behaviors individually. At this level, each pedestrian is treated separately and discrete models attempt to illustrate what happens collectively to the crowd when each heterogeneous individual moves autonomously but with a specified set of interaction rules which govern behavior.

2.1.1 Social Force Model

Originally introduced by Helbing and Molnár in the 1990s [16], the microscopic Social Force Model (SFM) treats each individual pedestrian i as a particle, subject to social and physical forces, and applies Newtonian physics, where force equals mass times acceleration (Equation 1), to generate pedestrian trajectories. The social force term $\mathbf{f}_i(t)$ in Equation 1 represents the sum of all environmental influences such as the individual's driving force due to his will, repulsive forces such as the desire to avoid other pedestrians and obstacles, and attractive forces such as the desire to stay together in a group or look at an information display. The additional term $\xi_i(t)$ is referred to as the fluctuation term, and it accounts for random individual behavioral variations [17].

Equation 1 Social Force Model [17]

$$\begin{aligned} \frac{d\mathbf{x}_i}{dt} &= \mathbf{v}_i(t) \\ m_i \frac{d\mathbf{v}_i}{dt} &= \mathbf{f}_i(t) + \xi_i(t) \end{aligned} \quad i = 1, \dots, N$$

Using the SFM as a basis for modeling at the microscopic level, many researchers have adapted and modified the model in an attempt to produce more realistic behaviors. In 2000, Helbing joined with Farkas and Vicsek [18] and better defined Equation 1 into what is now commonly referred to as the Helbing-Molnár-Farkas-Vicsek (HMFV) model [19]. The social force term $\mathbf{f}_i(t)$ in Equation 1 was expanded to explicitly model the internal (will) force where each pedestrian i has mass m_i , desired velocity $\mathbf{v}_i^0(t)$, and a desired direction of travel $\mathbf{e}_i^0(t)$, but tends to adapt his/her actual velocity $\mathbf{v}_i(t)$ with

relaxation time τ_i as shown in Equation 2. In addition, the HMFV model defines the social force term $\mathbf{f}_i(t)$ seen in Equation 1 as the sum of the external interaction forces from pedestrian-pedestrian interactions \mathbf{f}_{ij} and pedestrian-wall interactions \mathbf{f}_{iW} .

Equation 2 HMFV Social Force Model [18]

$$\begin{aligned} \frac{d\mathbf{x}_i}{dt} &= \mathbf{v}_i(t) \\ m_i \frac{d\mathbf{v}_i}{dt} &= m_i \frac{\mathbf{v}_i^0(t) \mathbf{e}_i^0(t) - \mathbf{v}_i(t)}{\tau_i} + \sum_{i \neq j} \mathbf{f}_{ij} + \sum_W \mathbf{f}_{iW} \end{aligned} \quad i = 1, \dots, N$$

where

$$\begin{aligned} \mathbf{f}_{ij} &= A_i e^{(r_{ij} - d_{ij})/B_i} \mathbf{n}_{ij} + kg(r_{ij} - d_{ij}) \mathbf{n}_{ij} + Kg(r_{ij} - d_{ij}) \Delta v_{ji}^t \mathbf{t}_{ij} \\ \mathbf{f}_{iW} &= A_i e^{(r_{ij} - d_{iW})/B_i} \mathbf{n}_{ij} + kg(r_{ij} - d_{iW}) \mathbf{n}_{iW} + Kg(r_{ij} - d_{iW}) (\mathbf{v}_i \cdot \mathbf{t}_{iW}) \mathbf{t}_{iW} \end{aligned}$$

As described by Helbing et al. [18], the pedestrian-pedestrian interactions \mathbf{f}_{ij} shown in Equation 2 consist of a social interaction term $A_i e^{(r_{ij} - d_{ij})/B_i} \mathbf{n}_{ij}$, physical contact term $kg(r_{ij} - d_{ij}) \mathbf{n}_{ij}$, and friction term $Kg(r_{ij} - d_{ij}) \Delta v_{ji}^t \mathbf{t}_{ij}$. The social interaction term is modeled by a repulsive interaction force (the assumption is that people want to stay away from each other) where A_i and B_i are constants, r_{ij} is the sum of their individual radii r_i and r_j , d_{ij} is the distance between their centers, and \mathbf{n}_{ij} is a normalized vector orthogonal to the vector pointing from j to i . The physical contact term is also applied in the direction of the normal vector \mathbf{n}_{ij} and is modeled by a large constant term k multiplied by a ‘‘contact’’ function $g(r_{ij} - d_{ij})$, which is zero if $r_{ij} - d_{ij} < 0$ (pedestrians are not in contact with each other) and equal to $r_{ij} - d_{ij}$ (the overlap) otherwise. The friction term is applied in the direction of the tangential vector \mathbf{t}_{ij} and

modeled by the product of a large constant term K , the “contact” function $g(r_{ij} - d_{ij})$ and the tangential velocity difference $\Delta v_{ji}^t = (\mathbf{v}_j - \mathbf{v}_i) \cdot \mathbf{t}_{ij}$. Note that the physical contact term and friction term only apply when contact between pedestrians occurs; that is, the sum of the pedestrian radii is greater than or equal to the distance between them. The pedestrian-wall interaction \mathbf{f}_{iW} term is analogous to the pedestrian-pedestrian interaction term.

In 2005, Lakoba et al. [20] modified the HMFV model. First, they added an “attraction-to-exit” force $f_{iE} = -Ae^{(\delta_{iE} - d_{iE})/B} \mathbf{n}_{iE}$ which is very similar to the repulsive social interaction term used by Helbing et al. except with different values for A and B and the use of the negative sign to indicate attraction rather than repulsion. They also added a velocity-correction term $f_v = -m \frac{v - v_0}{\tau}$ where the pedestrian’s current velocity is \mathbf{v} and the pedestrian’s preferred velocity is $\mathbf{v}_0 = (1 - p)V_0 \mathbf{e}_i + p \langle \mathbf{v}_j \rangle_i$ is based on the assumption that the speed at which a pedestrian prefers to walk is a weighted average of a pedestrian’s own (unimpeded) desired velocity V_0 and the average velocity of the people around him within a specified radius $\langle \mathbf{v}_j \rangle_i$. In addition to adding these forces, Lakoba et al. provided two additional recommendations for improvement to the HMFV model. First, they noticed that the HFMV model, under certain conditions, would allow pedestrians to occupy the same space (overlap) which is unrealistic. To compensate for this, they recommended the implementation of a maximal squeezing factor s_{max} , such that the simulated radius of a pedestrian would never be less than $r_i - s_{max}$. Second, they noticed that the values used for the magnitude A (2000 N)

and fall off length B (0.08 m) were unrealistic and recommended modifications to the force equations in the HMFV model as shown in Equation 3.

Equation 3 Modified HMFV Social Force Model [20]

$$\begin{aligned}\frac{dx}{dt} &= v \\ \frac{dv}{dt} &= -\frac{v - v_0(1 + E)}{\tau} - \frac{f_{social}(r_{||})}{m} + b \frac{f_{social}(r_{||})}{m} \\ \frac{dE}{dt} &= -\frac{E}{T} + \frac{E_m}{T} \left(1 - \frac{v}{v_0}\right)\end{aligned}$$

where

$$\frac{f_{social}(r_{||})}{m} = \frac{\omega_0(1 + E_m)e^{-1,91(D_0+r_{||}-\frac{1}{\rho_{max}})}}{\tau(1 - b)}$$

In Equation 3, $v_0(1 + E)$ is the effective preferred velocity with the constant E representing what Lakoba et al. describe as the “excitement” factor. The second term shown for the acceleration equation $\left(\frac{dv}{dt}\right)$ is the repulsive force which prevents a pedestrian from following too closely, while the third term in the acceleration equation is the force an individual feels from those behind him/her. Lakoba et al. explain that the value for b must be less than 1, and stated that they used a value of $b = 0.3$ for their simulation runs. The third equation $\left(\frac{dE}{dt}\right)$ describes the change in “excitement” and is based upon values chosen for lag time T and the maximum value for E_m . In normal situations, Lakoba et al. state that $E_m \approx 1$, but in “panic” situations $E_m = \frac{1}{(1+H)}$ where the “hurry” factor is $H = \frac{v_0}{\omega_0} - 1$ and desired velocity v_0 is much, much greater than the

speed of an isolated pedestrian ω_0 . It is important to note that the equation representing the pedestrian-pedestrian social repulsion forces $\frac{f_{social}(r_{ij})}{m}$ shown in Equation 3 was derived from the equations of motion listed in Equation 3 and the empirical fundamental diagram (density versus velocity) relationship (Figure 3) provided by Weidmann [21].

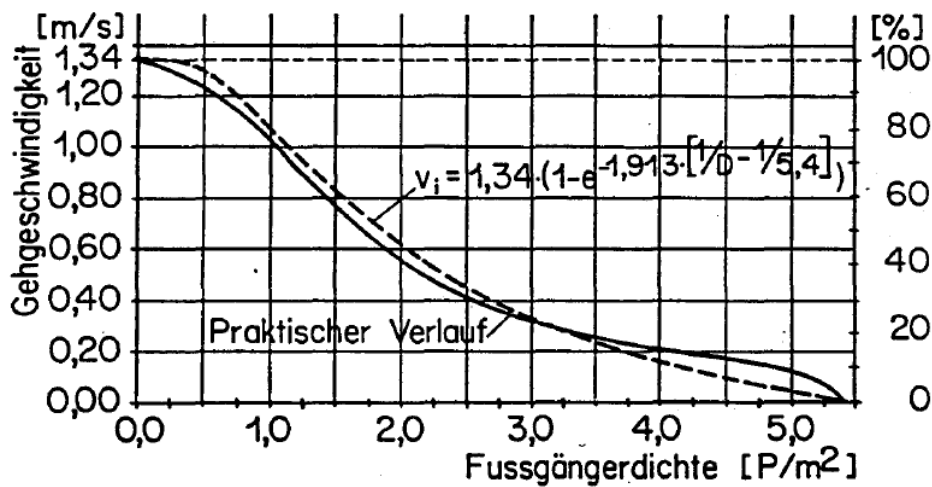


Figure 3 Weidmann Velocity vs Density Fundamental Diagram (extracted from [21])

Lakoba et al. [20] claimed that their modified HMFV model allowed a more realistic reproduction of the behaviors of a single pedestrian or a small group of pedestrians while still maintaining the realism of the original HMFV model for simulation of large crowds. However, they also acknowledged that some problems seen with the original HMFV model (such as problems with lane formation, the use of alternate exits, and oscillation of flux at doors) still existed following their modifications.

Since the introduction of the SFM, many researchers have continued to work on the model and suggested new forces. Each adaptation and modification to the SFM

attempts to exploit the model's advantages and mitigate its disadvantages. One of the most often challenged assumptions in the SFM is the use of symmetric forces between pedestrians; just because pedestrian i is trying to avoid pedestrian j does not necessarily mean that pedestrian j is trying to avoid pedestrian i . Similarly, because the SFM is based upon particle-particle interactions often seen in molecular dynamics modeling, the researchers assume that each pedestrian i influences all other pedestrians within a specified neighborhood (cut-off distance); however, it seems more logical that pedestrian i is only influenced by the "nearest" neighbors. Simply stated, if the pedestrians closest to pedestrian i are not moving, then pedestrian i cannot move. Lastly, as was previously seen, the SFM has a small number of parameters which, once calibrated, can be applied to a variety of situations and scenarios without the need for recalibration. However, initial calibration of the parameters may be difficult and research has shown a wide disparity between parameter estimations for the different SFM variations [22].

2.1.2 Cellular Automata Model

A second type of microscopic model is the cellular automata (CA) model which consists of spatial-temporal discretization, sequential or simultaneous position updating, and the application of a set of transition rules which govern pedestrian motion.

Foundational to the CA model is the definition of the movement grid which can be of differing dimensions and shapes. Two typical grids most often used in the modeling of pedestrians are square and hexagonal lattices where each cell in the lattice represents the personal space required by one pedestrian (Figure 4).

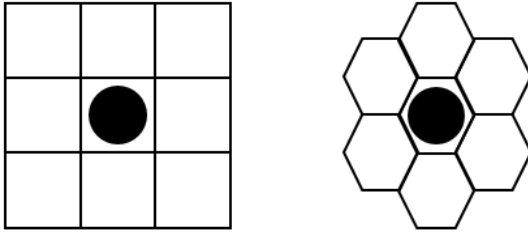


Figure 4 Most Common CA Pedestrian Grids – Square Lattice (left) and Hexagonal Lattice (right)

Given the spatial breakdown of the geometry into one of the aforementioned lattices, pedestrian locations are designated by the simple use of a Boolean (0 or 1) state indicator, where 0 represents an unoccupied cell and 1 indicates an occupied cell. Movement of pedestrians is governed by the type of neighborhood used, typically a von Neumann (Figure 5) or Moore (Figure 6) neighborhood, the associated transition probability matrices, and the subsequent set of local rules chosen to govern behavior. Typically, the transition probabilities and rule set are determined from a pedestrian's desired destination, his/her interactions with other pedestrians, and the interactions with walls and other inanimate obstacles.

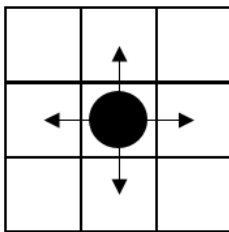


Figure 5 Pedestrian Movement Directions Allowed using a Von Neumann Neighborhood on a Square Lattice

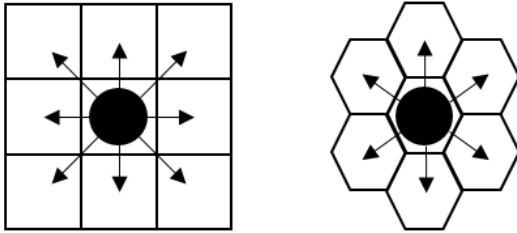


Figure 6 Pedestrian Movement Directions allowed using a Moore Neighborhood on a Square Lattice (left) and Hexagonal Lattice (right)

Blue and Adler first explored the use of CA for modeling unidirectional pedestrian walkways in 1998 [23] and extended their CA model to include bidirectional flow in 2001 [24] using an intuitively developed pedestrian rule set which induced seemingly realistic fundamental diagrams (speed and flow versus density). In their unidirectional study [23], Blue and Adler used a square lattice where the length of each side was 0.457 meters long, a modified von Neumann neighborhood where the only possible moves were straight ahead, step left then forward, or step right then forward, and a two-stage set of local rules. The algorithm governing the first stage determined the directional “lane” for each pedestrian while the second stage determined how many cells to advance the pedestrian during the time step. Blue and Adler used three different pedestrian categories defined by their desired velocities: 90% of the pedestrians had a desired velocity of 1.3 meters per second (which corresponded to a desire to move three cells during each one second time step), 5% had a desired velocity of 0.85 meters per second (two cells per time step), and 5% had a desired velocity of 1.8 meters per second (four cells per time step). As long as space was available in a particular lane, pedestrians would move to their new positions in accordance with their desired velocities; otherwise,

they would move based on space available. In their 2001 paper [24], they extended the unidirectional rule set to bi-directional pedestrian flow (shown in Table 1).

Table 1 CA Model Bi-directional Rule Set (extracted from [24])

CA-Ped Microsimulation rule set

Lane change (parallel update 1)

- (1) Eliminate conflicts: two walkers that are laterally adjacent may not sidestep into one another
 - (a) an empty cell between two walkers is available to one of them with 50/50 random assignment
- (2) Identify gaps: same lane or adjacent (left or right) lane is chosen that best advances forward movement up to v_{\max} according to the gap computation subprocedure that follows the step forward update
 - (a) For dynamic multiple lanes (DML):
 - (i) step out of lane of a walker from opposite direction by assigning $\text{gap} = 0$ if opposing pedestrian is within 8 cells
 - (ii) step behind a same direction walker when avoiding an opposite direction walker by choosing any available lane with $\text{gap}_{\text{same, dir}} = 0$ when $\text{gap} = 0$
 - (b) ties of equal maximum gaps ahead are resolved according to:
 - (i) Two-way tie between the adjacent lanes: 50/50 random assignment
 - (ii) Two-way tie between current lane and single adjacent lane: 80/20 random assignment for stay in lane/ adjacent lane
 - (iii) Three-way tie: 80/10/10 assignment for stay in lane or either adjacent lane
- (3) Move: each pedestrian p_n is moved 0, +1, or -1 lateral sidesteps after (1) and (2) are completed

Step forward (parallel update 2)

- (1) Update velocity: Let $v(p_n) = \text{gap}$, where gap is from gap computation subprocedure below
- (2) Exchanges: IF $\text{gap} = 0$ or 1 AND $\text{gap} = \text{gap}_{\text{opp}}$ (cell occupied by an opposing pedestrian) THEN with probability p_{exchg} $v(p_n) = \text{gap} + 1$ ELSE $v(p_n) = 0$
- (3) Move: each pedestrian p_n is moved $v(p_n)$ cells forward on the lattice after (1) and (2) are completed.

Subprocedure: Gap computation

- (1) Same direction: Look ahead a max of 8 cells ($8 = 2 * \text{largest } v_{\max}$) IF occupied cell found with same direction THEN set gap_{same} to number of cells between entities ELSE $\text{gap}_{\text{same}} = 8$
 - (2) Opposite direction: IF occupied cell found with opposite direction THEN set gap_{opp} to INT ($0.5 * \text{number of cells between entities}$) ELSE $\text{gap}_{\text{opp}} = 4$
 - (3) Assign $\text{gap} = \text{MIN}(\text{gap}_{\text{same}}, \text{gap}_{\text{opp}}, v_{\max})$
-

In 2001, Schadschneider [25] and Burstedde et al. [26], [27] introduced the concept of static and dynamic “floor fields” to the CA model. Rather than having a fixed set of transition probabilities, $p_{ij} = M_{ij}$, representing a pedestrian’s preference to move in the (i, j) direction (as was the case in Blue and Adler’s model) the transition probabilities are now updated using additional environmental information provided by

floor fields. A static floor field does not change with time, is position dependent, and exists even when no pedestrians are present. An example of a static floor field would be a distance-to-exit floor field. However, a dynamic floor field changes with time, depends on the locations and prior movements of the pedestrians, and is updated throughout the simulation. As the pedestrians move through the simulation, they leave a (virtual) “trace” which is recorded in the floor field thus enticing others to follow. The dynamic floor field F is subject to diffusion $\alpha \in [0, \frac{1}{8}]$ and decay $\delta \in [0, \frac{1}{2}]$, governed by Equation 4, which means that the trace disperses and eventually vanishes with time.

Equation 4 Dynamic Floor Field Diffusion and Decay Model

$$\frac{\partial D}{\partial t} = \alpha \Delta D - \delta D$$

As described by Burstedde et al. [26], [27], the transition probability p_{ij} for each of the nine cells in Figure 6, where (i, j) represents the direction of movement is shown in Equation 5.

Equation 5 Generalized Transition Probability for CA Model with Floor Field Interactions

$$p_{ij} = NM_{ij}D_{ij}S_{ij}(1 - n_{ij})$$

$$\sum_{(i,j)} p_{ij} = 1$$

If a particular cell is occupied, p_{ij} should equal zero; therefore, n_{ij} represents the occupation status of a particular cell. If $n_{ij} = 1$, the cell is occupied and if $n_{ij} = 0$, the cell is unoccupied. For an unoccupied cell, the transition probability p_{ij} for a particular cell is equal to the product of the static preference matrix M_{ij} (basic Blue and Alder transition), dynamic floor field value D_{ij} , and static floor field value S_{ij} multiplied by a normalization factor N to ensure that all of the probabilities sum to 1. The implementation algorithm proceeds according to Table 2.

Table 2 Basic Implementation Algorithm of a CA Model with Floor Field Interactions

Step	Action
1	Update dynamic floor field F according to diffusion and decay rules.
2	For each pedestrian, compute transition probabilities matrix p_{ij} using Equation 5.
3	For each pedestrian, determine target cells based on transition matrix probabilities.
4	Resolve conflicts between two or more pedestrians with same target cell.
5	Move pedestrians to new cells.
6	Alter dynamic floor field of cells previously occupied by pedestrians.

In a separate publication, Burstedde et al. [27] demonstrate the application of this model in simple evacuation scenarios and also demonstrate how their model improves on the previous CA models because they are able to reproduce collective behaviors such as lane formation in corridor counterflow situations and oscillations at entry ways. In 2002, Kirchner and Schadschneider [28] improved on the use of the CA model with floor field interactions in evacuation scenarios. First, when computing the transition probabilities p_{ij} , they removed the preference matrix M_{ij} from Equation 5 under the

assumption that pedestrians will not have a preferred direction at the beginning of an evacuation, therefore allowing the floor fields to determine direction of motion for the pedestrians as described in Equation 6. In addition, the level of contribution from each of the floor fields D_{ij} and S_{ij} is controlled through the use of two sensitivity parameters, k_D and k_S . The parameter k_S is coupled to the static field S and represents the knowledge the pedestrians have concerning the location of the exit. If k_S is large, pedestrians will follow the floor field to the closest exit; however, if k_S is small ($k_S \ll 1$), pedestrians will wander randomly and find the door by chance. The parameter k_D is coupled to the dynamic field D and represents the social influence tendency of the pedestrians. If k_D is large, pedestrians have a strong herding tendency and will follow the lead of others.

Equation 6 Transition Probability During Evacuations for CA Model with Floor Field Interactions [28]

$$p_{ij} = N e^{k_D D_{ij}} e^{k_S S_{ij}} (1 - n_{ij}) \xi_{ij}$$

with

occupation number: $n_{ij} = 0$ (empty) or 1 (occupied)

obstacle number: $\xi_{ij} = 0$ (forbidden cells) or 1 (else)

$$\text{normalization: } N = \left[\sum_{(i,j)} e^{k_D D_{ij}} e^{k_S S_{ij}} (1 - n_{ij}) \xi_{ij} \right]^{-1}$$

Expanding the CA model even farther, Kretz and Schreckenberg presented the Floor field- and Agent-based Simulation Tool (F.A.S.T.) in 2006 [29]–[31]. The F.A.S.T. model consists of three processes for each time step: 1) choose an exit, 2) choose a destination cell, and 3) move. At the beginning of each time step, each pedestrian i selects an exit E according to the probability formula shown in Equation 7.

Equation 7 Probability Pedestrian i Selects Exit E for F.A.S.T Model [29]–[31]

$$p_E^i = N \frac{1 + \delta_{iE} k_E(i)}{S(i, E)^2}$$

In Equation 7, δ_{iE} is a Boolean indicator describing the exit E selection history of pedestrian i . If pedestrian i chose exit E during the last timestep, $\delta_{iE} = 1$; otherwise, $\delta_{iE} = 0$. The parameter $k_E(i)$ models the persistence of pedestrian i to stick with exit E and the value $S(i, E)$ is the distance between exit E and the current position of pedestrian i . Following the selection of an exit, the second process is the selection of a destination cell. The destination cell is selected based on probabilities assigned to each cell in the neighborhood of a pedestrian (currently located at position (a, b)) according to Equation 8, where p_{xy}^X are partial probabilities based on the external influences on the pedestrian.

Equation 8 Probability Pedestrian i Selects Destination Cell (x, y) for F.A.S.T Model [29]–[31]

$$p = N p_{xy}^S p_{xy}^D p_{xy}^I p_{xy}^W p_{xy}^P$$

where

$$\begin{aligned} \text{influence of static floor field :} & \quad p_{xy}^S = e^{-k_S S_{xy}} \\ \text{influence of dynamic floor field :} & \quad p_{xy}^D = e^{k_D (D_x(x,y)(x-a) + D_y(x,y)(y-b))} \\ \text{influence of inertia effects :} & \quad p_{x_{t+1}y_{t+1}}^I = e^{k_I (v_{t+1} + v_t) \sin \frac{|\varphi|}{2}} \\ \text{influence of nearby walls :} & \quad p_{xy}^W = e^{-k_W W_{xy}} \\ \text{influence of nearby pedestrians :} & \quad p_{xy}^P = e^{-k_P N_p(x,y)} \end{aligned}$$

After all pedestrians have selected their destination cells, the pedestrians begin to move towards them. In [31], Kretz describes the various method that could potentially be used to move the pedestrians to their destination cells. Pedestrians could “jump” directly to their destination cell or move cell by cell in a more realistic manner. In addition, the order in which each pedestrian moves could be managed in a variety of ways. The order could be predetermined and constant for each timestep, predetermined and shifted during each timestep, partially randomized, or fully randomized. Most of the work by Kretz uses a fully randomized, cell by cell movement scheme.

The CA approach to pedestrian science has many advantages. First, it simplifies the computational complexity associated with the SFM by modeling complex scenarios with a simple set of behavioral rules. The use of these rule sets and the ability to define individual properties for each pedestrian allow for the inclusion of psychological attributes. With simple rules, the simulations are quick and the results provide detailed analysis on an individual level and reproduce many observed collective phenomena. On the other hand, the CA approach also has several disadvantages. Perhaps the biggest disadvantage of the CA model is the restrictions imposed by the underlying grid. Pedestrian movement is restricted to a cell by cell update scheme, thus establishing a predetermined set of possible velocities for each pedestrian and restricting freedom of movement to pre-determined directions. Since speed is typically defined by the grid, it may be difficult to adapt the model when pedestrians need to transition from normal behavior to a “hurried” behavior (as in emergency situations). A finer discretization may be used, but that would increase the computational demands potentially negating the

computational efficiency of the CA approach. In addition, the underlying grid presupposes a maximum density, making the study of high-density simulations using a CA model extremely unlikely.

2.1.3 Agent-based Microscopic Model

A third type of microscopic model, which also models pedestrians as heterogeneous individuals but attempts to also incorporate a realistic interactive decision-making process at a local level, is the Agent-Based Model (ABM). According to an editorial describing the current state of agent-based modeling by Batty in 2001 [32], ABMs are “structures in which the behavior of any agent or object is always a function of other objects in the system.” In contrast to the SFM or the CA model where the model itself controls pedestrian movement, in ABMs the agents are autonomous, able to gather environmental information and make independent movement decisions based upon their perceptions of the environment.

In 2001, Kukla et al. [33] introduced an autonomous ABM which used a set of pre-defined rules attached to each agent through the use of parameters. The pedestrians evaluate their current local situation at each step and make decisions based upon their specific rule set in order to traverse an area which is defined by a rectangular grid. All pedestrians have the same basic set of rules, but individual behavior varies based on the local environment and specific parameters assigned to each pedestrian, such as preferred gap size (PGS) and personal space measure (PSM). For example in the prototype described by Kukla et al., distance categories include “close”, “gap”, “aware”, and “far”; speed categories include “same” and “faster”; and direction categories include “same”,

“opposite”, and “different”. Further definition led to seven entity types: person moving in same direction and faster; person moving in same direction and slower; person moving in opposite direction; person moving in a different direction; environmental edge; blockage; and curb which could appear in three distance ranges (close, gap, and aware) on each of three possible travel lanes. These combinations led to more than 10,000 possible situations which could occur during one instance of the simulation, all of which had to be mapped to rule outputs consisting of a combination of four directions (left, straight, right, choice) and three speed choices (full, match, avoid). These specific rule sets (if A then do B) direct the movement of the individual agents.

The Centre for Advanced Spatial Analysis (CASA) in London has contributed much to the study of agent-based pedestrian modeling through a series of published working papers [34]–[36]. These papers include the development of STREETS [35], a mesoscopic ABM which will be described later (see section 2.3.3). In the 2003 publication [36], Batty demonstrates the use of random walks as a path finding technique within agent-based simulations. His model was calibrated against actual path information (trajectory mapping) and density values obtained through direct observation and video analysis. Batty et al. [37] describe the practical use of their ABM as a crowd control planning tool for the Notting Hill Carnival, Europe’s largest street festival, which attracts more than a million pedestrians annually.

In 2010, researchers at the University of North Carolina-Chapel Hill (Guy et al.) teamed with programmers at Intel Corporation [38] to present an ABM and simulation which used the principle of least effort (PLE) to generate the individual pedestrian

trajectories and collective crowd dynamics. The main idea in the PLE model is that a pedestrian will select a velocity which will minimize the expected effort to reach the goal. Guy et al. assumed that total effort is minimized if a pedestrian is able to walk at his/her preferred speed along the shortest path to the goal. The PLE objective function used to determine the optimal velocity \mathbf{v}_A^{new} from a previously determined set of permissible velocities PV_A for each agent A is shown in Equation 9. The first term represents the energy consumption per unit time, described in a book on gait analysis by Whittle [39], as $E = e_s + e_w|\mathbf{v}|^2$ where $e_s = 2.23$ and $e_w = 1.26$ represent the values for an average human. In their model, Guy et al. [38] describe e_s and e_w as per-agent constants, noting that $\sqrt{e_s/e_w} = \sqrt{2.23/1.26} = 1.33$ m/s, the average walking speed of humans, such that these constants describe the preferred velocity of the agents. The second term is based upon a corollary presented by Guy et al. where the minimum amount of effort expended by a pedestrian of mass m to traverse a path of length L is $2mL\sqrt{e_s e_w}$, where $L = |\mathbf{G}_A - \mathbf{p}_a - \tau\mathbf{v}_A^{new}|$ and \mathbf{G}_A is the goal of agent A , \mathbf{p}_a is the current position, and $\Delta t\mathbf{v}_A^{new}$ represents the next movement by agent A over a period of Δt seconds.

Equation 9 PLE Objective Function [38]

$$\min \Delta t(e_s + e_w|\mathbf{v}_A^{new}|^2) + 2|\mathbf{G}_A - \mathbf{p}_a - \Delta t\mathbf{v}_A^{new}|\sqrt{e_s e_w} \quad \text{where } \mathbf{v}_A^{new} \in PV_A$$

The components of the agent-based algorithm used by Guy et al. is shown in Figure 7. At each time step, a “goal selection” module determines the desired goal of

each agent. Then a “guiding path computation” module determines the path from each agent’s current position to their destination using a pre-computed roadmap. The “local collision avoidance” module returns the set of permissible velocities PV_A . The path information, set of permissible velocities, and Equation 9 are then used in the “velocity computation” module to determine the new velocity v_A^{new} for agent A . The model proposed by Guy et al. generates energy-efficient paths based on PLE and was shown to generate many of the pedestrian behaviors (congestion, arching at exits, lane formation, etc.) seen in the other microscopic models.

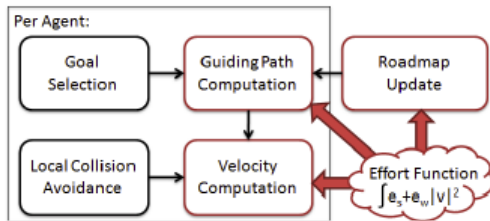


Figure 7 Multi-Agent Navigation Incorporating PLE (extracted from [38])

To avoid pedestrian-pedestrian collisions, Curtis and Manocha [40] use velocity obstacles (VO) and a local collision avoidance routine known as Optimal Reciprocal Collision Avoidance (ORCA). However, they found that the ORCA routine fails to reproduce the fundamental diagram; agent speeds remain constant regardless of density. To account for this deficiency, they use a behavior model to introduce behaviors consistent with the fundamental diagram into ORCA. The behavior model is based upon

a physiological constraint (Equation 10) due to stride length and a psychological constraint (Equation 11) due to an individual's desire to maintain a zone of privacy.

Equation 10 Physiological Constraint due to Natural Stride Length

$$L(v) = \frac{H}{\alpha} \sqrt{v}$$

Equation 11 Psychological Constraint due to Desired Privacy Space

$$B(v) = \beta L(v)$$

In Equation 10, H represents the normalized height of an individual ($H = h/1.72$ m), α represents the stride factor ($\alpha = 1.57$), and v represents the current walking speed of the pedestrian. Curtis and Manocha elect to use a quadratic relationship between stride length L and walking speed v , rather than the more common linear relationship. However, in order for the dimensions of Equation 10 to be correct, the velocity, as shown under the square root sign, must be normalized as well. A possible way of doing this is to divide the velocity by a typical velocity v_0 , where typical values of this constant may be $v_0 = 1.0$ m/s or $v_0 = 1.33$ m/s (Equation 12).

Equation 12 Physiological Constraint due to Natural Stride Length (corrected)

$$L(v) = \frac{H}{\alpha} \sqrt{\frac{v}{v_0}}$$

In Equation 11, the psychological constraint is simply a linear function of the physiological space constraint shown in Equation 12, controlled by the stride buffer parameter, β . Therefore, the space required for a pedestrian to move at a specified speed (as postulated by Curtis and Manocha) is shown in Equation 13 and its inverse, the natural speed for a given space is shown in Equation 14. These equations are used to modify the preferred speed of the agent; the agent will move at the natural speed for the perceived space available or at his/her desired velocity, whichever is less.

Equation 13 Space Required for Specified Speed v

$$S(v) = B(v) + L(v) = (1 + \beta) \frac{H}{\alpha} \sqrt{\frac{v}{v_0}}$$

Equation 14 Natural Speed for Available Space S

$$v(S) = \left(\frac{S \alpha}{H(1 + \beta)} \right)^2$$

In 2011, three University of North Carolina-Chapel Hill researchers (Curtis, Guy, and Manocha) teamed with a member of the Hajj Research Institute, Umm al-Qura University [41], to show how an ABM could simulate the Tawaf, an Islamic ritual performed by Muslims, by characterizing each agent with a physical state, a behavior state, and a scenario-specific property set. The researchers presented an ABM which instead used a Finite State Machine (FSM) coupled to a “reciprocal velocity obstacles”

(RVO) local collision avoidance algorithm to model the individual Tawaf-specific behaviors of the pedestrians (Figure 8).

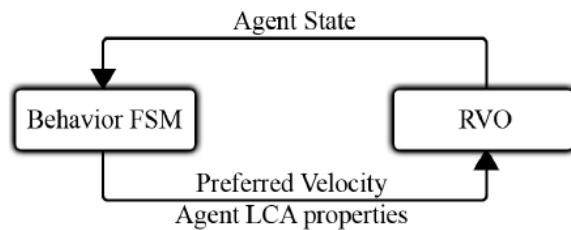


Figure 8 FSM and RVO Coupling (extracted from [41])

Each agent has a physical state (position, velocity, size, etc.), a behavior state (represented by the FSM), and a scenario driven property set. The FSM controls the agents' behavior transitions based upon spatial, property, temporal, or stochastic conditions. A spatial transition is triggered by the agent's location; a property transition occurs when the agent's property set meets a certain condition; a temporal transition begins when an agent meets (or exceeds) a pre-determined time-in-state; and a stochastic transition begins based upon a pre-defined probability distribution. This high-level FSM is coupled with a low-level local collision avoidance (LCA) algorithm to model pedestrian movement during the Tawaf as depicted in Figure 8.

Microscopic ABMs are models where decisions are driven by the current state of the individual pedestrian and his/her local environment; decisions are made at the local level and driven from the bottom-up. The agents typically have fairly complicated decision trees (rule sets) which define how to interact with obstacles and other pedestrians or they have rather complex collision-avoidance routines. It seems that a

pedestrian's will force, the desire to be at a specific place at a specific time, is taken into consideration but it does not have the dominating presence that it has in the SFM. Lastly, the collision-avoidance routines used in ABMs prevent contact, so it is impossible to determine inter-pedestrian contact forces which may be necessary for safety in high-density situations.

2.2 Pedestrian Literature: Macroscopic Models

At the macroscopic level, pedestrian science focuses mainly on the aggregate movement of large homogeneous crowds and high-level rational pedestrian behaviors such as overall trip planning. Researchers at this level make no distinction between individuals and look at the strategic behaviors of pedestrians as a collective whole rather than individual behaviors. That is, the behaviors of large groups with a common objective instead of individual pedestrians with differing intentions. At the macroscopic level of pedestrian behaviors, pedestrians collectively select their origin and destination, allocate time for their trip, and may even choose their desired path.

2.2.1 Gas-Kinetic Macroscopic Model

Pioneering macroscopic modeling in the 1970s, Henderson [42] demonstrated how some crowds (typically those that are less dense) could be modeled as an homogeneous crowd gas using Maxwell-Boltzmann theory to describe the motion of the crowd. From Henderson's perspective, crowds had three differing energy levels (standing still, walking, and running). He described a loosely packed crowd as a "crowd gas" and a densely packed crowd as a "crowd liquid". Henderson applied the Maxwell-Boltzmann equation to the gaseous crowd phase using the following assumptions: 1) the surface was

continuous at any time t in both position and velocity; 2) the crowd is homogeneous, therefore each particle has the same mass and probability of velocity; 3) particles could be composite (people walk in pairs and/or groups) or prime (single individuals); 4) regardless of composite or prime, the particles are statistically independent in position and velocity; 5) velocity is uncorrelated with position; and 6) the crowd is in equilibrium, therefore its statistical properties can be obtained. From Maxwell-Boltzmann statistical theory, Henderson presented probability density functions for velocity (Equation 15, Equation 16, and Equation 17) and speed (Equation 18).

Equation 15 Probability Density Function for Velocity (x-component) [42]

$$P(v_x) \equiv \frac{1}{N} \frac{dN_{v_x}}{dv_x} = \frac{1}{\sqrt{2\pi}v_{r.m.s.}} e^{-\frac{1}{2} \frac{v_x^2}{v_{r.m.s.}^2}}$$

where

$$v_{r.m.s.} = \sqrt{\frac{1}{2}(v_x^2 + v_y^2)}$$

Equation 16 Probability Density Function for Velocity (y-component) [42]

$$P(v_y) \equiv \frac{1}{N} \frac{dN_{v_y}}{dv_y} = \frac{1}{\sqrt{2\pi}v_{r.m.s.}} e^{-\frac{1}{2} \frac{v_y^2}{v_{r.m.s.}^2}}$$

Equation 17 Probability Density Function for Velocity (resultant) [42]

$$P(V) \equiv \frac{1}{N} \frac{dN_V}{dV} = \frac{1}{2\pi v_{r.m.s.}^2} e^{-\frac{1}{2} \frac{V^2}{v_{r.m.s.}^2}}$$

Equation 18 Probability Density Function for Speed [42]

$$P(|V|) \equiv \frac{1}{N} \frac{dN_v}{dv} = \frac{\pi v^2}{4 \bar{v}^2} e^{-\frac{\pi}{4} \frac{v^2}{\bar{v}^2}}$$

where

$$\bar{v} = \sqrt{\frac{\pi}{2}} v_{r.m.s.}$$

In order to allow for more sophisticated comparisons with observational crowd data, Henderson extended his work in 1974 [43] by identifying the circumstances which allow the conservation laws of mass, momentum, and kinetic energy, as shown in Equation 19, to be applied to the collective motion of pedestrians.

Equation 19 Henderson's Conservation Equations [43]

$$\text{Energy: } \frac{1}{2} m \sum_i \bar{n}_i V_i^2 = \text{constant}$$

$$\text{Momentum: } m \sum_i \bar{n}_i V_i \mathbf{V}_i = \text{constant}$$

$$\text{Mass and Particle Quantity: } m \sum_i n_i = \text{constant}$$

In Equation 19, \mathbf{V} is the pedestrian's velocity represented in polar coordinates (V, ϕ) and is assumed to be constant in magnitude and direction (at least for a short time). Based on the values of the velocity vectors, each pedestrian is then categorized into a speed class interval i which allows the construction of histograms and probability density functions. Therefore, the occupation number, \bar{n}_i , represents the average number of pedestrians in the i th speed class interval (V_i) and direction class interval (ϕ_i). According

to Henderson's model, the pedestrians (modeled as particles) exchange momenta and kinetic energies through a collision process. This leads to the equation of state shown in Equation 20, where P is pressure (defined as average force per unit length), $\bar{\rho}$ is the average pedestrian density, and \bar{v}^2 is the mean square of velocity fluctuations.

Equation 20 Henderson's Equation of State [43]

$$P = \bar{\rho} \frac{1}{2} m \bar{v}^2$$

Henderson next had to model the interaction between the different energy modes (standing still, walking, and running) and pedestrian density phases (loosely packed "gas", densely packed "liquid"). When more than one energy mode and/or density phase exists, the conservation equations shown in Equation 19 are not necessarily conserved which leads to a set of revised equations for flow in a variable channel of width l shown in Equation 21.

Equation 21 Henderson's Conservation Equations – Interactive Speed Modes and Density Phases [43]

$$\begin{aligned} \text{Energy:} \quad & E + m\bar{\rho}\bar{v}^2 + \frac{1}{2}m\bar{\rho}\bar{V}^2 = \text{constant} \\ \text{Momentum:} \quad & l\left(\frac{1}{2}m\bar{\rho}\bar{v}^2 + \frac{1}{2}m\bar{\rho}\bar{V}\bar{V}\right) = \text{constant} \\ \text{Mass and Particle Quantity:} \quad & m\bar{\rho}l\bar{V} = \text{constant} \end{aligned}$$

In the energy conservation equation given in Equation 21, E represents the stored energy in the system and Henderson likens it to potential energy. The second term in the

energy conservation equation is the sum of flow work and random kinetic energy, each contributing $\frac{1}{2}m\bar{\rho}\bar{v}'^2$ to the overall energy. The final term in the energy conservation equation is the convective kinetic energy. In the momentum conservation equation, the first term is the pressure generated by the motion of the crowd as given by the state equation (Equation 20) while the second term is the average momentum along the channel.

2.2.2 Fluid-dynamic Macroscopic Model

In the early 2000s, Hughes [44], [45] acknowledged that crowds are typically more often rational than irrational and referred to his fluid mechanic application to pedestrians as that of “thinking fluids” where crowd research focuses on the theoretical development of scientific rules governing collective pedestrian motion. Hughes [44] developed the governing equations shown in Equation 22 on the basis of three hypotheses. First, the speed of pedestrians is governed by the density of the surrounding pedestrians, their behavioral characteristics, and the ground. This means that speed is the product of the crowd speed $f(\rho)$ and direction of the motion $\hat{\phi}$. Second, Hughes hypothesized that pedestrians have a common view of the goal or task at hand (called potential ϕ) such that two individuals at different locations would see no reason to exchange places. Thus, motion is in the direction perpendicular to potential (unit gradient vector). Lastly, Hughes postulated that pedestrians wish to minimize travel time and, yet, avoid exposure to areas with extremely high densities. This means that the distance between potentials must be inversely proportional to the pedestrian speed $f(\rho)$. This

proportionality factor, denoted by $g(\rho)$, is a function of density and allows for discomfort at very high densities.

Equation 22 Governing Equations for Crowd Flow [45]

$$-\frac{\partial \rho}{\partial t} + \frac{\partial}{\partial x} \left(\rho g(\rho) f^2(\rho) \frac{\partial \varphi}{\partial x} \right) + \frac{\partial}{\partial y} \left(\rho g(\rho) f^2(\rho) \frac{\partial \varphi}{\partial y} \right) = 0$$

with

$$g(\rho) f(\rho) = \frac{1}{\sqrt{\left(\frac{\partial \varphi}{\partial x}\right)^2 + \left(\frac{\partial \varphi}{\partial y}\right)^2}}$$

In its most basic form, this hydrodynamic model introduced by Hughes is a coupled set of non-linear, hyperbolic, partial differential equations. The first partial differential equation (Equation 23) is the mass conservation equation with density $\rho(t, \mathbf{x}) \in \mathbb{R}^2$, velocity $\mathbf{v}(t, \mathbf{x}) \in \mathbb{R}^2$, and position $\mathbf{x}(t) \in \mathbb{R}^2$. For a detailed discussion on the development of this conservation of mass equation beginning from the definition of flux ($\mathbf{q} = \rho \mathbf{v}$), see Kachroo [46]. Similarly, to derive the momentum conservation equation (Equation 24), Kachroo begins with the definition of momentum ($\mathbf{p} = \rho \mathbf{v}$) and the definition of the flux for momentum ($\mathbf{p} \mathbf{v} = \rho \mathbf{v}^2$), applies Newton's second law where the force is equal to the product of pressure $\mathbf{P}(t, \mathbf{x}) \in \mathbb{R}^2$ and area.

Equation 23 Mass Conservation

$$\frac{\partial \rho}{\partial t} + \nabla \cdot (\rho \mathbf{v}) = 0$$

Equation 24 Momentum Conservation

$$\rho \left(\frac{\partial \mathbf{v}}{\partial t} + \mathbf{v} \cdot \nabla \mathbf{v} \right) = -\nabla P$$

Key to the utilization of these equations for pedestrian flows is the method chosen to model the flux (density-velocity relationship) and the method of computing the “pressure”. In his book, Kachroo [46] describes many of the models used to compute the flux density-velocity ($\mathbf{q} = \rho \mathbf{v}$) relationship. As an example, some of these models, where v_f is the unimpeded free-flow speed (speed when density is zero) and ρ_m is the maximum density (density where speed is zero), are described in Equation 25 and their corresponding density-velocity fundamental diagrams are shown in Figure 9.

Equation 25 Example Density-Velocity Models [46]

Greenshield Model: $V(\rho) = v_f \left(1 - \frac{\rho}{\rho_m} \right)$

Greenberg Model: $V(\rho) = v_f \ln \left(\frac{\rho_m}{\rho} \right)$

Underwood Model: $V(\rho) = v_f e^{-\frac{\rho}{\rho_m}}$

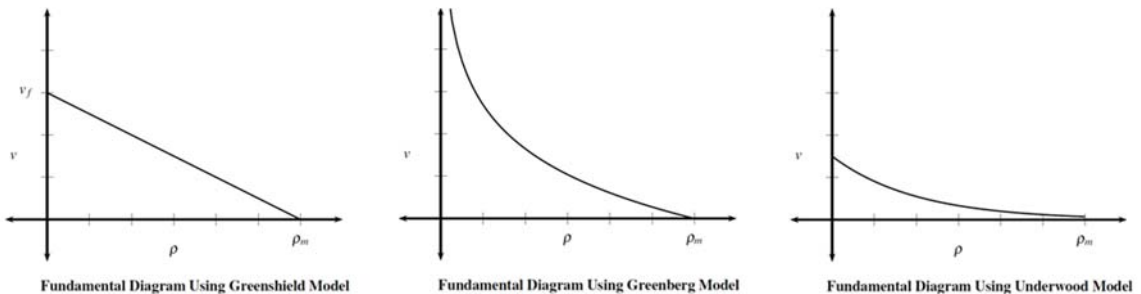


Figure 9 Example Fundamental Diagrams derived from Density-Velocity Models (extracted from [46])

Since the concept of pressure when dealing with crowds directly conflicts with crowd safety, the pressure term $\mathbf{P}(t, \mathbf{x})$ must be replaced; Kachroo describes three models (all of which were first proposed for use in vehicular traffic models): the Payne-Whitham (PW) model, the Aw and Rascle (AR) model, and the Zhang micro-to-macro model. The PW model, which was first proposed in the 1970s, replaces the pressure term shown in Equation 24 with a relaxation term P_τ , an anticipation term P_A which is the product of a coefficient and density, and a viscosity term P_V . The one-dimensional PW model, with corresponding definitions for the relaxation, anticipation, and viscosity terms, is shown in Equation 26.

Equation 26 One-Dimensional Payne-Whitham (PW) Model

$$\frac{\partial \rho}{\partial t} + \frac{\partial(\rho v)}{\partial x} = 0$$

$$\frac{\partial v}{\partial t} + v \frac{\partial v}{\partial x} = P_\tau - P_A + P_V$$

with

$$\text{relaxation term: } P_\tau = \frac{V(\rho) - v}{\tau}$$

$$\text{anticipation term: } P_A = \frac{1}{\rho} \frac{\partial A(\rho)}{\partial x} \quad \text{where } A(\rho) = c_0^2 \rho$$

$$\text{viscosity term: } P_V = \mu \frac{v \partial^2 v}{\rho \partial x^2}$$

In Equation 26, $V(\rho)$ is the chosen density-velocity model, τ is the relaxation time, c_0 is a constant, and μ is the constant coefficient of viscosity. The AR model, shown in Equation 27, was proposed in the early 2000s as an improvement to the PW

model, arguing that the “anticipation term” should be anisotropic, that is, directionally dependent based on the flow of traffic.

Equation 27 One-Dimensional Aw and Rascle (AR) Model

$$\frac{\partial \rho}{\partial t} + \frac{\partial(\rho v)}{\partial x} = 0$$

$$\frac{\partial v}{\partial t} + v \frac{\partial v}{\partial x} = P_\tau - P_A$$

with

$$\text{relaxation term: } P_\tau = \frac{V(\rho) - v}{\tau}$$

$$\text{anticipation term: } P_A = \frac{\partial A(\rho)}{\partial t} + \frac{\partial A(\rho)}{\partial x} \quad \text{where } A(\rho) = c_0^2 \rho^\gamma$$

The Zhang micro-to-macro model, proposed first in 1998, is very similar to the AR model; however, Zhang argued that the “anticipation term” is not constant and is actually density-dependent (Equation 28).

Equation 28 One-Dimensional Zhang Model

$$\frac{\partial \rho}{\partial t} + \frac{\partial(\rho v)}{\partial x} = 0$$

$$\frac{\partial v}{\partial t} + v \frac{\partial v}{\partial x} = P_\tau - P_A$$

with

$$\text{relaxation term: } P_\tau = \frac{V(\rho) - v}{\tau}$$

$$\text{anticipation term: } P_A = \rho V'(\rho) \frac{\partial v}{\partial x}$$

2.2.3 Advantages and Disadvantages of Macroscopic Models

Modeling pedestrian motion at the macroscopic scale has several advantages.

First, quantitatively it is possible to reproduce a realistic fundamental diagram without conducting detailed analysis on an individual level. Since pedestrian flow is typically characterized in aggregate quantities of density, velocity, and flow, using macroscopic modeling techniques is less computationally demanding. Macroscopic modeling is also well suited for the application of control theory and seems to be applicable when self-organizing behaviors such as herding occur, where such models may be used to predict collective evacuation times [46].

A key assumption of the macroscopic model is that the removal of individual pedestrian analysis has very little effect on the collective movement. However, individual evasive actions such as collision avoidance and deceleration do impact the overall collective movement patterns and such actions do not obey the laws of momentum and energy conservation [47]. There is no way to incorporate these individual behaviors in a purely macroscopic gas-kinetic or fluid-dynamic model. In addition, gases and fluids typically flow in one direction, whereas pedestrians often flow in opposing directions and cross paths at intersections. In response to these shortcomings, some mesoscopic models have been developed [48], [49] and will be discussed in section 2.3.

2.3 Pedestrian Literature: Mesoscopic Models

Mesoscopic pedestrian science bridges the gap between the macro- and microscopic scales. Researchers using a mesoscopic approach may use one of two typical methods. The first macro-to-microscopic method models the collective pedestrian behaviors among a crowd or large group while still considering and accounting for the

individual forces among the pedestrians. The second method is just the reverse; the micro-to-macroscopic method focuses on and models individual pedestrian behaviors while maintaining an aggregate view of the entire crowd [50].

2.3.1 Gas-Kinetic Mesoscopic Model

The most common mathematical formulation at the mesoscopic scale is a modified version of the Boltzmann-like gas-kinetic formulation. This formulation was popular in the 1960s and 1970s to represent vehicular traffic flow and was reenergized on a mesoscopic scale in the early 1990s by Helbing [48]. Helbing noted that the conservation of energy and momentum assumptions made by Henderson were unrealistic and instead, Helbing develops a “special theory for pedestrians” which incorporates terms that account for microscopic individual pedestrian desires and interactions into the macroscopic scale equations previously described for ordinary gases and fluids. Helbing groups pedestrians by their desired direction and velocity creating “coupled equations of several fluids”, where these equations include terms that account for a pedestrian’s tendency to change direction and avoid other pedestrians.

In 2000, Hoogendoorn and Bovy [49] presented a novel gas-kinetic model for pedestrian traffic flow. In its most basic form, the gas kinetic equation (Equation 29) describing the dynamics of pedestrian phase-space density (P-PSD) $\rho(t, \mathbf{x}, \mathbf{v}, w)$ is an accumulation of changes due to smooth processes (continuum) such as convection and acceleration and non-smooth processes (non-continuum) such as interactions between the pedestrians.

Equation 29 Pedestrian Gas-Kinetic Equation

$$\frac{\partial \rho}{\partial t} + \nabla_x \cdot (\rho \mathbf{v}) + \nabla_v \cdot (\rho \mathbf{A}) = \left(\frac{\partial \rho}{\partial t} \right)_{event}^+ + \left(\frac{\partial \rho}{\partial t} \right)_{event}^-$$

The continuum processes are on the left hand side of Equation 29. The second term on the left hand side of Equation 29, $\nabla_x \cdot (\rho \mathbf{v})$, represents the changes due to convection (that is, the balance of outflow versus inflow), where $\mathbf{v} = \frac{dx}{dt}$. The third term, $\nabla_v \cdot (\rho \mathbf{A})$, accounts for the change due to the desire to accelerate toward a desired (absolute) velocity w and move in a desired direction \mathbf{d} . Equation 30 shows the derivation of the acceleration term \mathbf{A} where $v_r = \|\mathbf{v}\|$, τ_r is the acceleration time and τ_α is the angle of movement adaptation time, $\cos \alpha = \frac{v_1}{v_r}$, and $\sin \alpha = \frac{v_2}{v_r}$.

Equation 30 Derivation of the Acceleration Term \mathbf{A} in Equation 29

$$A_1 = \frac{dv_1}{dt} = \frac{d}{dt} v_r \cos \alpha = \left(\frac{w - v_r}{\tau_r} \right) \cos \alpha - v_r \left(\frac{\alpha_0 - \alpha}{\tau_\alpha} \right) \sin \alpha$$

$$A_2 = \frac{dv_2}{dt} = \frac{d}{dt} v_r \sin \alpha = \left(\frac{w - v_r}{\tau_r} \right) \sin \alpha + v_r \left(\frac{\alpha_0 - \alpha}{\tau_\alpha} \right) \cos \alpha$$

where

$$\text{desired angle of movement: } \alpha_0 = \tan^{-1} \left(\frac{d_2 - x_2}{d_1 - x_1} \right)$$

$$\text{exponential acceleration laws: } \frac{dv_r}{dt} = \frac{w - v_r}{\tau_r} \quad \text{and} \quad \frac{d\alpha}{dt} = \frac{\alpha_0 - \alpha}{\tau_\alpha}$$

Terms reflecting the non-continuum processes, such as interactions due to dynamic events, are on the right hand side of Equation 29. The modified gas-kinetic equations described by Hoogendoorn and Bovy can serve as a macroscopic model by

applying the method of moments and applying an appropriate numerical scheme. Similarly, the gas-kinetic equations can be applied directly but this quickly leads to computational difficulties. To simplify the complexity involved when solving a high-dimensional system, Hoogendoorn and Bovy adopt a microscopic-like particle approach. Central to the approach is the idea that pedestrians are considered individually with desired destinations and velocities, but their behavior is described in aggregate terms over some locally determined domain. The interactions between pedestrians within the region is considered through aggregate terms such as density, average velocity, and velocity variance. This approach has several advantages. Individual descriptive behaviors due to pedestrian interaction, such as acceleration, deceleration, and change of direction, can be obtained without having to individually account for interactions and the discrete integration of each pedestrian through space and time. Updating of pedestrian locations and velocities can be accomplished through parallel computations, thus saving computational speed. Lastly, this type of model allows researchers to distinguish between different classes of pedestrians, categorized by pedestrian classes or pre-determined attributes.

2.3.2 Fluid-dynamic Mesoscopic Model

Another example of a mesoscopic model is the 2006 work by Treuille et al. [51] from the University of Washington. Their crowd model is based on continuum dynamics and extends the earlier macroscopic crowd dynamic work of Hughes [44], [45]. Specifically, the work by Treuille et al. adds a microscopic particle representation to the continuum work of Hughes. The University of Washington researchers used dynamic

potential fields to integrate global navigation and local collision avoidance into a single framework and added a discrete particle representation to enable crowd simulation. In practice, they discretized pedestrian movement in time and space where, at each time step, the crowd was converted to a density field, the average velocity field was created, then the potential field was dynamically created from the eikonal equation, the gradient was subsequently determined, and then the pedestrian locations were updated ensuring a minimum distance between pedestrians was maintained. The work by Treuille et al. is analogous to particle-particle particle-mesh methods (PPPM). Instead of solving Laplace's equation for the potential field, the eikonal equation is solved instead.

To compute the density field, the discretized grid structure such as the one shown in Figure 10 was used. For each pedestrian in the simulation, the cell center with coordinates less than the coordinates of the pedestrian in both the x and y directions was found and the relative position of the pedestrian $(\Delta x, \Delta y)$ was computed with respect to the cell center. Then a density contribution from pedestrian i was added to the grid as described in Equation 31 where λ is the density exponent and represents the speed of density falloff such that each pedestrian contributes at least $\bar{\rho}$ to their grid cell and no more than $\bar{\rho}$ to the neighboring cells where $\bar{\rho} = \left(\frac{1}{2}\right)^\lambda$.

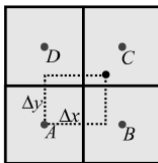


Figure 10 Example Discretized Grid Used to Compute Density Field (extracted from [51])

Equation 31 Density Contribution Equations for Pedestrian i

$$\begin{aligned}\rho_A^i &= \min(1 - \Delta x, 1 - \Delta y)^\lambda & \rho_B^i &= \min(\Delta x, 1 - \Delta y)^\lambda \\ \rho_C^i &= \min(\Delta x, \Delta y)^\lambda & \rho_D^i &= \min(1 - \Delta x, \Delta y)^\lambda\end{aligned}$$

After the crowd is converted to a density field, then a unit cost field C is constructed for each group. This cost field arises from some underlying assumptions made by the researchers that people choose the paths which minimize distance, time, and discomfort g according to Equation 32 where α , β , and γ are the weights for each respective term.

Equation 32 Path Objective Function

$$\min \alpha \int_P 1 ds + \beta \int_P 1 dt + \gamma \int_P g dt$$

If f represents the speed field, then the relationship between differential path length ds and dt is $ds = f dt$. Therefore, Equation 32 can be rewritten as shown in Equation 33 to clearly define the unit cost field C in terms of the weights (α , β , and γ), speed field f , and discomfort field g .

Equation 33 Path Objective Function w/Unit Cost Field C

$$\min \int_P C ds \quad \text{where} \quad C \equiv \frac{\alpha f + \beta + \gamma g}{f}$$

After the construction of the unit cost field C , the dynamic potential field ϕ (and $\nabla\phi$) was computed such that ϕ satisfies the eikonal equation: $\|\nabla\phi\| = C$. The velocity field \mathbf{v} was then computed from the normalized gradient and each pedestrian's position \mathbf{x} was updated by interpolating the velocity field and ensuring that a minimum distance between people was maintained.

An advantage of the model proposed by Treuille et al. is that it provides the macroscopic perspective in crowd dynamics while accounting for local collision avoidance between individual pedestrians. It seems that their implementation algorithm could be integrated with other microscopic models, such as ABMs. However, at the core of their model is the individual pedestrian's location and velocity, from which everything else is derived. The model never considers forces between pedestrians, nor does it include contact between pedestrians (a brute force "minimum closeness" algorithm prevents contact). Lastly, the underlying assumption that one's path choice depends only on path length, time to destination, and a desire to avoid discomfort may be too simplistic. All of the factors involved in modeling the forces involved in the SFM seem to indicate that the decision-making process is slightly more complex.

2.3.3 Agent-based Mesoscopic Model

In one of the very first working papers published by the Centre for Advanced Spatial Analysis (CASA), Batty [34] describes a mesoscopic ABM where the model is based upon the location, connectivity (geometric paths), and flows (in terms of volume) between agent origins and destinations. Origins are modeled as "nodes" in the system

from which pedestrians begin movement. Destinations, on the other hand, are not necessarily specific places, but modeled as “attraction surfaces” – areas of the geometry that are desirable for pedestrians, such as an exhibit inside a museum. In 1999, Schelhorn et al. [35] introduced STREETS, an agent-based mesoscopic model which utilizes several GIS datasets to generate the simulation environment. The environment consists of three process components: 1) the built environment which includes the building attributes as well as the street network and way points; 2) the agents with specified route plans based upon socio-economic factors; and 3) the movement environment which includes the underlying surface data for attractiveness and walkability (i.e., walking on a sidewalk is preferred to walking in the street). To model pedestrian movement, the agent process interacts with itself (pedestrian-pedestrian interactions) and interacts with the other two processes. This model was developed using SWARM, a software package developed by the Santa Fe Institute. Even though interactions between pedestrians are at the microscopic level, SWARM does not have the ability to provide microscopic detail such as the trajectories of pedestrians, group movements, behaviors at intersections, or individual pedestrian velocities. However, SWARM does have the ability to provide aggregate statistical information often seen at the macroscopic level such as density, flow, and overall patterns of movement.

2.4 Pedestrian Literature: Combined Models

It seems that the future of pedestrian modeling will require the coupling of the best attributes from each of the levels of pedestrian science. As the models become increasingly more sophisticated, researchers will attempt to develop combined methods

which assemble the separate models into all-encompassing realistic behaving (and looking) simulations.

One such researcher is Dr. Paul Torrens from the Geosimulation Research Laboratory at Arizona State University. In a January 2012 paper [52], Torrens simultaneously models micro-, meso-, and macro-level pedestrian behaviors using an ABM that incorporates geographical information and multiple theories behind pedestrian science. Torrens takes advantage of existing models for high-level trip and path planning and couples this with techniques to describe medium- and low-level behaviors. These medium level behaviors include vision (awareness of one's local surrounding), steering (reactive, interactive, and proactive behaviors), and collision avoidance. At the lowest-level Torrens models the kinematics of a pedestrian to make the agent locomotion look realistic. Torrens' comprehensive approach to pedestrian science not only encompasses every behavioral level, but also spans the past five decades of research efforts with more than 170 cited references.

3 LITERATURE SURVEY II: EVACUATION DYNAMICS

Within pedestrian science, the study of pedestrian response to emergency situations encompasses a multitude of research areas and disciplines and is commonly referred to collectively as the study of “evacuation dynamics”. Evacuation dynamics is an extremely important and interesting research topic, at the intersection of psychology and sociology, mechanics and kinematics, mathematical modeling and analysis, numerical methods, parallel computing, visualization, and data collection. The mathematical models and techniques behind pedestrian science described in the first literature survey represent the collection of mathematical tools most often used in computer simulations to model the evacuation process. The computer-aided study of evacuation processes is most often used for optimization (evacuate efficiently as possible), simulation (realistic representation of behaviors and movement), or risk assessment (identify hazards and quantify risk) [14].

3.1 Evacuation Modeling Software Reviews

In 1999, Gwynne et al. [53] published a review of methodologies used in computer evacuation simulations. They noted that computer simulations could be useful in understanding how the “system” (defined as a particular building, occupancy level, and scenario) might behave given a set of pre-defined conditions. At the time when Gwynne et al. published their paper in 1999, there were 22 different evacuation models of which

16 were currently in use and 6 were still in development. To categorize the models, Gwynne et al. evaluated their primary purpose (simulation, optimization, risk assessment); their geometric description of the domain (fine network, coarse network); the perspective of the population (global, individual); and the behavioral perspective (none, functional analogy, implicit, rule based, and artificial intelligence) and categorized each of the 16 models as shown in Figure 11. In conclusion, Gwynne et al. highlight the necessity of understanding the governing principles in a computer evacuation model prior to using the model in applications.

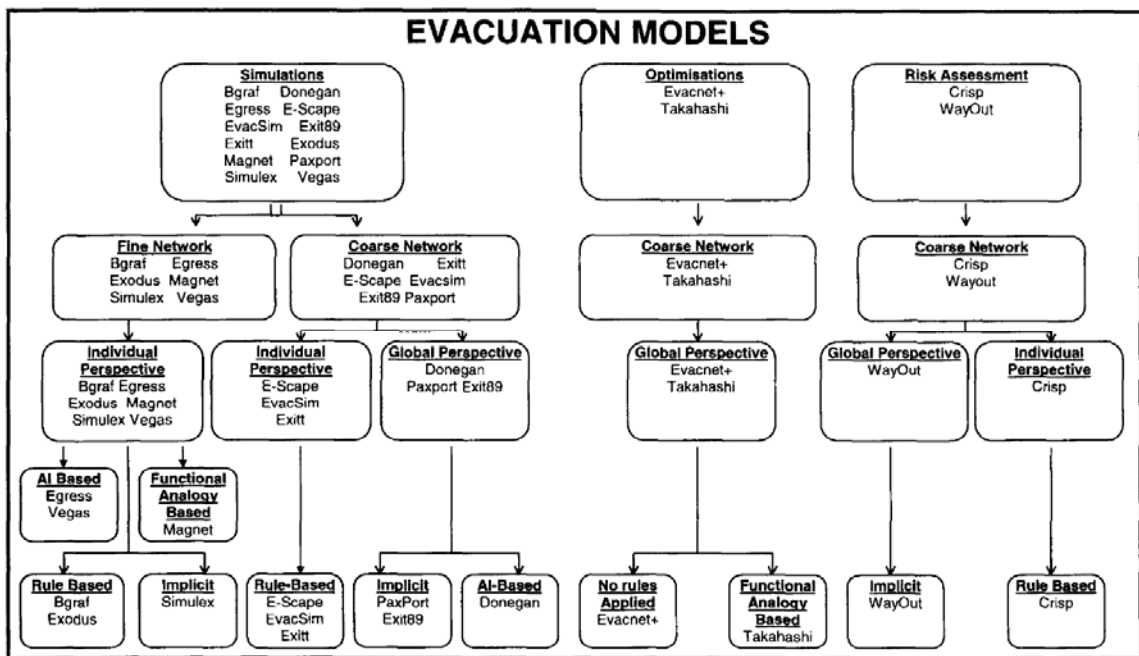


Figure 11 Evacuation Models (circa 1999) Classified According to Methodology (extracted from [53])

However, following the events of September 11th, 2001, the simulation of emergency evacuations grew at an exceptional rate. In July 2005, Kuligowski and

Peacock [54] published a review of building evacuation models for the United States' National Institute of Standards and Technology (NIST). In their review, Kuligowski and Peacock expand the descriptions of the models previously categorized by Gwynne et al. in 1999, provide additional information on newly developed evacuation models, and describe the mathematics behind each model. The purpose of their paper was to provide a set of evaluation criteria and software descriptions to aid users in the selection of an appropriate evacuation model for a specific project. In all, Kuligowski and Peacock reviewed 30 models, grouped in Figure 12 by their method of availability (from top to bottom): available to the public, on a consultancy basis, not yet released, no longer in use, and unknown.

Model	Available to public	Modeling Method	Purpose	Grid/ Structure	Perspective of M/O	Behavior	Movement	Fire data	CAD	Visual	Valid
FPETool	Y	M	1	N/A	G	N	UC	N	N	N	N
EVACNET4	Y	M-O	1	C	G	N	UC	N	N	N	FD
TIMTEX	Y	M	4	C	G/I	N	D	N	N	N	PE
WAYOUT	Y	M	5	C	G	N	D	N	N	N	2-D FD
STEPS	Y	M/PB	1	F	I	N/I	P, E	N	Y	3-D	C
PedGo	Y	M/PB	1	F	I	I	P, E (CA)	N	Y	2-D	FD
PED/PAX	Y/N3	PB	3	C	G	I	D	N	Y	2,3-D	N
Simulux	Y	PB	1	Co.	I	I	ID	N	Y	2-D	FD, PE
GridFlow	Y	PB	1	Co.	I	I	D	N	Y	2,3-D	FD, PE
ASERI	Y	B-RA	1	Co.	I	R/C, P	ID	Y1.2	N, F	2,3-D	FD
BldEXO	Y	B	1	F	I	R/C, P	P, E	Y1.2	Y	2,3-D	FD
EXITT	Y	B	2	C	I	R/C	C	Y1.2	N	2-D	N
Legion	Y	B	1	Co.	I	AI	D, C	Y2	Y	2,3-D	FD, OM
PathFinder	N1	M	1	F	I/G	N	D	N	Y	2-D	N
EESCAPE	N1	M	5	C	G	N	D	N	N	N	FD
Myriad	N1	M	1	N/A	I	N	D	N	Y	2-D	3P
ALLSAFE	N1	PB	5	C	G	I	Un.F	Y1.2	N	2-D	OM
CRISP	N1	B-RA	1	F	I	R/C, P	E, D	Y3	Y	2,3-D	FD
EGRESS 2002	N1	B	1	F	I	R/C, P	P, D (CA)	Y2	N	2-D	FD
SGEM	N2	M/PB	1	F	I	N/I	E, D (CA)	N	Y	2-D	FD, OM
Egress Complexity	N2	M/PB	5	C	G/I	N	Ac K, FA	N	N	N	OM
EXIT89	N2	PB	1	C	I	I/C(smK)	D	Y1	N	N	FD
BGRAF	N2	B	1	F	I	R/C, P	UC?	Y1.2	N, F	2-D?	FD
EvacSim	N2	B	1	F	I	R/C, P	D	Y2	N	N	N
Takahashi's Fluid	N3	M-O	1	C	G	N	FA-D	N	N	2-D	FD
EgressPro	N3	M	5	C	G	N	D	Y2	N	N	N
BFIRES- 2	N3/U	B-RA	4	F	I	R/C, P	UC	Y2	N	N	N
VEgAS	N3/U	B	1	F	I	AI	ID	Y1?	Y	3-D	N
Magnetic Model	U	M	1	F	I	I	FA	N	N	2-D	N
E-SCAPE	U	B	1	C	I	R/C, P	OML	Y2	N	2-D	N

? indicates that a category is unclear or unknown

Figure 12 Evacuation Models (circa 2005) Classified According to Main Features (extracted from [54])

In 2010, Kuligowski et al. published another NIST technical report [55] reviewing building evacuation models as an update to their 2005 publication. In this review, Kuligowski et al. provide updated information (where applicable) to 16 of the models described in the 2005 report and provide additional information on 10 newly developed models. If a model contained in the 2005 report had no significant change in the period between the two reviews, Kuligowski et al. refer the reader to the original 2005 report. In all, Kuligowski and Peacock reviewed 26 models, grouped in Figure 13 by their method of availability (from top to bottom): available to the public, on a consultancy basis, and not yet released.

Model	Available to public	Modeling Method	Purpose	Grid/ Structure	Perspective of M/O	Behavior ^a	Movement ^a	Fire data	CAD	Visual	Valid
EVACNET4	Y	M-O	1	C	G	N	UC	N	N	N	FD
WAYOUT	Y	M	5	C	G	N	D	N	N	2-D	FD
STEPS ^c	Y	B	1	F	I	C, P	P, E	Y1,2	Y	2,3-D	C,FD,PE
PEDROUTE	Y	PB	3	C	G	I	D	N	Y	2,3-D	N
Simulex ^b	Y	PB	1	Co.	I	I	ID	N	Y	2-D	FD,PE, 3P
GridFlow	Y	PB	1	Co.	I	I	D	N	Y	2,3-D	FD, PE
FDS+Evac ^c	Y	PB	1	Co.	I	I, C, P	ID	Y3	N/Y	2,3-D	FD,PE,OM
Pathfinder 2009 ^c	Y	PB	1	Co.	I/G	I	D, ID	N	Y	2,3-D	C,FD,PE,OM
SimWalk ^c	Y	PB	1,3	Co.	I	C, P	P	N	Y	2,3-D	FD,PE,3P
PEDFLOW ^c	Y	B	1	Co.	I	C, P	ID	Y2	Y	2,3-D	PE
PedGo ^c	Y,N1	PB/B	1	F	I/G	I/C, P	P,E (CA), C	Y2	Y	2,3-D	FD,PE,OM,3P
ASERF ^c	Y	B-RA	1	Co.	I	C, P	ID	Y1,2	Y	2,3-D	FD, PE
BldEXO ^b	Y	B	1	F	I	C, P	P, E	Y1,2	Y	2,3-D	FD,PE,OM,3P
Legion ^c	Y,N1	B	1	Co.	I	AI, P	ID, C	Y1	Y	2,3-D	C,FD,PE,3P
SpaceSensor ^c	Y	B	3	Co.	I	C, P	C, Ac_K	N	Y	2,3-D	FD,OM
EPT ^c	Y,N1	B	1	F	I	AI	UC,C	Y2	Y	2,3-D	FD
Myriad II ^c	Y, N1	B	1	C, F, Co.	I	AI	D, UC, IP, Ac_K	Y1	Y	2,3-D	PE, 3P
MassMotion ^c	Y, N1	B	1	Co.	I/G	AI,P	C	N	Y	2,3-D	C,FD,PE,OM
PathFinder	N1	M	1	F	I/G	N	D	N	Y	2-D	N
ALLSAFE	N1	PB	5	C	G	I	Un_F	Y1,2	N	2-D	OM
CRISP	N1	B-RA	1	F	I	C, P	E,D	Y3	Y	2,3-D	FD
EGRESS 2002	N1	B	1	F	I	C, P	P,D (CA)	Y2	N	2-D	FD
SGEM ^c	N1	PB	1	Co.	I	I	D	N	Y	2-D	FD,OM
EXIT89 ^c	N2	PB	1	C	I	I/C, P	D	Y1	N	N	FD,3P
MASSEgress ^b	N2	B	1	Co.	I	C, AI	C	N	Y	2,3-D	PE,OM
EvacuatioNZ ^c	N2	B	1	C	I/G	I, C, P	D, UC	Y2	Y	2-D	FD, PE,OM

^aOnly the underlying methods used by the algorithm are listed. In some instances users can define other options

^bModel developers/NIST provided an update on the model's development in Spring 2009.

^cModel developers/NIST provided an update on the model's development in Fall 2010.

Figure 13 Evacuation Models (circa 2010) Classified According to Main Features (extracted from [55])

Combining the two NIST technical reports, Kuligowski et al. have provided detailed descriptions and analysis for a total of 40 past, present, and future evacuation models. As is abundantly clear from the published reviews, evacuation modeling is an extremely relevant field of study and new evacuation models are being developed and introduced at a high rate. To aid in research collaboration and keep pace with the current state of evacuation modeling, the EvacMod.net [56] portal was created. The portal is dedicated to the simulation of human behavior during emergency situations and is available to anyone with an interest in this area of pedestrian science. The methodologies and the criteria used by Kuligowski et al. in their NIST technical reports have been adopted by EvacMod.net as a way to evaluate the numerous evacuation simulation tools that are currently available. EvacMod.net maintains a current listing of available evacuation models and, as of March 2016, 64 models were listed there.

3.2 Pre-Evacuation Phase: Modeling Using Distributions

In the case of an emergency situation, subsequent individual actions can be divided between two phases: a decision-making phase and post-decision action phase. During the decision-making phase, an individual must recognize the emergency, evaluate the situation, and make a deliberate decision as to the appropriate action to take. Once the decision is made, the post-decision phase commences and the individual carries out the specified action. For example in an evacuation scenario, if an individual determines during the decision-making phase that the appropriate action to take is to evacuate the area (or building), then the post-decision phase begins when the individual starts movement. In 1999, MacLennan et al. [57] provided an accident sequence model (Figure

14) which clearly delineates the steps involved in an emergency scenario. In Figure 14, the decision-making phase would consist of the perception, cognition, and decision steps. The figure also clearly shows that failure to perform any of these steps leads to a probabilistic opportunity for an accident to occur.

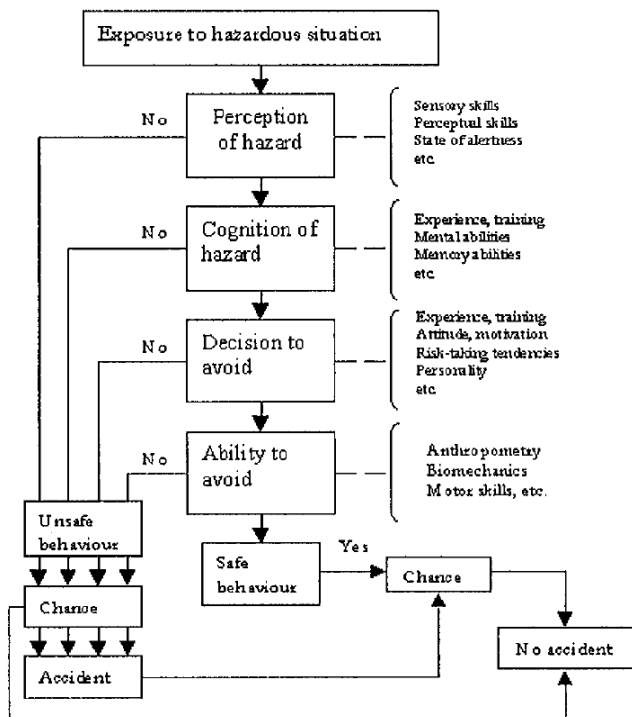


Figure 14 Accident Sequence Model (extracted from [57])

In evacuation dynamics, the decision-making phase is typically modeled using a pre-evacuation “delay” and the post-decision phase is modeled through evacuation simulations. During their assessment of the evacuation models, Kuligowski et al. [55] assessed each model’s ability to account for the pre-evacuation delay period. As depicted

in Figure 15, 23 of the 26 models assessed in 2010 had the ability to somehow account for the pre-evacuation phase.

<i>Model</i>	<i>Counter-flow</i>	<i>Exit Block</i>	<i>Fire Conditions</i>	<i>Toxicity</i>	<i>Groups</i>	<i>Disabled / slower</i>	<i>Delays/pre-evacuation</i>	<i>Elevator use</i>	<i>Route choice</i>
EVACNET4	N	N	N	N	N	N	N	Y	Optimal routes
WAYOUT	N	N	N	N	N	N	Y	N	1 route, flows merge
STEPS ^c	Y	Y	Y	Y	Y	Y	Y	Y	Conditional
PEDROUTE	N	N	N	N	Y	Y	Y	N	Shortest, optimal, or signage
Simlex ^b	Y	Y	N	N	Y	Y	Y	N	Shortest or altered distance map
GridFlow	Y	Y	N	Y	N	Y	Y	N	Shortest, random, user-def.
FDS+Evac ^c	Y	Y	Y	Y	N	Y	Y	N	Optimal, conditional
Pathfinder 2009 ^c	Y	Y	N	N	Y	Y	Y	N	Shortest, user-def.
SimWalk ^c	Y	N	N	N	Y	Y	Y	Y	Shortest
PEDFLOW ^c	Y	Y	Y	Y	Y	Y	Y	Y	Shortest, conditional
PedGo ^c	Y	Y	Y	N	Y	Y	Y	N	Probabilistic/conditional, user-def.
ASERJ ^c	Y	Y	Y	Y	Y	Y	Y	N	Shortest, user-def., conditional
BldEXO ^b	Y	Y	Y	Y	Y	Y	Y	N	Various
Legion ^c	Y	Y	Y	Y	Y	Y	Y	Y	Conditional
SpaceSensor ^c	N	Y	N	N	N	N	N	Y	Conditional – visual perception
EPT ^c	Y	Y	Y	Y	Y	Y	Y	Y	Shortest, conditional
Myriad II ^c	Y	Y	Y	Y	Y	Y	Y	Y	Various
MassMotion ^c	Y	Y	Y	N	Y	Y	Y	Y	Shortest, conditional
PathFinder	N	N	N	N	N	N	N	N	User's choice – 2 choices
ALLSAFE	N	N	Y	N	Y	N	Y	N	1-Choice
CRISP	Y	Y	Y	Y	Y	Y	Y	N	Shortest, user-def., conditional
EGRESS 2002	Y	Y	Y	Y	Y	Y	Y	N	Conditional
SGEM ^c	Y	Y	N	N	N	Y	Y	Y	Shortest time, conditional
EXIT89 ^c	Y	Y	Y	Y	N	Y	Y	N	Shortest distance, user-def.
MASSEgress ^b	Y	Y	N	N	Y	Y	Y	N	Conditional – visual perception
EvacuationNZ ^c	N	Y	Y	N	Y	Y	Y	N	Various

^bModel developers/NIST provided an update on the model's development in Spring 2009.

^cModel developers/NIST provided an update on the model's development in Fall 2010.

Figure 15 Evacuation Models (circa 2010) Classified According to Special Features (extracted from [55])

In 2012, Gwynne et al. [58] identified five core performance components of evacuation simulations: 1) pre-evacuation time, 2) travel speeds, 3) route usage/choice, 4) route availability, and 5) flow conditions/constraints. Gwynne et al. describe the most common methods to incorporate the pre-evacuation time component into an evacuation simulation and the effect on overall evacuee response (Figure 16). Two hypothetical settings include the instantaneous setting (no evacuee delay) and the distributed setting (evacuation begins over a period of time). In addition, pre-evacuation times could be

explicitly estimated from empirical data. Lastly, the evacuation could be initiated according to a specified procedure or according to external conditions from the environment.

Core performance component	Example component setting	Considerations for evacuee response given a component setting
Pre-evacuation times	Instantaneous (hypothetical)	No delay
	Distributed (hypothetical)	Evacuation begins over a period of time
	Estimated	Estimated response from comparable empirical data
	According to procedure	Evacuation starts according to the procedure assumed during the scenario
	According to external conditions	Start time derived from the external environmental/structural/social conditions faced

Figure 16 Description of Pre-evacuation Times Performance Component (extracted from [58])

Currently, the most common method of accounting for the pre-evacuation period is the establishment of a (hypothetical) time delay; a period of time that occupants will wait before initiating movement. Typically, this information is a user-provided input to the simulation, a discrete value or modeled using distributions obtained from direct measurements. In their 1999 paper, MacLennan et al. [57] evaluated numerous probability distributions of pre-evacuation times, noting that the Weibull distribution may be the most suitable.

In 2005, Lord et al. published a NIST Grant/Contract Report (GCR) [59] intended to serve as a guide to evaluate the predictive abilities of computer evacuation models. In Appendix B, they provided a summary of evacuation-related data discovered through an

extensive literature search. Among the data provided was consolidated pre-evacuation distributions for office buildings (Figure 17) and apartment buildings (Figure 18).

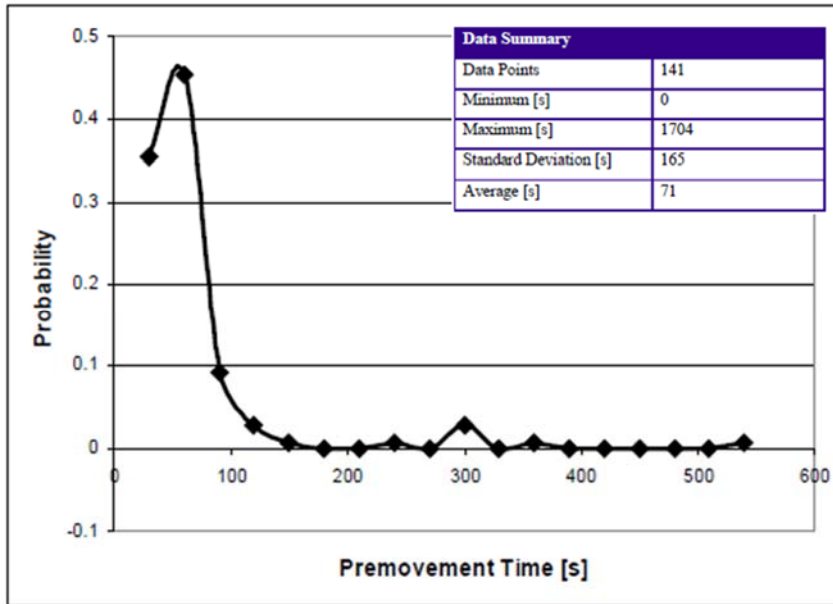


Figure 17 Distribution of Office Building Pre-evacuation Times (extracted from [59])

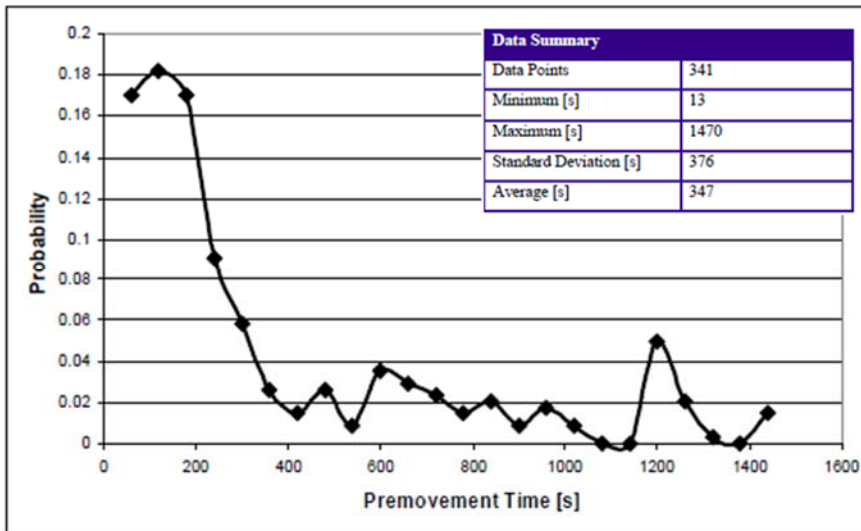


Figure 18 Distribution of Apartment Building Pre-evacuation Times (extracted from [59])

A comparison of Figure 17 and Figure 18 highlights one of the unique aspects of evacuation modeling. The type of building being evacuated impacts the amount of time occupants take to start evacuation. As seen from Figure 17 and Figure 18, the average pre-evacuation delay in office buildings was 71 seconds whereas the average evacuation time seen in apartment buildings was 347 seconds, almost five times greater. Research has shown that an analysis of occupant type and their pre-evacuation activities can help account for the differences seen in pre-evacuation delay times. A more thorough description of the reasons for these differences in evacuation delay will be discussed further in section 5.2.

In 2004, Spearpoint [60] examined how distributions of pre-evacuation times affect the movement phase during computer simulated evacuations. He concludes that if the average pre-evacuation time is small then pedestrian movement and queuing dominate the overall evacuation time; however, if the mean pre-evacuation time is large then the pre-evacuation distribution dictates the overall evacuation time.

3.3 Pre-Evacuation Phase: Modeling Using Decision Models

Rather than requiring the user to input hypothetical or estimated values (or distributions) for the pre-evacuation phase, researchers have started to look for more dynamic ways to model the pre-evacuation phase. The implementation of a procedure-based or scenario-driven routine would allow the simulation to determine the time required for the pre-evacuation phase. The length and sequence of events during the pre-evacuation phase may have a significant impact on the movement phase. In early 2013, Reneke [61] developed the Evacuation Decision Model (EDM) which addresses how

occupants make decisions to evacuate. Specifically, the EDM incorporates many of the physical, social, and psychological factors identified in Kuligowski's [62] qualitative model of pre-movement evacuation behaviors.

The purpose of Reneke's EDM is to predict the amount of decision-making time required by each individual in an evacuation simulation. It is based upon each individual's perception of risk, which in turn determines an individual's subsequent actions. Reneke assumes that individuals have three states: normal, investigating, and evacuating. The time an individual spends in the normal and investigating states determines the overall amount of time in the pre-evacuation phase.

The basic risk perception model, shown in Equation 34, describes an individual's change in risk perception as a differential equation, modeled as $\dot{R}_i(t)$. The change in risk perception is proportional to an individual's current level of risk perception $R_i(t)$. Reneke chooses to use the impact of a constant continuous cue, given as A_i , as the constant of proportionality. A continuously sounding alarm would be one example of a constant continuous cue as defined by Reneke.

Equation 34 Basic Risk Perception Model

$$\dot{R}_i(t) = A_i R_i(t)$$

Expanding the basic model, Reneke makes several assumptions which govern an individual's change in risk perception. First, Reneke assumes that an individual's change in risk perception is proportional to the environmental cues (alarm, smoke, etc.) and the

agent's current level of perceived risk. Second, he assumes that an individual's past experiences can increase or decrease the rate of change in risk perception (modeled as a prior knowledge). Lastly, he assumes that the observed state of other agents can increase or reduce the risk perception of an agent (modeled as a social influence).

Equation 35 Complete Risk Perception Model

$$\dot{R}_i(t) = \begin{cases} A_{I,i} \left(\left\{ \begin{matrix} environ \\ cues \end{matrix} \right\} + \left\{ \begin{matrix} prior \\ knowledge \end{matrix} \right\} + \left\{ \begin{matrix} social \\ influence \end{matrix} \right\} \right) R_i(t) & R_i(t) < R_I \\ A_{E,i} \left(\left\{ \begin{matrix} environ \\ cues \end{matrix} \right\} + \left\{ \begin{matrix} prior \\ knowledge \end{matrix} \right\} + \left\{ \begin{matrix} social \\ influence \end{matrix} \right\} \right) R_i(t) & R_I \leq R_i(t) < R_E \end{cases}$$

where

investigating state proportionality constant: $A_{I,i} = \frac{\ln R_I}{t_{I,i}}$

evacuating state proportionality constant: $A_{E,i} = \frac{\ln C_E}{\Delta t_{E,i}}$

Equation 35 describes Reneke's complete risk perception model in general terms where R_I and R_E represent the risk perception levels (on a Likert scale) required for an individual to transition from the normal state to the investigating state (R_I) and from the investigating state to the evacuating state (R_E). Any appropriate Likert scale could be used to describe the risk perception levels. For example, Reneke describes a scale from 1 to 7 where 1 represents "no risk" and 7 represents "about to die." A more thorough description, implementation, and analysis of Reneke's model (for a single continuous alarm) will be provided in Chapter 4.

4 EVACUATION DECISION MODEL SINGLE ALARM IMPLEMENTATION

Incorporating pre-movement pedestrian behaviors such as event detection, denial, deliberation, and/or reaction into pre-existing evacuation simulations serves two purposes. First, the implementation of a pre-movement model avoids the typical practice of user-assigned input and instead allows the model to predict the time required for the pre-movement phase. Secondly, pre-evacuation behaviors may have a significant impact on the movement phase and a pre-evacuation model would demonstrate the impact of these behaviors on the subsequent movement phase. One dynamic, recently developed method to simulate pre-evacuation delay is Reneke's Evacuation Decision Model (EDM) [61]. The EDM addresses how occupants make decisions to evacuate and, in theory, attempts to incorporate many of the physical, social, and psychological factors identified by Kuligowski [62]. This section describes a single continuous alarm implementation of the EDM as a sub-model to a pre-existing CA evacuation model.

4.1 Basic Model

In its most basic form, the EDM collects environmental information from the perspective of each pedestrian, determines the current level of risk perception using a Likert scale, and selects an appropriate action. The Likert scale suggested by Reneke [61] is a scale from 1 to 7 "with 1 representing no risk and 7 representing about to die". As the risk perception level changes, pedestrians will transition through three states: a normal

behavioral state at the lower end of the Likert scale, an investigating behavioral state in the middle of the Likert scale, and an evacuation behavioral state towards the upper end of the Likert scale. Therefore, it is important to define two values, R_I and R_E , at which point the pedestrian state changes from normal to investigating and from investigating to evacuating, respectively.

If $R_i(t)$ describes the level of risk perception of pedestrian i at time t , then the change in risk perception can be computed using an ODE solver according to the formula shown in Equation 36 where $t_{I,i}$ is the point in time where pedestrian i reaches the investigating state with only a single alarm and $\Delta t_{E,i}$ is the change in time between pedestrian i 's entrance in the evacuating state and entrance in the investigating state, that is $\Delta t_{E,i} = t_{E,i} - t_{I,i}$. The values of $t_{I,i}$ and $\Delta t_{E,i}$ for each pedestrian are user-assigned EDM inputs.

Equation 36 Basic Risk Perception Model (Single Continuous Alarm)

$$\dot{R}_i(t) = \begin{cases} \frac{\ln R_I}{t_{I,i}} (1) R_i(t) & R_i(t) < R_I & \text{(normal state)} \\ \frac{\ln C_E}{\Delta t_{E,i}} (1) R_i(t) & R_I \leq R_i(t) < R_E = C_E R_I & \text{(investigating state)} \end{cases}$$

As described by Reneke, risk perception attributed to a single continuous alarm is represented by an exponential growth model and implementation of this model using the formula shown in Equation 36 may seem trivial, but it is important to understand the nuances of this basic model (and its impact on the pre-movement phase) before

incorporating other social or psychological factors. For example, suppose in this model the point on the Likert scale where the transition to the investigating state occurs is defined as $R_I = 2.0$ and the transition to evacuating state as $R_E = 5.0$. Furthermore, assume pedestrian i takes 6 seconds to begin investigating following an alarm ($t_{I,i} = 6.0$) and does not change behavior once in the investigating state, then pedestrian i 's risk perception curve is shown as the blue line in Figure 19 and calculations show that pedestrian i spends 7.93 seconds in the investigating state before transitioning to the evacuating state. However, if the user defines the parameters such that pedestrian i will spend no more than 4 seconds investigating (perhaps due to an increased sense of awareness) before deciding to evacuate such that $\Delta t_{E,i} = 4.0$ seconds, then pedestrian i 's risk perception curve is sharper during the investigation phase as illustrated by the green line in Figure 19.

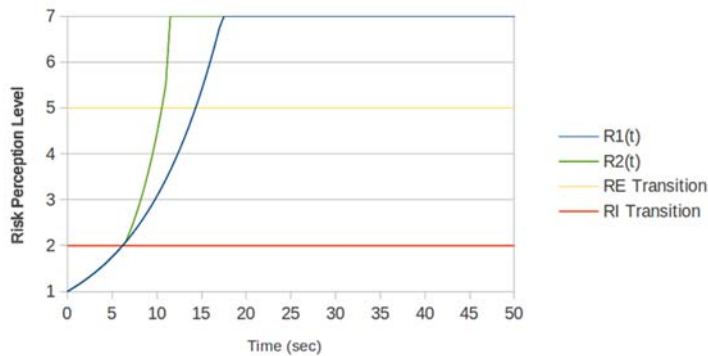


Figure 19 Risk Perception Curve (Single Pedestrian)

In the absence of prior knowledge or social influence, risk perception levels depend only on the global model inputs for R_I and R_E , and individual pedestrian user-

assigned values for $t_{I,i}$ and $\Delta t_{E,i}$. However, it can be argued that due to the increased sense of awareness in the investigating state, the value of $\Delta t_{E,i}$ must be less than or equal to the “no awareness (or change in behavior) during the investigating state” value which can be computed analytically as a function of $t_{I,i}$ using Equation 37.

Equation 37 Maximum Value of $\Delta t_{E,i}$ for Pedestrian i

$$\Delta t_{E,i,MAX} = \frac{\ln C_E}{\ln R_I} t_{I,i}$$

In order to demonstrate the implementation of this time-dependent basic EDM in a pre-existing CA evacuation simulation, 50 pedestrians were randomly dispersed in a 16 meter by 16 meter square room with a single exit. Each pedestrian inside the room was randomly assigned one of three initial activity choices (exiting the room, standing still, or wandering randomly about the room) as shown in Figure 20.

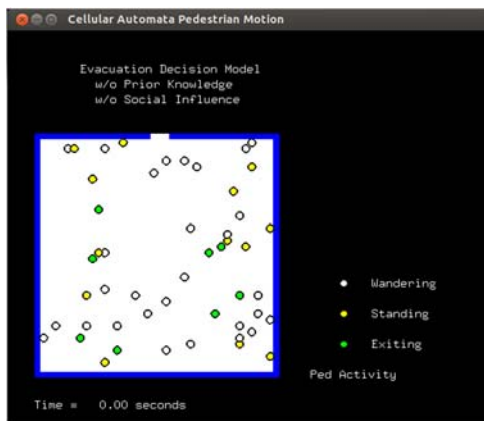


Figure 20 Pedestrian Initial Locations and Activities within Room

The following values were used with the basic EDM: $R_I = 2.0$, $R_E = 5.0$, $t_{l,i} = 15 \pm 5$ s, and $\Delta t_{E,i}(t_{l,i}) = \max(\Delta t_{E,i})$. The value of $\Delta t_{E,i}$ was first chosen to illustrate what happens to risk perception when the pedestrians fail to show any increased awareness (no change in behavior) upon entering the investigating state. A second simulation was conducted with values normally distributed such that $\Delta t_{E,i} = 10 \pm 5$ s. Figure 21 and Figure 22 show the pedestrian risk perception curves for each situation, respectively.

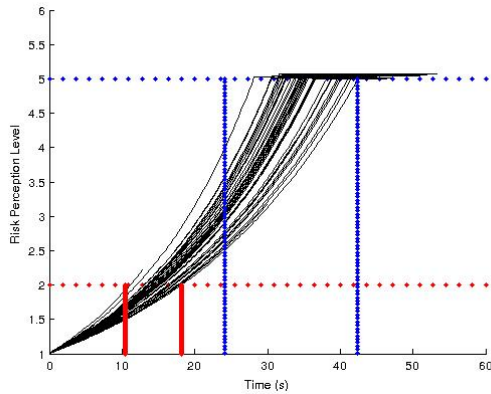


Figure 21 Risk Perception Curves for Pedestrians with Normal Awareness

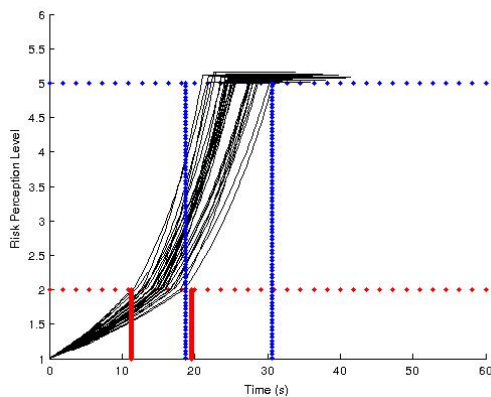


Figure 22 Risk Perception Curves for Pedestrians with Increased Awareness

Figure 21 clearly shows that in a model with normal awareness, prior knowledge, or social influence, all pedestrians enter the investigating state based on their normally distributed simulation-assigned value of $t_{I,i}$, which can be represented by a maximum window of $10 \leq t \leq 20$ seconds, and enter the evacuation state based on the computed value of $\Delta t_{E,i}(t_{I,i})$ such that $t = t_{I,i} + \Delta t_{E,i}$, which analytically has a maximum window of $23.2 \leq t \leq 46.4$ seconds. The actual windows based on the simulation-generated random values for $t_{I,i}$ are shown by the red (window for pedestrian transition into investigating state) and blue (window for pedestrian transition into evacuating state) vertical lines in Figure 21 and Figure 22. Similarly, in the model containing user-assigned values for individual pedestrian urgency where $\Delta t_{E,i}$ was normally distributed such that $\Delta t_{E,i} = 10 \pm 5$ seconds, pedestrians now enter the evacuating state sooner. The analytically computed maximum window for this second simulation ranges from $15 \leq t \leq 35$ seconds and the risk perception curves shown in Figure 22 clearly enter the evacuation state within this window (blue lines).

As Reneke points out and as the discussion in the previous paragraphs illustrate, incorporating just the basic time-dependent EDM fails to move the evacuation simulation away from a user-defined pre-movement time. The pre-movement period is determined by a hypothetical distribution as was previously described in Figure 16. The maximum pre-movement time for the basic EDM is easily computed using the user-assigned values of R_I , R_E , $t_{I,i}$, and $\Delta t_{E,i}$.

4.2 Prior Knowledge

As defined by Reneke [61], prior knowledge is information a pedestrian recalls following a trigger (such as an alarm or interaction with neighboring pedestrians) that impacts decisions made by an individual after the trigger. According to Reneke [61], “the cue value can take all real values both positive and negative but is normally 0.” If the prior knowledge cue is greater than 0, then the pedestrian is hyper-vigilant in emergency situations and if the prior knowledge cue is less than 0, then the pedestrian is typically more complacent than normal in emergency situations.

The parameter $k_{p,i}$ describes the prior knowledge cue value of pedestrian i relative to a single external cue (such as a continuous alarm). If pedestrian i is not subjected to any external triggers and pedestrian i 's risk perception level is normal ($R_i(t) = 1$), then the prior knowledge cue is not activated, that is $k_{p,i} = 0$. However, once triggered, pedestrian i 's prior knowledge cue value continues to impact pedestrian i 's pre-movement decisions until pedestrian i is safely evacuated. For a single external trigger, this interaction can be represented according to the formula shown in Equation 38.

Equation 38 Prior Knowledge Cue Value

$$K_{p,i} = \begin{cases} 0 & \text{if no external trigger and } R_i(t) = 1 \\ k_{p,i} & \text{else} \end{cases}$$

Returning to the basic EDM model described by Equation 36 in the previous section, the modified formula for the change in risk perception is given by Equation 39 where the external cue and prior knowledge cue are summed in the formula.

Equation 39 Modified Risk Perception Model (Single Continuous Alarm with Prior Knowledge Cue)

$$\dot{R}_i(t) = \begin{cases} \frac{\ln R_I}{t_{I,i}} (1 + K_{P,i}) R_i(t) & R_i(t) < R_I \\ \frac{\ln C_E}{\Delta t_{E,i}} (1 + K_{P,i}) R_i(t) & R_I \leq R_i(t) < R_E = C_E R_I \end{cases}$$

Given this modified formula, it is now desirable to quantify the appropriate range of values for the prior knowledge cue value as well as understand the impact of the prior knowledge on the individual pedestrian's overall risk perception level. The green curve shown in Figure 23 is the same risk perception curve shown earlier in Figure 19 where $R_I = 2.0$, $R_E = 5.0$, $t_{I,i} = 6.0$ seconds, $\Delta t_{E,i} = 4.0$ seconds, and the knowledge cue value was zero ($k_{P,i} = 0$). As explained by Reneke, Figure 23 clearly shows that if $k_{P,i} > 0$, the pedestrian is hyper-vigilant and moves into the investigating and evacuating stages more quickly. Similarly, if $k_{P,i} < 0$ then the pedestrian is more complacent and takes longer to move through the stages. Interestingly, as the value of the prior knowledge variable nears a value of -1.0, the pedestrian fails to reach the evacuating state in a reasonable amount of time. In fact, for any pedestrian with a prior knowledge cue value $k_{P,i} = -1.0$ (and no other external influences), Equation 39 clearly indicates there is never a change in risk perception for pedestrian i and pedestrian i will not evacuate.

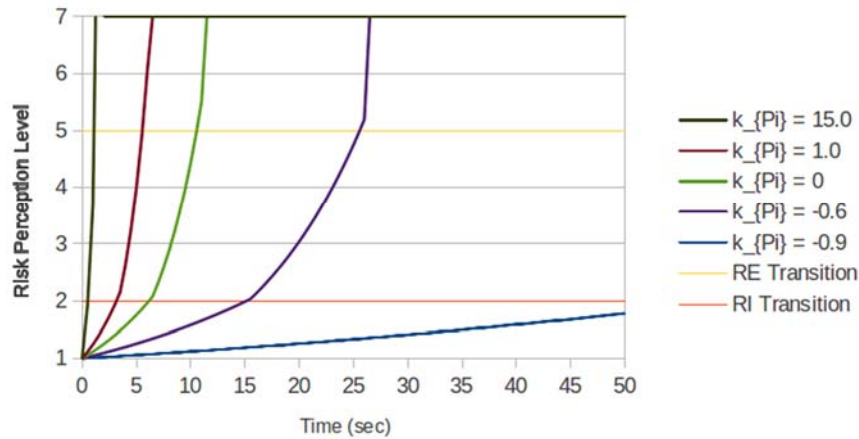


Figure 23 Effect of Knowledge Cue Value on Risk Perception Level (Single Pedestrian)

Once again using the example pedestrian with $R_I = 2.0$, $R_E = 5.0$, $t_{I,i} = 6.0$ seconds, and $\Delta t_{E,i} = 4.0$ seconds, Figure 24 illustrates pedestrian i 's pre-evacuation times for various values of $k_{P,i}$. As the value of $k_{P,i}$ approaches -1 , the time required to enter the investigating state and evacuating state approaches positive infinity, indicating that it is likely that an extremely complacent individual may elect to not evacuate. Similarly, as $k_{P,i}$ approaches positive infinity, the time required to transition to evacuation approaches zero. For this particular pedestrian, a hyper-vigilant prior knowledge value of 12.0 would mean that this pedestrian evacuates almost immediately (with a transition to evacuation time of 1.0 second after the alarm).

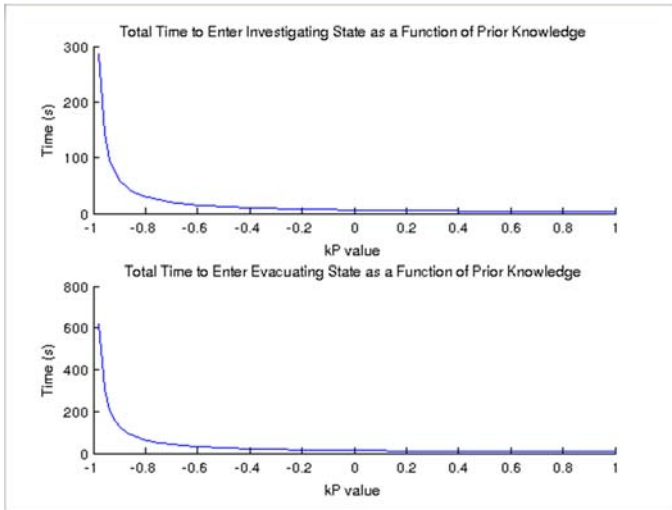


Figure 24 Impact of Prior Knowledge Values on Transition Times

Armed with the knowledge discovered in the previous investigation, it seems logical to use prior knowledge cue values which are normally distributed with $\mu = 0$ and $\sigma \leq 1/3$. Figure 25 shows the results obtained when the “normal awareness” simulation shown in Figure 21 was repeated with the addition of prior knowledge.

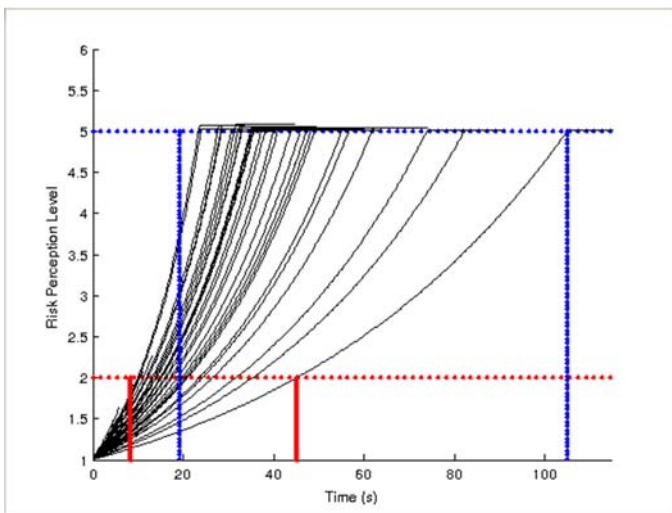


Figure 25 Risk Perception Curves for Pedestrians with Prior Knowledge and Normal Awareness

It is clear that prior knowledge increased the complacency of at least five pedestrians, slowing the rate of change in risk perception, and lengthening the amount of time each pedestrian spends in the pre-movement stage. Similarly, Figure 26 shows the results obtained when the “increased urgency” simulation shown in Figure 22 was repeated with the addition of prior knowledge. Here, the effects of hyper-vigilance and complacency are clearly seen as some pedestrians spend as little as 10 seconds in the pre-movement phase, while others spend more than 50 seconds which is almost 20 seconds longer than was seen with just the basic EDM.

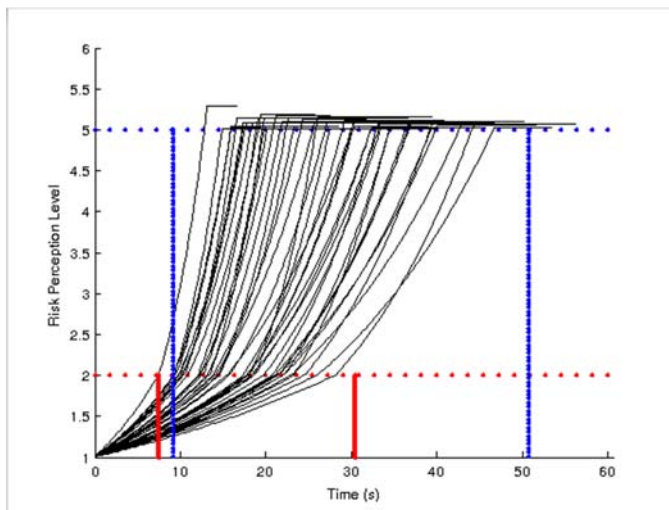


Figure 26 Risk Perception Curves for Pedestrians with Prior Knowledge and Increased Urgency

Even with the inclusion of the prior knowledge cue value, it is still possible to analytically predict how long the pre-movement phase will take (these analytically predicted values are again shown by the red and blue vertical lines in Figure 25 and Figure 26). As the prior knowledge value approaches -1, individual pedestrian

complacency increases exponentially which greatly effects the duration of the pre-movement phase. In fact, in some simulations where the prior knowledge cue value is close to -1.0, pedestrian complacency dominates and the pedestrian fails to evacuate. An example of such a complacent person would be the office employee who has witnessed several false fire alarms and independently makes the decision to continue working and not evacuate the next time the alarm sounds.

4.3 Social Influence

When alone, a pedestrian relies solely on their estimate of the situation, as seen in the time-dependent EDM, and previous experiences, as seen with the addition of the prior knowledge cue value, when evaluating risk. However, in a group setting, the actions of other pedestrians can influence the decision making process (and perception of risk). In his model, Reneke includes a social influence cue computed using Equation 40 which describes how the observed actions of other pedestrians (neighbors) influence a pedestrian's perception of risk. To compute social influence, Equation 40 uses a time-dependent observed neighbor vector, $\mathbf{N}_i(t) = \{N_{E,i}(t), N_{I,i}(t), N_{N,i}(t)\}$, where $N_{E,i}(t)$ is the number of neighbors observed in the evacuating state by pedestrian i at time t ; $N_{I,i}(t)$ is the number of neighbors observed in the investigating state by pedestrian i at time t ; and $N_{N,i}(t)$ is the number of neighbors observed in the normal state by pedestrian i at time t .

Equation 40 Social Influence Cue

$$S_i(\mathbf{N}_i(t)) = \begin{cases} 2 \frac{N_{E,i}(t) + N_{I,i}(t) - N_{N,i}(t)}{N_{E,i}(t) + N_{I,i}(t) + N_{N,i}(t) + N_{0,i}} & R_i(t) < R_I \\ 2 \frac{N_{E,i}(t) - N_{N,i}(t)}{N_{E,i}(t) + N_{I,i}(t) + N_{N,i}(t) + N_{0,i}} & R_i(t) \geq R_I \end{cases}$$

If $N_i(t) = N_{E,i}(t) + N_{I,i}(t) + N_{N,i}(t)$ represents the total number of observed neighbors, then pedestrian i observes other pedestrians in the evacuating or investigating state whenever the number of neighbors in the normal state is less than the total number of observed neighbors, that is when $N_{N,i}(t) < N_i(t)$. In addition, Equation 40 utilizes a user-assigned parameter, $N_{0,i}$, which represents the number of neighbors observed in the normal state by pedestrian i which will prevent pedestrian i from responding to a single alarm.

Returning to the basic EDM model described by Equation 36, the modified formula for the change in risk perception is given by Equation 41 where the external cue (single alarm) and social influence cue are summed in the formula. The prior knowledge cue described in the previous section has temporarily been removed for clarity.

Equation 41 Modified Risk Perception Model (Single Continuous Alarm with Social Influence Cue)

$$\dot{R}_i(t) = \begin{cases} \frac{\ln R_I}{t_{I,i}} (1 + S_i(\mathbf{N}_i(t))) R_i(t) & R_i(t) < R_I \\ \frac{\ln C_E}{\Delta t_{E,i}} (1 + S_i(\mathbf{N}_i(t))) R_i(t) & R_I \leq R_i(t) < R_E = C_E R_I \end{cases}$$

Given this modified formula, it is now desirable to return to the basic EDM and investigate the impact of social influence on a single pedestrian's risk perception level. The first scenario demonstrates how risk perception is impacted by neighbors observed in the normal state. Recall that $N_{0,i}$ represents the number of neighbors observed in the normal state by pedestrian i which will prevent pedestrian i from responding to a single alarm. Therefore, if all of pedestrian i 's neighbors are in the normal state and that value equals $N_{0,i}$, that is $N_i(t) = N_{N,i}(t) = N_{0,i}$, then $S_i(\mathbf{N}_i(t)) = -1$ by Equation 40 and pedestrian i 's risk perception level does not change (Equation 41). However, if $N_i(t) = N_{N,i}(t) < N_{0,i}$, then $S_i(\mathbf{N}_i(t)) > -1$ and the risk perception level of pedestrian i increases. Similarly, if $N_i(t) = N_{N,i}(t) > N_{0,i}$, then $S_i(\mathbf{N}_i(t)) < -1$ and pedestrian i 's risk perception level decreases. Figure 27 illustrates this concept for a pedestrian with $N_{0,i} = 5$. Notice that pedestrian i 's risk perception level drops below 1 when $S_i(\mathbf{N}_i(t)) < -1$ (blue curve); however, the Likert scale ranges from 1 to 7, therefore care must be taken to ensure $R_i(t) \geq 1$ for all t . It is also important to note that this analysis is performed for a pedestrian who has continuous observation of all neighbors and those neighbors never change state. While not a likely scenario for an evacuation simulation, it is a useful method to understand the impact of social influence on a single pedestrian.

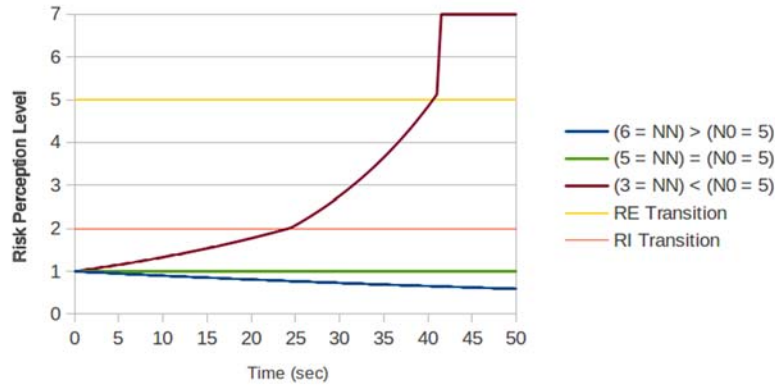


Figure 27 Effect of $N_{N,i}$ (Observed Neighbors in Normal State) on Pedestrian i

Next consider how neighbors observed in the investigating and evacuating states impact risk perception. From Equation 9, it is clear that if the number of observed neighbors in the normal state is less than or equal to $N_{0,i}$ and any other neighbors of pedestrian i are investigating and/or evacuating, then $S_i(\mathbf{N}_i(t)) > 0$ and pedestrian i 's overall risk perception level increases. However, when the number of observed neighbors in the normal state exceeds $N_{0,i}$, some interesting situations arise. For example, when $N_{0,i} = 5$, $N_{N,i} = 6$, $N_{I,i} = 1$, $N_{E,i} = 0$, and $R_i(t) > R_I$ it appears that it is once again possible for $S_i(\mathbf{N}_i(t)) = -1$ and pedestrian i enters the investigating state and remains there in perpetuity. In addition, when the value of $N_{N,i}$ is changed to 7 in the example above, the risk perception level oscillates above and below the R_I value with risk perception increasing when pedestrian i is in the normal state and risk perception decreasing when pedestrian i is in the investigating state. These example risk perception curves for a single agent are shown in Figure 28.

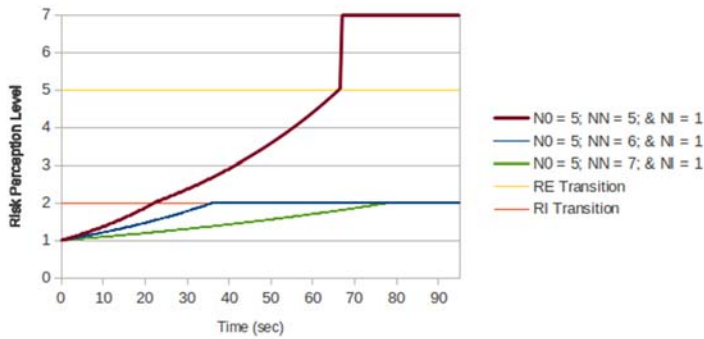


Figure 28 Example Risk Perception Curves for Pedestrian i when $N_{N,i} \geq N_{O,i}$ and $N_{I,i} = 1$

The risk perception curves shown in Figure 27 and Figure 28 are for a single pedestrian in continuous observation of neighbors who never change state. However, during an actual evacuation scenario, the number of observed neighbors surrounding pedestrian i and their states most likely will fluctuate during the simulation. Therefore, the instantaneous observed neighbor vector, $\mathbf{N}_i(t)$, for each pedestrian i must be evaluated at each time step during a simulation. To illustrate the impact of social influence on an evacuation, the “normal awareness” simulation shown in Figure 21 was again repeated with the addition of social influence. During initialization, the value of $N_{0,i}(t)$ was randomly assigned using a normal distribution with $\mu = 5$ and $\sigma = 2$. Assuming that pedestrians will turn and scan 360 degrees to observe neighbors during an emergency scenario and only neighbors within a radius of 2.4 meters influence each pedestrian, a pedestrian neighborhood of approximately 18 m² was defined for the simulation. Figure 29 demonstrates the impact of social influence on the pre-movement phase.

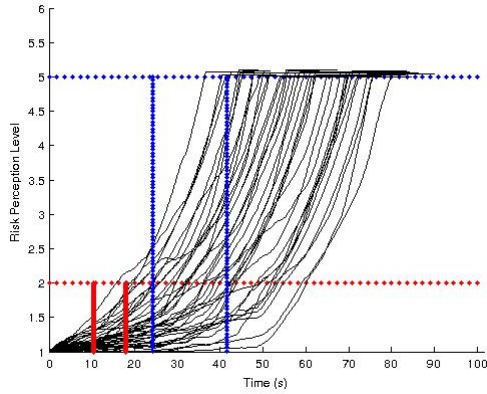


Figure 29 Risk Perception Curves for Pedestrians with Social Influence and Normal Awareness

The blue and red lines represent the analytically computed windows for the basic time-dependent EDM. As can be seen by the various risk perception curves shown in Figure 29, social influence doubles the time required for all pedestrians to complete the pre-movement phase and begin evacuation. Figure 30 shows the results obtained when the “increased urgency” simulation shown in Figure 22 was repeated with the addition of social influence.

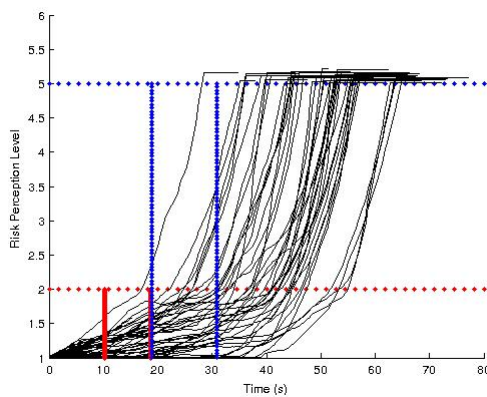


Figure 30 Risk Perception Curves for Pedestrians with Social Influence and Increased Awareness

The risk perception curves shown in Figure 30 again demonstrate the delayed desire to investigate and evacuate due to social influence. The time needed for all pedestrians to complete the pre-movement phase is more than twice as long as the analytically computed values from the basic time-dependent EDM.

Since the observed neighbor vector, $N_i(t)$, continually changes during the evacuation simulation, it is no longer possible to analytically predict the length of the pre-movement phase. As was seen in the two simulations described above, it appears that social influence roughly doubles the length of time it takes for all pedestrians to make the decision to begin evacuation.

4.4 Complete EDM (Single Alarm)

Following individual analysis of each component of Reneke's EDM, the final step is to run simulations which combine the basic EDM with the prior knowledge and social influence factors. Equation 42 shows the complete risk perception model for a single continuous alarm.

Equation 42 Complete Risk Perception Model (Single Continuous Alarm)

$$\dot{R}_i(t) = \begin{cases} \frac{\ln R_I}{t_{I,i}} (1 + K_{P,i} + S_i(N_i(t))) R_i(t) & R_i(t) < R_I \\ \frac{\ln C_E}{\Delta t_{E,i}} (1 + K_{P,i} + S_i(N_i(t))) R_i(t) & R_I \leq R_i(t) < R_E = C_E R_I \end{cases}$$

where $K_{P,i} = \begin{cases} 0 & \text{if no external trigger, } R_i(t) = 1, \text{ and } N_{N,i}(t) = N_i(t) \\ k_{P,i} & \text{else} \end{cases}$

$$S_i(N_i(t)) = \begin{cases} 2 \frac{N_{E,i}(t) + N_{I,i}(t) - N_{N,i}(t)}{N_{E,i}(t) + N_{I,i}(t) + N_{N,i}(t) + N_{0,i}} & R_i(t) < R_I \\ 2 \frac{N_{E,i}(t) - N_{N,i}(t)}{N_{E,i}(t) + N_{I,i}(t) + N_{N,i}(t) + N_{0,i}} & R_i(t) \geq R_I \end{cases}$$

Implementation of the complete model requires a slight modification to the model described by Reneke. In his model, Reneke explains that if $\dot{R}_i(t) < 0$ while $R_i(t) = 1$, then $\dot{R}_i(t) = 0$ (to ensure adherence to the Likert scale). However, upon implementation, it is also possible for $\dot{R}_i(t) < 0$ while $R_i(t)$ is slightly larger than 1 causing the newly computed value of $R_i(t)$ to fall below 1. Therefore, the following restriction was also included: if the computed value $R_i(t) = R_i(t - 1) + \Delta t \dot{R}_i(t)$ is less than 1, then $R_i(t) = 1$. Figure 31 shows the output from the “normal awareness” simulation using the previously defined values for the parameters.

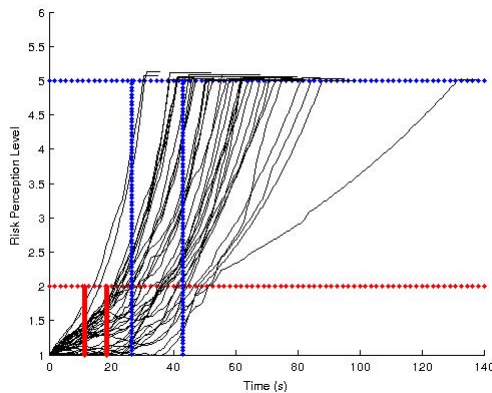


Figure 31 Complete EDM Simulation with Normal Awareness

The pedestrian curve on the far right of Figure 31 is a complacent individual with a randomly generated prior knowledge value of $k_{p,i} = -0.7477$ with a rather high randomly generated time to investigating stage value of $t_{i,i} = 17.16$. During the initial phases of the

evacuation, this pedestrian is influenced by his neighbors and increases his risk perception at rate which is faster than if the pedestrian was alone in the room. In Figure 32, the blue curve represents this pedestrian's risk perception curve predicted by this individual's parameters without social influence. The second curve (green) shows the results of the simulation where pedestrian i is initially impacted by social influence. Without social influence, this particular pedestrian would wait approximately 158 seconds prior to evacuating; however, with social influence, pedestrian i 's risk perception level increases faster and pedestrian i makes the decision to evacuate approximately 131 seconds following the initiation of the alarm, saving almost 30 seconds of precious evacuation time.

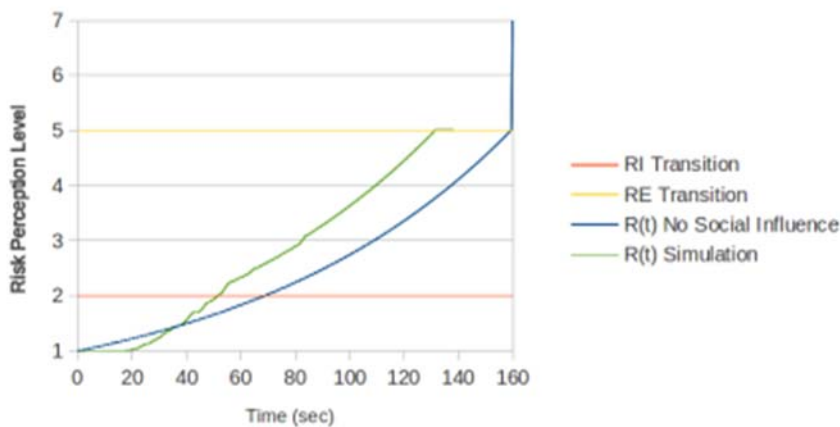


Figure 32 Positive Effect of Social Influence on the Risk Perception Curve

Figure 33 shows the output from the “increased awareness” simulation again using the previously defined values for the parameters. In this simulation, the pedestrian who decides to evacuate last is a more complacent individual with a randomly generated

prior knowledge value of $k_{p,i} = -0.7662$, but with a close to average randomly generated time to investigating stage value of $t_{I,i} = 10.89$. For this individual pedestrian, it appears that social influence negatively impacted his natural risk perception and delayed his transition to the investigating stage and in effect, his overall decision to begin evacuating as shown in Figure 34.

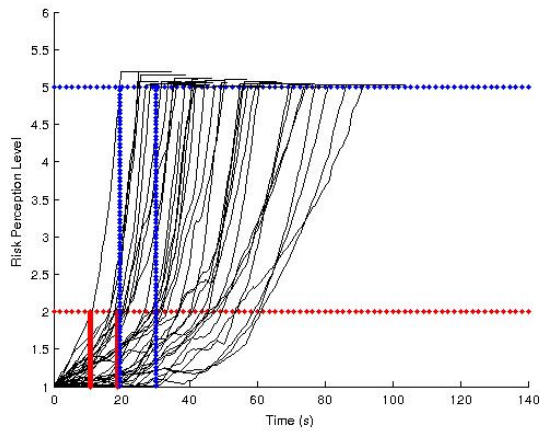


Figure 33 Complete EDM Simulation with Increased Awareness

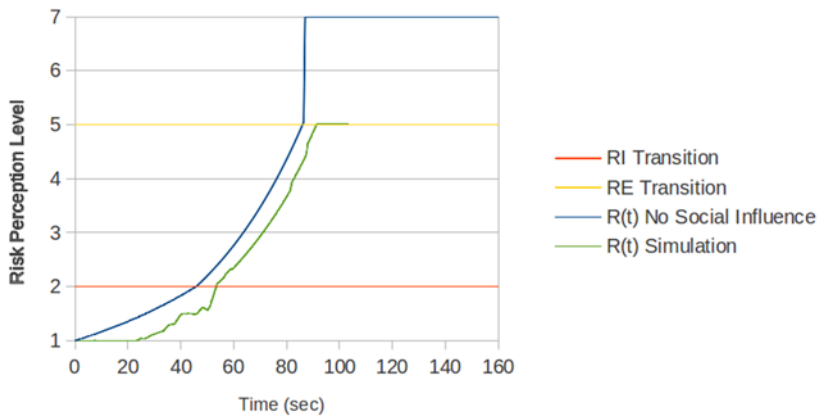


Figure 34 Negative Effect of Social Influence on the Risk Perception Curve

4.5 Discussion

This chapter walks the reader through a single continuous alarm implementation of Reneke's Evacuation Decision Model as a sub-model to a pre-existing CA evacuation model. Without regard to parametric calibration, the EDM appears to incorporate many of the physical, social, and psychological factors previously identified by Kuligowski [62]. More research and empirical data is needed to determine the appropriate values and distributions for the various parameters in the EDM.

Future modifications to the model should include behavioral adaptations upon initial alarm and entrance into the investigating state. For this implementation, the assumption is that the pedestrians continue their previous activity (exiting the room, standing still, or wandering randomly about the room) without interruption until their risk perception level causes them to begin evacuation. It may be more realistic for the pedestrians to pause upon initial alarm activation prior to continuing previous activities. In addition, appropriate behavior options should be considered for the investigating state. For example, once pedestrian i enters the investigating state, he or she may not continue his or her previous activity, but instead may approach others in the investigating and/or evacuating state to discuss the situation. Or pedestrian i may be drawn towards some information providing object (such as a window, computer, telephone, alarm panel, etc.) during the investigating state.

Another potential modification would be to allow the pedestrians to "remember" what has already happened during the evacuation. As currently modeled, social influence is instantaneous and once all of the observed neighbors leave the room, pedestrian i doesn't remember that those individuals departed and pedestrian i 's change in risk

perception is now void of social influence. However, it may be more realistic that if pedestrian i was in a room with 49 other pedestrians and within two minutes all 49 of those individuals have departed the room, pedestrian i 's risk perception would be influenced by their sudden departure.

5 LITERATURE SURVEY III: EVACUATION DATA COLLECTION EFFORTS

Although a terrorist attack on the World Trade Center buildings triggered the September 11th evacuation, the need to evacuate or take some other protective action in an airplane, ship, building, stadium, or other facility can stem from a variety of sources. Some of the most common are fires; active shooter situations; active bombings, bomb threats, or other acts of terrorism; overcrowding; power outages; and effects of nature, such as damage caused by earthquakes, rain, hail, wind, etc. Regardless of origin, all protective actions taken by occupants should be efficient and safe, and under emergency conditions, they should minimize stress so as not to induce panic. Applicable to both outdoor and indoor pedestrian traffic ways, design consultants and engineers implement the aforementioned modeling techniques of pedestrian science and evacuation dynamics in order to ensure the comfort and safety of occupants while optimizing the utility of the space or pedestrian facility.

Research has shown that typical calculations of evacuation and egress times based solely upon engineering standards often represent the best case scenarios. These computations often ignore pedestrian pre-movement behaviors and situation-dependent crowd psychology in favor of egress estimations using pedestrian travel-to-exit distances and times, where each pedestrian in the simulation knows the exact location of the exit. In a 1995 paper, Sime [63] argued that crowd psychology and engineering are mutually

supportive and highlighted the need to validate computer simulations “against psychological as well as engineering criteria”. Sime illustrated the need to incorporate pre-movement activities into evacuation and egress models citing reports from several recent disasters and empirical studies. The disasters cited by Sime include egress disasters such as the 1973 Summerland fire on the Isle of Man, the 1987 King’s Cross Fire in London, and the 1997 Beverly Hills Supper Club fire and he cites an empirical underground station study conducted in 1989 and 1990. Specifically, Sime discussed the observance of co-operative, competitive, affiliative, and sometimes complacent behaviors in evacuation situations. In conclusion, he indicated that specific attention should be placed on evacuation delay (response) times as it pertains to behaviors resulting from psychological factors. Sime concluded that most published evacuation times are based upon design and engineering factors such as the population density (people in relation to floor space), exit capacity, and degree of fire protection and then argues that evacuation simulations must include pre-movement behaviors such as event recognition, investigation, and response times which result from the previously cited psychological factors.

5.1 Literature Survey: Evacuation Dynamics and Data Collection

Numerous consolidated reviews exist on the topic of building evacuation [14], [15], [53], [64]–[66]. In 2008, Schadschneider et al. [14] published a theoretical review of pedestrian science, including a summary of current empirical results, typical modeling approaches, and potential applications for simulation tools. In their paper, Schadschneider et al. described a possible classification scheme for empirical data.

Assuming all environments can be described as either controlled or uncontrolled and further described as a normal or emergency situation, Schadschneider et al. categorized four possible types of empirical data: accident reports (emergency situation and uncontrolled environment), evacuation exercises (emergency situation but controlled environment), observations (normal situation but uncontrolled environment), and movement experiments (normal situation and controlled environment) as shown in Figure 35.

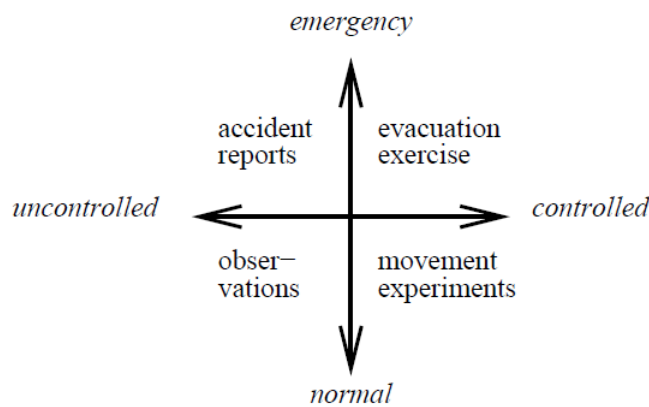


Figure 35 Empirical Data Classifications (extracted from [14])

Empirical data collection through observations occurs when pedestrian movement data is collected through the surveillance of everyday normal activities. Some of the data reported in Predtechenskii and Milinskii's *Planning for Foot Traffic Flow in Buildings* [2] and Fruin's *Pedestrian Planning and Design* [3] was obtained through direct observation of pedestrians in normal situations. However, direct observation was not enough, as mentioned in their forward, Predtechenskii and Milinskii admit that the methodologies

and results published in their book are the culmination of more than 30 years of experimental and theoretical studies. Back in 1958, when the operational research section of London Transport was asked to study the flow of passengers in the subway [1], they found that direct observation was too complex and therefore opted to collect data by conducting controlled experiments utilizing participants at a boys' school in southern England. Movement experiments, therefore, provide valuable data used to inform the methods for mathematical calculations and computations related to the study of pedestrian science. Specifically, pedestrian movement experiments occur when researchers set up a specific scenario, obtain volunteers to participate, and obtain movement data by running trials. Empirical data collected by direct observation and through movement experiments under normal conditions, while beneficial to researchers concerned with general, as well as scenario-specific, modeling of pedestrian movement, does not provide relevant data to researchers who are concerned with evacuation (and pre-evacuation) decision making processes, behaviors and activities.

Although there have been efforts in the past to formalize evacuation data acquisition methods [67] and consolidate evacuation data [68], no approved methodology or integrated database exists. Since a consolidated database of evacuation data does not exist, evacuation data must come through the systematic review of literature published and data collected from accident reports and evacuation exercises. In 2005, Whiting [66] published a comprehensive international summary of research efforts geared specifically towards gathering information on occupant pre-movement behaviors and response times in fire situations. Interestingly, in his report Whiting listed a relatively small number

(forty-three) of potential pre-movement data sources which illustrates the immaturity of the field.

Following a tragic incident, the deliberate review of accident reports and attempts to recreate the life-threatening scenario often provides valuable data and insight into pedestrian reactions and responses to serious emergency situations. The most common type of accident report used to collect information on pre-evacuation behaviors, activities, and corresponding times comes from post-fire accident reports and interviews. A thorough review of specific fire incidents allows researchers to examine the causes of evacuation delay as well as the factors involved in route-to-exit selection.

Evacuation exercises allow the collection of pedestrian movement data through the surveillance of individual responses to emergency-like situations within buildings. Through the observation of evacuation exercises, researchers attempt to collect valuable qualitative and quantitative information on individual occupant pre-alarm activities, post-alarm behaviors, evacuation route choices, exit selection, pre-evacuation delay times, and overall evacuation times.

5.2 Evacuation Delay: Psychological Factors and Empirical Data

One major cause of evacuation delay relates to the number of actions an occupant performs prior to beginning evacuation. These actions are definitely different for each scenario and may include activities such as notifying others, finding family and friends, collecting personal belongings, making telephone calls, securing property, waking up, and getting dressed. In 1986, Horiuchi et al. [69] utilized a post-fire investigation to study evacuation in a multi-purpose office building. Of interest here was their

categorization of building occupants as either “regular” or “less-familiar” users. Regular users performed several actions such as trying to extinguish the fire, alerting others, and helping others to evacuate; whereas, less-familiar users tended to evacuate immediately. They concluded that occupant familiarity determined the number of actions taken prior to beginning evacuation, the quantity of actions taken influenced the pre-evacuation phase, and the length of the pre-evacuation phase directly impacted the total evacuation time.

A second major cause of evacuation delay relates to the type and number of cues an individual receives. In an emergency situation, cues include things such as the activation of an alarm, the smell of smoke, notification by others, loud unexplained noises, noticeable flames, explosions, mass exodus of occupants or the arrival of emergency personnel. In 1997, Brennan [70] looked at two fire incidents, a fire in a fourteen-story office building and a fire in an eighteen-story residential building hoping to obtain behavioral information on the types of actions and patterns of behavior that occur; the probability of the occurrence of such actions by different populations and in different occupancies; and the time taken for each of the actions and periods of inactivity. From her study, she concluded that the majority of overall evacuation time is determined by the response time and is directly related to the cues received by the occupants.

In 1997, Proulx and Fahy [71] found that the evacuation delay time is often longer in actual fires because of the uncertainty of the situation and the ambiguity of the cues. In addition, they found that the audibility of the alarm (arguably the most important cue) also had a significant impact in reducing evacuation start time. It was found that in the buildings with barely audible alarm systems, occupants did not evacuate until they were

alerted by the arrival of the fire trucks or told to leave in the building sweep conducted by emergency personnel.

In an attempt to better understand the human factors involved in evacuation decision making, Kuligowski and Mileti [72] used regression analysis to identify the predictors of evacuation delay as experienced by the evacuees of the World Trade Center towers. In this context, the authors cited several factors that contributed to evacuation delay: quantity of environmental cues, closeness to safety, amount of information available and/or obtainable, and number of pre-evacuation activities.

The study of evacuation exercises allows researchers to better determine the types of actions an individual performs prior to starting evacuation. Some of the actions performed during an evacuation drill may be the same as those actions previously derived from accident reports. Certainly, these actions, when performed in a controlled environment, may be executed with less urgency than in an actual emergency. However, the type of actions performed in a regulated evacuation drill may also differ greatly than the actions performed in a life-threatening situation. At the 1994 Human Factors and Ergonomics Society Meeting, Proulx [73] presented the evacuation delay times collected from a series of evacuation drills in four Canadian mid-rise apartment buildings. Upon initiation of the alarm, the first occupants began evacuating as early as 30 seconds and the majority of the residents evacuated within the first five minutes; however, some occupants took more than 24 minutes to begin evacuating (Figure 36). In post-event surveys, Proulx found that most occupants spent time after the alarm sounded conducting some type of pre-evacuation activity such as finding pets or children, getting dressed or

gathering valuables, or looking in the corridor presumably to see what other occupants were doing.

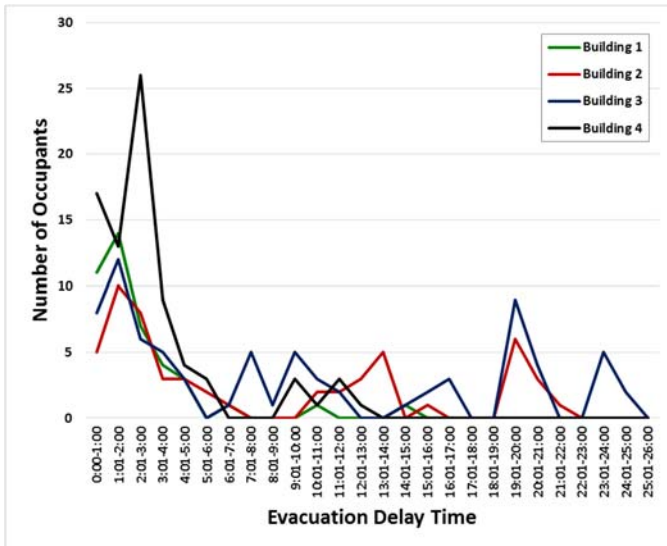


Figure 36 Evacuation Delay Times from Four Mid-Rise Apartment Buildings [73]

In 1997, Proulx and Fahy [71] published a review of five case studies which included the results from the mid-rise apartment buildings mentioned in the preceding paragraph as well as five other evacuation drill studies: three high-rise apartment buildings and two office buildings. In their analysis, they found that occupants in buildings with highly audible alarm systems began to evacuate, on average, almost six minutes faster than buildings with barely audible alarm systems. It was found that in the buildings with barely audible alarm systems, occupants did not evacuate until they were alerted by the arrival of the fire trucks or by the building sweep conducted by the firefighters. In addition, she noted that in the high-rise study weather had a significant

impact. One drill occurred during a snowfall and the occupants had to dress in appropriate outer garments prior to leaving their apartments. In the office building case studies, Proulx found that the average evacuation delay was much smaller than in the cases of the apartment buildings and attributed this to good alarm audibility, occupant training, and the presence of fire “wardens” to prompt evacuation. Most pre-movement activities included gathering belongings, getting dressed, and notifying others.

A study that is fairly similar to the Johnson Center evacuation study contained within this dissertation is the March 2, 2000 study of the Dreadnaught educational facility at the University of Greenwich [74]. In their 2003 report, Gwynne et al. [74] examined the pre-evacuation time distributions and analyzed the behavioral factors which influenced the pre-evacuation times (Figure 37). The number of actions performed prior to evacuating had a significant impact on the pre-evacuation times. These actions included activities such as shutting down the computer, disengaging socially, collecting items, and investigating the incident. Many of these same activities were seen in the video analysis of the Johnson Center evacuation. In addition, the level of prompting also influenced the pre-evacuation times. A little more than one-half of the occupants evacuated the building with no prompting by other students or staff members. However, the remainder of the occupants required prompting to leave the building, thus indicating the importance of identifying staff members who are responsible for clearing the building.

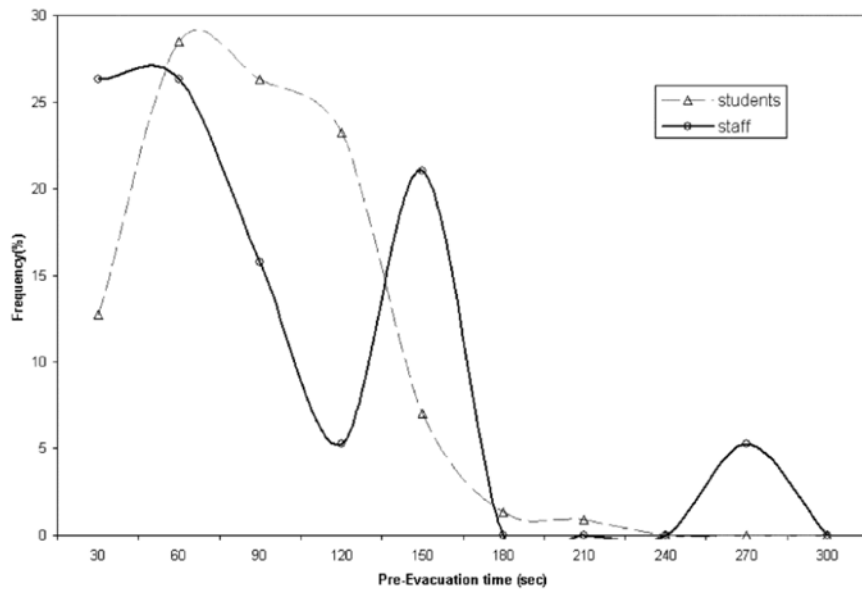


Figure 37 Pre-eva-cuation Times (extracted from [74])

In 1989, Kimura and Sime [75] monitored the evacuation of two theaters in order to study occupant exit choice with and without instruction. Their research confirmed the importance of proximity to exit, route familiarity, and social influence in evacuation situations. Additional research [76], conducted at the same two theaters one year later demonstrated that approximately two-thirds of the total evacuation time was spent on pre-movement behaviors (referred to as “time to start” in the report). In a 2003 master’s thesis, Ko [77] used this same study to compare the results obtained using the EvacuationNZ and SIMULEX computer-based evacuation simulation software. The foundations of a theater evacuation case study could be established in a pedestrian simulation utilizing the information from the original report, along with the extracted initialization data from Ko’s thesis. For validation purposes, the theater evacuation

simulation could also be compared to the qualitative data obtained during a 1995 evacuation of a theater in Finland, as reported by Weckman [78].

5.3 Route-to-Exit Choices: Psychological Factors and Empirical Data

Once an evacuation begins and an individual decides to begin movement, he/she must make a deliberate decision on which exit to use and the route to get there. The exit chosen may be a familiar exit (affiliation), the closest exit (shortest time-to-exit), an exit the individual is directed to use (fixed path), or an exit the individual witnesses being used by others (social influence). Similarly, how an individual gets to an exit may be influenced by normal routines (affiliation), route cues such as emergency exit signage, or herding behavior (social influence). In their 1986 study, Horiuchi et al. [69] determined that familiarity impacted the exit route selection where the regular users chose to evacuate by a regularly used route (path affiliation), whereas those who were less-familiar had to follow or rely on others because it was difficult to find an exit (social influence).

In a 1983 article published in the journal of environmental psychology, Sime [79] analyzed flight from a fire using two contrasting models: a “panic” model and an “affiliative” model. The panic model assumes the escape involves a homogeneous population individually concerned with self-preservation and competing for available exits. The affiliative model assumes individuals will move towards familiar people (thus escaping in groups) and places (thus escaping via familiar routes of escape). In a 1985 follow-up to his earlier publication, Sime [80] highlights an engineering model of escape behavior which he describes as the “physical science” model which assumes a physically

deterministic relationship between the location of a fire, proximity of an exit, and direction of movement. The earlier mentioned “panic” model closely overlaps the physical science model in that both models treat people as non-thinking objects in motion. Through log-linear casual analysis, Sime demonstrates that even in emergency situations, people are less likely to use unfamiliar (affiliation) escape routes and exits. He further postulates that evacuation drills should be used to familiarize persons with unfamiliar exit routes and choices. Sime’s research [76] resulted in a three-year research project intend to “determine what factors may deter people who are escaping from a fire from using internal escape routes.” Sime finds that familiarity with escape choices is as important as travel distance and all routes should be used routinely to familiarize occupants with their options.

Horiuchi et al. [69] conducted a post-fire study of an April 1984 fire in a multi-purpose office building. The results contained within the post-fire report show significant differences between regular users and less-familiar users in terms of actions taken, exit route selection, and egress success. Typically, regular users initially performed non-evacuation actions such as fighting the fire, alerting others, and/or helping others to evacuate whereas the less-familiar users elected to immediately evacuate. In addition, the less familiar users had a difficult time finding an exit route and most had to rely on others to successfully evacuate. The choice of exit by regular users depended on the amount of smoke, directions from the PA system, sex, job, and building familiarity. Familiarity affected all phases of the evacuation and directly impacted the speed and ease of evacuation. In 1996, Proulx et al. [81] published a comprehensive report on occupant

behaviors, route selection, and speed during the evacuation of two office buildings.

Although it may not be possible to determine the exact inputs to recreate these types of evacuations in pedestrian simulations, the qualitative conclusions provided by Horiuchi et al. [69] and the quantitative data provided by Proulx et al. [81] could potentially be used to validate pedestrian simulation tools. Similarly, in 2005, Gwynne et al. [82] attempted an analogous type of validation, comparing predictions obtained using the buildingEXODUS evacuation software with experimental data collected during a 1991 fire drill conducted at Milburn House, an eight floor, multi-occupied office building. Although the office building contained eight floors, the buildingEXODUS simulations were limited to just two floors and eight cases.

The route and exit selection process during an evacuation drill is very similar to the selection process described in accident reports. Individuals must still decide which exit to use and how to get there. One important distinction, however, is that in the case of a typical evacuation drill all exits are available and the individuals have no external life-threatening cues (such as smoke, fire, or heat) to influence their selection of the closest exit from the building.

A more comprehensive report on the evacuation data previously shown in Figure 36 was published by Proulx in a 1995 edition of the Fire Safety Journal [83]. In her report, Proulx found that 62% of the occupants traveled in groups during the evacuations (pairs, groups of three, or family units). From an affiliation standpoint, Proulx observed that most occupants also exited via a familiar direction of travel. Interestingly, Proulx found that (once evacuation begins) the total time to evacuate does not vary considerably

among the evacuees and in conclusion, Proulx remarked that “it appears essential to develop strategies to shorten time to start the evacuation as a means to reduce the total evacuation time of all occupants.” Analogously, it therefore seems essential to develop evacuation simulation models that account for pre-evacuation behaviors and activities.

In fact, in his 1999 master’s thesis, Crawford [84] concluded that the time needed for pre-movement activities, that is any and all activities after an alarm sounds but prior to initiation of a protective action (such as evacuation), is often underestimated in deterministic design calculations.

6 PEDFLOW

The pedestrian flow simulation tool (PEDFLOW) [85] is a discrete microscopic model where each pedestrian is treated individually and motion is influenced by Newtonian dynamics (similar to Helbing's Social Force Model [17]). PEDFLOW has been in development at GMU for more than 10 years and currently contains a complete suite of pre- and post-processing tools. The computer aided design tool included in PEDFLOW allows the user to input all information required to set up the test case including the geometric definitions; boundary conditions; pedestrian types, characteristics and desired paths; as well as any scenario-specific information (such as evacuation). In addition, the user may use the computer aided design tool to specify required diagnostics as a means of collecting all necessary quantitative and qualitative information during the simulation run for analysis during post-processing. Once pre-processing is complete, the PEDFLOW tool runs the simulation and outputs all requested diagnostic information to data files for post-processing.

6.1 Model Considerations

Many factors need to be considered when modeling pedestrian motion with a force-based model. The model begins simply enough with an individual's motivation to reach a desired place at a given time (i.e., evacuate a building as soon as possible) and

then is expanded as considerations are made for the physiological, sociological, and psychological interactions.

A physiological interaction is a reaction to environmental factors which affects the capabilities of the pedestrian. The model should consider an individual's physical fitness level and take into account an individual's physical reaction to numerous environmental factors such as geographical knowledge or familiarity with ones surroundings, obstacles, climatic conditions, and/or terrain conditions. An individual who slows due to exhaustion when climbing stairs or delays evacuation due to the weather outside are two examples of physiological interactions. Within PEDFLOW, physiological interactions are modeled using accurate pedestrian demographic information to initially define the pedestrians and adjustments are made within the simulation using a set of subroutines related to the health of the pedestrians.

Sociological interaction concerns an individual's association with other pedestrians and the influence others have on the subsequent behaviors of the individual. This is often described in pedestrian literature as social influence. Sociological factors such as group affiliation, familiarity with ones surroundings, supervisory responsibilities and heroic tendencies may influence an individual's subsequent behaviors. A family who evacuates together, a supervisor who clears the floor of a building, and an individual who battles the blaze rather than retreating from it are all examples of behaviors influenced by sociological factors. Sociological interactions are modeled within PEDFLOW using accurate pedestrian demographic information to initially define the pedestrians/groups

and, in cases of evacuation, through specific path definitions which define duties and/or responsibilities after the initiation of an emergency.

In a manner similar to sociological influence, psychological factors also influence subsequent behaviors of a pedestrian. Psychological factors relate to one's risk perception level and include such things as privacy radius (comfort zone), available information (or cues), past experiences, and directives. An individual who waits for a directive to evacuate from emergency personnel and an occupant who evacuates immediately because of prior experiences are two examples of behaviors influenced by psychological factors. Within PEDFLOW, psychological interactions are modeled using accurate pedestrian demographic information to initially define the pedestrians and, in cases of evacuation, through evacuation delay distributions obtained from empirical studies.

6.2 Mathematical Model Formulation

During the simulation, the PEDFLOW model starts with the basic equations of motion shown again in Equation 43, where m represents the mass of the pedestrian, \mathbf{f} are the internal and external forces acting on the pedestrian, \mathbf{v} is the pedestrian's velocity vector and \mathbf{x} represents the position vector of the pedestrian within the simulation.

Equation 43 Newton's Equations of Motion

$$m \frac{d\mathbf{v}}{dt} = \sum \mathbf{f}$$
$$\frac{d\mathbf{x}}{dt} = \mathbf{v}$$

The differential equations are integrated within PEDFLOW using a first-order explicit time-stepping technique. First, PEDFLOW aggregates all of the internal and external forces for each pedestrian as shown in Figure 38.

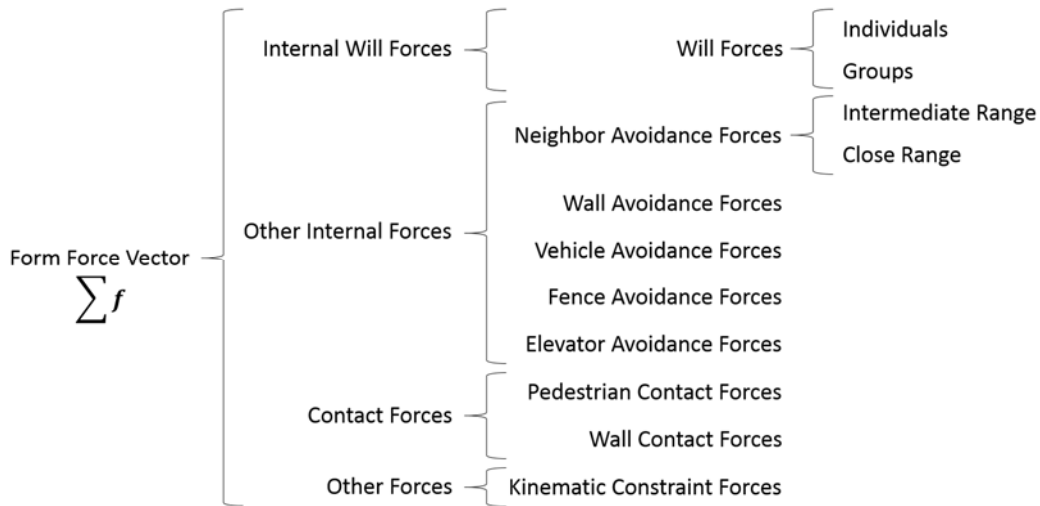


Figure 38 Creation of the Force Vector in PEDFLOW

As was the case with the SFM, the main modeling effort (and often the distinction between microscopic simulation programs) concerns the methods used to determine the forces f which act on the pedestrian (Figure 38). Within PEDFLOW, global movement is controlled by the individual's desired destination, modeled as an internal will force. Local movement is controlled by additional internal forces such as intermediate collision avoidance, near-range collision avoidance, and wall/obstacle avoidance forces, as well as external pedestrian-pedestrian and pedestrian-object contact forces.

6.2.1 Internal Will Force

The internal will force models a person's desire to get to a certain point with a certain speed. Within PEDFLOW the force due to will is computed based on a number of considerations such as the pedestrian's desired path, urgency, physical fitness level, and whether or not the individual is a member of a group. As was seen previously in the SFM, the will force f_{will} could be modeled as a function g_w multiplied by the difference between the desired velocity v_d and the current velocity v (Equation 44).

Equation 44 Will Force

$$f_{will} = g_w(v_d - v)$$

While it is true that, in a non-linear case, g_w could be modeled as a function of $(v_d - v)$, one can also assume g_w is a constant. To derive a mathematical value for g_w , assume that the only force acting on the pedestrian is the will force and the pedestrian begins from a position of rest such that initial velocity is zero. Then the initial value problem is as shown in Equation 45.

Equation 45 Initial Value Problem (IVP)

$$m \frac{dv}{dt} = g_w(v_d - v), \quad v(0) = 0$$

Using the separation of variables integration technique to solve for v and the given initial condition, yields the particular solution shown in Equation 46.

Equation 46 Solution to the IVP given in Equation 45

$$\mathbf{v} = \mathbf{v}_d(1 - e^{-\alpha t}) \quad \text{where} \quad \alpha = \frac{g_w}{m} = \frac{1}{\tau_r}$$

Differentiating the velocity equation shown in Equation 46 with respect to t , provides the acceleration equation and, when $t = 0$, initial acceleration equals $\alpha \mathbf{v}_d$. Therefore, g_w must be proportional to the inverse of the relaxation time τ_r and represents the time required to reach a desired velocity. An individual's desired velocity is often scenario dependent and depends greatly on an individual's health and fitness level, purpose, and the level of determination involved to reach a certain place at a certain time. Appropriate values for desired velocity are based on the fact that pedestrians typically stroll at $0.4 - 0.8 \text{ m/s}$, walk at $0.8 - 1.5 \text{ m/s}$, jog at $1.5 - 4.0 \text{ m/s}$, and run at $4.0 - 10.0 \text{ m/s}$ [85]. The time it takes a pedestrian to reach his or her desired velocity (starting from rest) is typically in the range of $0.5 - 1.0 \text{ s}$; however, this value is also dependent on the individual's fitness and determination levels, as well as environmental factors.

6.2.2 Other Internal Forces

An individual's desire to avoid collisions with other pedestrians and inanimate objects such as walls, vehicles, and virtual fences lead to the development of force-based models within PEDFLOW. This section will describe the intermediate- and close-range pedestrian-pedestrian collision avoidance models as well as the pedestrian-object collision avoidance models. In general, PEDFLOW conducts collision avoidance by first

checking to see if a collision will occur and then applies forces in the appropriate directions to elicit the desired collision avoidance behavior. A key assumption in the implementation of these models is that individuals are only influenced by their nearest neighbors and nearest inanimate objects.

6.2.3 Neighbor Avoidance Force: Intermediate-Range

As currently defined in PEDFLOW, “intermediate range” refers to only the nearest (closest) neighbors within a range of approximately 2 to 20 times the combined radii of two neighbors. Given pedestrians 1 and 2 with positions \mathbf{x}_1 and \mathbf{x}_2 and velocities \mathbf{v}_1 and \mathbf{v}_2 , the (future) time Δt when the two pedestrians are the closest can be found by minimizing the distance between the two pedestrians as shown in Equation 47.

Equation 47 Objective Function to Find Δt that Minimizes the Distance between Two Moving Pedestrians

$$\min((\mathbf{x}_1 + \Delta t\mathbf{v}_1) - (\mathbf{x}_2 + \Delta t\mathbf{v}_2))^2$$

differentiating with respect to Δt and solving for Δt yields,

$$2(\mathbf{x}_1 + \Delta t\mathbf{v}_1 - \mathbf{x}_2 - \Delta t\mathbf{v}_2) \cdot (\mathbf{v}_1 - \mathbf{v}_2) = 0$$

$$((\mathbf{x}_1 - \mathbf{x}_2) + \Delta t(\mathbf{v}_1 - \mathbf{v}_2)) \cdot (\mathbf{v}_1 - \mathbf{v}_2) = 0$$

$$(d\mathbf{x} + \Delta t(d\mathbf{v})) \cdot (d\mathbf{v}) = 0$$

$$(d\mathbf{x}) \cdot (d\mathbf{v}) + \Delta t(d\mathbf{v}) \cdot (d\mathbf{v}) = 0$$

$$\Delta t_{min} = -\frac{(d\mathbf{x}) \cdot (d\mathbf{v})}{(d\mathbf{v}) \cdot (d\mathbf{v})}$$

Using the time Δt_{min} found in Equation 47, the minimum distance is therefore given by $\delta_{min} = (\mathbf{x}_1 - \mathbf{x}_2) + \Delta t_{min}(\mathbf{v}_1 - \mathbf{v}_2)$. If this expected distance is smaller than the pre-established closeness tolerance, then PEDFLOW adds a repelling force in the

tangential \mathbf{t} (i.e., along the direction of motion) and normal \mathbf{n} (i.e., perpendicular to the direction of motion) directions (Equation 48) to the current velocity vector \mathbf{v}_1 .

Equation 48 Tangential and Normal Directions for Vector \mathbf{v}

$$\mathbf{t} = \begin{bmatrix} \frac{v_x}{|\mathbf{v}|} \\ \frac{v_y}{|\mathbf{v}|} \end{bmatrix} \quad \mathbf{n} = \begin{bmatrix} \frac{-v_y}{|\mathbf{v}|} \\ \frac{v_x}{|\mathbf{v}|} \end{bmatrix}$$

Given that r_{12} represents the combined radii of pedestrians 1 and 2, as well as the privacy radius (comfort zone) of pedestrian 1, then the normalized distance δ between pedestrians 1 and 2 is shown in Equation 49 and the corresponding tangential δ_t and normal δ_n components are shown in Equation 50.

Equation 49 Normalized Distance δ Between two Pedestrians in PEDFLOW

$$\delta = \frac{|\mathbf{x}_1 - \mathbf{x}_2|}{r_{12}} = \frac{|d\mathbf{x}|}{r_{12}}$$

Equation 50 Tangential and Normal Components of the Normalized Distance δ

$$\delta_t = \frac{|\mathbf{t} \cdot d\mathbf{x}|}{r_{12}} \quad \delta_n = \frac{|\mathbf{n} \cdot d\mathbf{x}|}{r_{12}}$$

When changing direction to avoid a collision from afar, pedestrians move faster in the direction normal to the motion (lateral direction). Therefore, the maximum force in the normal direction f_{max_n} should be higher than the force in the tangential

direction f_{max_t} . In PEDFLOW, values of $f_{max_n} = 4.0$ and $f_{max_t} = 2.0$ are used. The maximum force in each direction is multiplied by desired velocity over relaxation time to ensure the dimensions are correct. Lastly, some scenario specific conditions are checked and, if they apply, the force is scaled appropriately by some value β . Some of these scenario specific situations include cases where the pedestrian is looking for a seat and therefore he/she has a reduced motivation to evade ($\beta = 0.25$); pedestrian 1 is a follower and therefore there is less motivation to evade pedestrian 2 ($\beta = 0.5$); the individual is “pushy”, defined by a pre-defined pushiness parameter $p \in [0,0.8]$, then there may also be less motivation to evade ($\beta = 1 - p$); and lastly if individual 1 is a typical pedestrian and individual 2 is modeled as a wheelchair, then pedestrian 1 has more desire to evade pedestrian 2 ($\beta = 1.5$). The final repulsive intermediate-range forces are then given by Equation 51.

Equation 51 Pedestrian-Pedestrian Intermediate-Range Forces

$$\mathbf{f} = -\mathbf{f}_t - \mathbf{f}_n = -\beta f_{max_t} \left(\frac{|v_d|}{\tau} \right) \frac{1}{1 + \delta_t^2} \mathbf{t} - \beta f_{max_n} \left(\frac{|v_d|}{\tau} \right) \frac{1}{1 + \delta_n^2} \mathbf{n}$$

6.2.4 Neighbor Avoidance Force: Close-Range

In contrast to the intermediate-range forces, “close range” refers to the nearest neighbors where the distance between the two pedestrians is closer than 2 times the combined radii of the two pedestrians. The objective function shown in Equation 47 is again used to determine if the pedestrians are getting closer and, if so, then a repelling

force is added that is proportional to the distance between the two pedestrians (Equation 52) and in the direction of the difference vector $\frac{d\mathbf{x}}{|d\mathbf{x}|}$.

Equation 52 Normalized Distance δ between Two Close-Range Pedestrians in PEDFLOW

$$\delta = \frac{|\mathbf{x}_1 - \mathbf{x}_2|}{r_1} = \frac{|d\mathbf{x}|}{r_1}$$

When a pedestrian approaches another pedestrian (or a group of pedestrians), velocity decreases greatly; therefore, in contrast to what was seen in the intermediate-range case, close-range avoidance forces will act in the direction of the normalized difference vector, $\frac{d\mathbf{x}}{|d\mathbf{x}|}$, and in the direction normal to this vector, $\frac{d\mathbf{x}_n}{|d\mathbf{x}|}$. Since the pedestrians are close, the maximum force in the direction of motion is now higher than the force in the normal direction. In PEDFLOW, values of $f_{max} = 4.0$ and $f_{norm} = 0.2$ are used. The maximum force in each direction is again multiplied by desired velocity over relaxation time to ensure the dimensions are correct. Lastly, the scenario specific conditions are again checked and, if they apply, the force is scaled appropriately by the value β . The final repulsive close-range forces are then given by Equation 53.

Equation 53 Pedestrian-Pedestrian Close-Range Forces

$$\mathbf{f} = -\beta f_{max} \left(\frac{|v_d|}{\tau} \right) \left(\frac{1}{1 + \delta^2} \right) \left(\frac{d\mathbf{x}}{|d\mathbf{x}|} \right) - \beta f_{norm} \left(\frac{|v_d|}{\tau} \right) \left(\frac{1}{1 + \delta^2} \right) \left(\frac{d\mathbf{x}_n}{|d\mathbf{x}|} \right)$$

6.2.5 Wall Avoidance Force

As part of the pre-processing tools available with PEDFLOW, the user is able to input the geographical information into PEDFLOW using a computer-aided design program. The user inputs all scenario specific information such as walls, entrances/exits, stairs, elevators, etc. Once added, this information is converted into a triangular background mesh. To compute wall avoidance forces, it is assumed that the force must act in the direction of the gradient which is given by a pre-computed distance-to-wall function $d_w(\mathbf{x})$ and stored in the elements of the background mesh. In the wall avoidance subroutine, PEDFLOW first checks to see if pedestrian i can reach his/her desired destination via a near neighbor search. If so, then there is no need for the wall avoidance. However, if it is determined that a wall lies between pedestrian i and his/her destination, then the force vector is computed as shown in Equation 54 where $f_{max} = 4.0$, v_d , r_i , and τ represent pedestrian i 's desired velocity, radius, and relaxation time, respectively.

Equation 54 Pedestrian-Wall Collision Avoidance Force

$$\mathbf{f}_{iW} = -f_{max} \left(\frac{|v_d|}{\tau} \right) \left(\frac{1 - d_w}{5.0 + r_i} \right) (\nabla d_w)$$

6.2.6 Virtual Fence Avoidance Force

In addition to inputting the physical geometry of the environment using the computer-aided design program, the user is also able to define temporary crowd and pedestrian control measures needed in the scenario. For example, portable barriers, such as the retractable barriers or removable stanchions used for crowd control (i.e., ticket

lines), can be defined in PEDFLOW and added or removed as the situation warrants. Similarly, a two-way doorway could be designated as entrance-only (due to presence of ticket takers, for example) at the beginning of the simulation, but the one-way directional constraint may be removed later, allowing for two way passage and facilitating rapid exit at the conclusion of the event. In PEDFLOW, control measures such as these are modeled as “virtual fences” – areas in the simulation that prohibit and/or restrict pedestrian movement for a prescribed amount of time as defined by the user.

The governing equation used by PEDFLOW to compute the virtual fence avoidance force is shown in Equation 55. A value of $f_{max} = 4.0$ is used again to represent the maximum force that can be exerted by the fence (as a multiple of the will force) and then multiplied by desired velocity v_d over relaxation time τ to ensure the dimensions are correct. This value is then multiplied by a reduction factor φ_F which is dependent on the pedestrian’s distance d_{iF} from the virtual fence. PEDFLOW uses the pedestrian’s current position and the location of the virtual fence to compute the distance to the virtual fence d_{iF} in both the normal and tangential directions. To account for the potential to have varying effectiveness of portable barriers and other crowd control measures represented by virtual fences, a user-defined blockage factor $\beta \in [0, 1]$ is used, where $\beta = 0$ represents no blocking and $\beta = 1$ represents a total blockage. Lastly, it is assumed that the force must act in the user-defined direction normal to the fence, \mathbf{r}_n .

Equation 55 Pedestrian-Fence Avoidance Force

$$\mathbf{f}_{iF} = -f_{max} \left(\frac{|v_d|}{\tau} \right) (\varphi_F) (\beta) \mathbf{r}_n \quad \text{where } \varphi_F = \max \left(0, 1 - \frac{d_{iF} - r_i}{d_{coff}} \right)$$

6.2.7 Elevator Avoidance Force

The formula used by PEDFLOW to compute the elevator avoidance force is very similar to the virtual fence avoidance (see Equation 56). A maximum force value of $f_{max} = 4.0$ is again used and multiplied by pedestrian's desired velocity v_d over relaxation time τ to ensure the correct dimensions. This value is then multiplied by a reduction factor φ_E which is dependent on the pedestrian's distance d_{iE} from the elevator, the cutoff distance d_{coff} , and pedestrian's radius r_i . This distance is based upon the pedestrian's current location and given by the distance-to-elevator function $d_E(\mathbf{x})$ which was pre-computed and stored in the elements of the background mesh. Just as was assumed with the wall avoidance forces, it is assumed that the elevator avoidance force must act in the direction of the gradient of the distance to the elevator ∇d_E .

Equation 56 Pedestrian-Elevator Avoidance Force

$$\mathbf{f}_{iE} = -f_{max} \left(\frac{|v_d|}{\tau} \right) (\varphi_E) (\nabla d_E) \quad \text{where } \varphi_E = \max \left(0, 1 - \frac{d_{iE}}{(d_{coff})(r_i)} \right)$$

6.2.8 Contact Forces

An individual's desire to avoid collisions with other pedestrians led to the development of force-based models within PEDFLOW to account for intermediate-range and close-range collision avoidance. PEDFLOW conducts collision avoidance by first

checking to see if a collision will occur and then applies forces in the appropriate directions to elicit the desired collision avoidance behavior. A key assumption in the implementation of this model is that individuals are only influenced by their nearest-neighbors.

6.2.9 Pedestrian-Pedestrian Contact Forces

Even though pedestrians subconsciously try to avoid collisions, sometimes contact between pedestrians occurs. Once contact occurs, the repulsive forces will increase markedly and will behave symmetrically between the two pedestrians. To compute the contact forces, PEDFLOW first computes the closest distance and/or penetration (if the pedestrians overlap) using the method of multiple circles. If it is determined that the pedestrians will make contact, then the centroid and radius of the closest distance circle for each pedestrian is used to determine the repelling force. Given two pedestrians i and j who are determined to come in contact with one another, the normalized distance δ_{ij} between them is shown in Equation 57 where r_{ij} represents the sum of the two closest distance radii that were determined using the method of multiple circles.

Equation 57 Normalized Distance δ_{ij} Between two Pedestrians in PEDFLOW

$$\delta_{ij} = \frac{|\mathbf{x}_i - \mathbf{x}_j|}{r_{ij}} = \frac{|d\mathbf{x}_{ij}|}{r_{ij}}$$

To ensure uniform contact between the pedestrians, PEDFLOW multiplies a maximum force value $f_{max} \leq 8.0$ by a standardized relaxation time, $\frac{v_d}{\tau}$, where $v_d = 1.35$ and $\tau = 0.1$. Next, PEDFLOW computes a damping coefficient, $\beta_{damping}$, multiplies the damping coefficient by the relative velocity $(\mathbf{v}_j - \mathbf{v}_i) \cdot d\mathbf{x}$, and subtracts this term from the uniform force $f_{uniform}$ term. Lastly, the scenario specific conditions are again checked and, if they apply, the force is scaled appropriately by the value β . An example of such scaling would be a group of pedestrians in a theater who are looking for a particular seat and inevitably must contact others as they make their way down a row to their particular seat; in order to allow contact (and therefore enable the simulated pedestrian to get to his/her seat), the pedestrian-pedestrian contact force is reduced by one-half ($\beta = 0.5$). The complete model for the pedestrian-pedestrian contact force is given by Equation 58. As was stated before, this force due to contact term is a symmetric force and is, therefore, inversely applied to both pedestrians i and j , such that $\mathbf{f}_i = -f_{contact}d\mathbf{x}$ and $\mathbf{f}_j = f_{contact}d\mathbf{x}$.

Equation 58 Pedestrian-Pedestrian Contact Forces

$$f_{contact} = \beta \left(f_{uniform} - \beta_{damping} ((\mathbf{v}_j - \mathbf{v}_i) \cdot d\mathbf{x}) \right)$$

where

$$f_{uniform} = f_{max} \left(\frac{v_d}{\tau} \right)_{uniform}$$

$$f_{max} = \begin{cases} \max(0, a_\beta + b_\beta \delta_{ij}) & \text{if } \delta_{ij} > 1.0 \\ \min(8.00, a_\alpha + b_\alpha \delta_{ij}) & \text{if } \delta_{ij} \leq 1.0 \end{cases}$$

$$\beta_{damping} = \sqrt{\frac{f_{uniform}}{\max(|d\mathbf{x}| - r_{ij}, 0.25(r_i + r_j))}}$$

6.2.10 Pedestrian-Wall Contact Force

Just as pedestrians try to avoid colliding with other pedestrians, pedestrians also try to avoid contact with walls and other solid objects (such as columns, pillars, furniture items, and other stationary objects). In PEDFLOW all solid objects are assigned the same boundary conditions as walls and therefore, the pedestrian-wall contact subroutine computes the repulsive forces when contact between a pedestrian and any inanimate object occurs. To compute the contact forces, PEDFLOW first identifies all pedestrians within the simulation that are within a specified closeness tolerance to a wall, where this closeness tolerance is a multiple of the pedestrian's radius, r_i . A typical value for the closeness tolerance is two times r_i . If a pedestrian is within this closeness tolerance, then the minimum distance δ_{iW} from pedestrian i to the wall W is computed. Next, PEDFLOW multiplies a maximum force value $f_{max} \leq 8.0$ by pedestrian i 's relaxation time, $\frac{v_d}{\tau}$. PEDFLOW uses the value obtained for $f_{\delta_{iW}}$ to compute a damping coefficient, $\beta_{damping}$, as shown in Equation 59. The damping coefficient is then multiplied by the pedestrian's velocity in the normal direction and subtracted from the distance-to-wall force term $f_{\delta_{iW}}$. In cases where the pedestrian is very close to the wall (i.e., touching the wall), the pedestrian's velocity is checked to see if the pedestrian is moving towards the wall or away from the wall. If the pedestrian is moving towards the wall, the force is multiplied by a scenario-specific scaling factor β to increase repulsion

and if the pedestrian is moving away from the wall, the force is multiplied by a different scaling factor β that will reduce the force.

Equation 59 Pedestrian-Wall Contact Force

$$f_{contact} = \beta \left(f_{\delta_{iW}} - \beta_{damping} (\mathbf{v}_i \cdot \nabla W) \right)$$

where

$$f_{\delta_{iW}} = f_{max} \left(\frac{v_d}{\tau} \right)$$

$$f_{max} = \begin{cases} \max \left(0, a_\beta + b_\beta \frac{\delta_{iW}}{r_i} \right) & \text{if } \delta_{iW} > r_i \\ \min \left(8.00, a_\alpha + b_\alpha \frac{\delta_{iW}}{r_i} \right) & \text{if } \delta_{iW} < r_i \end{cases}$$

$$\beta_{damping} = \sqrt{\frac{f_{\delta_{iW}}}{\max(r_i, \delta_{iW})}}$$

6.3 Advancing the Pedestrians

Following the computation of the force vector, PEDFLOW uses this value, the pedestrian's maximum desired velocity, and the pedestrian's radius to determine the best Δt to use. The argument is that a pedestrian's velocity should not change more than a fraction of his/her desired velocity. Once the appropriate Δt is found PEDFLOW then updates the pedestrian velocities as shown in Equation 60.

Equation 60 Velocity Update

$$\mathbf{v}_{n+1} = \mathbf{v}_n + \Delta t \sum \mathbf{f}$$

Following this update (and prior to moving the pedestrians), PEDFLOW checks to see if the pedestrian velocities should be adjusted in some way due to scenario-dependent situations (Figure 39); for example, a pedestrian’s velocity might be reduced due to high densities, closeness to walls or other obstacles, or an injury, but might be increased if pedestrian is on a moving walkway or traveling up an escalator, and finally the velocity might be set to zero if the pedestrian is seated, stopped by traffic lights, or riding in an elevator.

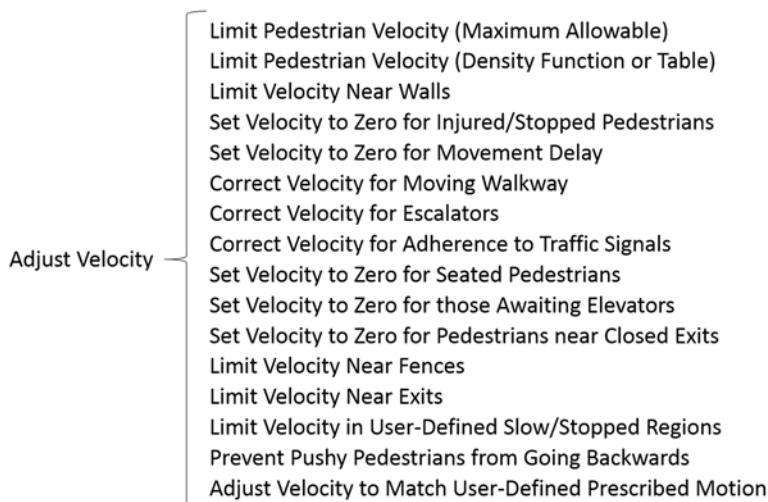


Figure 39 Velocity Adjustment Routines Available in PEDFLOW

Once the new velocity v_{adj} is determined, the pedestrian is advanced within the simulation according to Equation 61.

Equation 61 Position Update

$$\mathbf{x}_{n+1} = \mathbf{x}_n + \Delta t \mathbf{v}_{adj}$$

6.4 Evaluation of PEDFLOW as an Evacuation Model

Although the PEDFLOW simulation software described in this chapter has been in development and use at GMU for more than 10 years, it is not one of the ones currently evaluated by Kuligowski et al. [54], [55] nor has it been reviewed on the EvacMod.net portal [56]. Since the primary purpose of this dissertation concerns the use of PEDFLOW in evacuation simulations, a review of PEDFLOW using the evaluation criteria established by Kuligowski et al. was conducted at the start of this research project. Table 3 shows the initial evaluation of PEDFLOW using the main feature categories and corresponding labels as described by Kuligowski et al.

Table 3 Initial Evaluation of PEDFLOW According to Main Features [55]

Category	Remarks	Label
Available to Public	Yes, for a fee	Y
Modeling Method	Movement model	M (PB)
Purpose	Any type of building	1
Grid/Structure	Continuous	Co
Perspective of Model/Occupant	Individual/Global	I/G
Behavior	No behavior	N (I/P)
Movement	Inter-person distance	ID
Fire Data	Import	Y1
CAD	Import	Y
Visualization	In Paraview	Y
Validation	Past experiments	PE (FD)

In addition to the main features, Kuligowski et al. describe several special features that may interest users. These special features enable the simulation of more

sophisticated evacuation scenarios. At the start of this project, PEDFLOW contained the two-thirds of the special features described by Kuligowski et al. as shown in Table 4.

Table 4 Initial Evaluation of PEDFLOW According to Special Features [55]

Category	Label
Counterflow	Y
Exit block/obstacles	Y
Fire conditions	N
Toxicity	N
Defining groups	Y
Disabilities/slow occupant groups	Y
Delays/pre-evacuation times	N
Elevator use	Y
Route choice of the occupants	Optimal

At the start of this research project, PEDFLOW’s evacuation simulations were most basic; all pedestrians would start to evacuate immediately and choose an exit which would allow them to exit in the shortest-time available. PEDFLOW could not be used to run scenarios that would incorporate many of the special features of egress models described by Kuligowski et al. in their report. For example, PEDFLOW did not have the capability to account for pre-evacuation delay, could not demonstrate how environmental conditions affects pedestrian behaviors, nor simulate incapacitation due to toxicity. As will be shown in the subsequent chapters, the evacuation-inspired work contained in this dissertation led to some significant improvements within PEDFLOW.

7 VERIFICATION OF PEDFLOW

Realizing that several of the special features of evacuation models described by Kuligowski et al. in the previous chapter would require specific subroutine modifications and/or additions to PEDFLOW, this study began with the process of verifying PEDFLOW's current capabilities and making modifications as necessary. With no international standards for verification and validation of pedestrian flow and crowd dynamic simulation tools, researchers often apply inconsistent procedures, use unreliable data, or only partially test the simulation tools. In an attempt to develop a verification and validation standard for building fire evacuation models, researchers at NIST [86] recommended a set of seventeen verification tests spanning five core components: 1) pre-evacuation time, 2) movement and navigation, 3) exit usage, 4) route availability, and 5) flow constraints. The application of these seventeen verification tests to a PEDFLOW led to some rather significant improvements to the code for approximately half of the recommended tests (Table 5). In some cases, capabilities were added to PEDFLOW that did not exist before. In other cases, anomalous behaviors were found and the existing code was adjusted to remove these unexplained behaviors. This chapter summarizes the work on the verification tests, highlighting the lessons learned and modifications made to the code as a result. In addition, several recommendations for improvement were

provided to NIST during the 2014 PED conference and those recommended modifications are provided here.

Table 5 Summary of NIST Verification Tests as Applied to PEDFLOW

NIST ID	Sub-element	Capability Existed	Code Modified	Capability Added	Remarks
1.1	Pre-evacuation time distributions			√	
2.1	Speed in a corridor	√			
2.2	Speed on stairs		√		Adjusted pedestrian speed compensation on incline/decline
2.3	Movement around a corner	√			
2.4	Assigned demographics		√		
2.5	Reduced visibility vs walking speed			√	
2.6	Occupant incapacitation			√	
2.7	Elevator usage	√-			Not used in PEDFLOW evacuation scenarios
2.8	Horizontal counter-flows (rooms)		√		
2.9	Group behaviors	√			
2.10	People with movement disabilities		√		Modified test to represent ramp (8.33% grade); adjusted wheelchair speed on incline/decline
3.1	Exit route allocation	√			Occupants select nearest exit
3.2	Social influence			√	
3.3	Affiliation			√	
4.1	Dynamic availability of exit	√			
5.1	Congestion	√			
5.2	Maximum flow rates		√		Anomalous behavior discovered

7.1 Description of NIST Verification Tests

In November 2013, researchers from the United States' NIST Fire Research

Division in conjunction with researchers from the Department of Fire Safety Engineering and Systems Safety at Lund University published a set of seventeen hypothetical

verification test cases for use in quantitatively and qualitatively verifying results produced by the fire evacuation models. The NIST researchers developed this set of test cases, some of which were based on similar verification tests developed by the International Maritime Organization [87] and shared by the German RiMEA guidelines [88], [89], as a means to open a debate and contribute to an on-going effort by the International Standards Organization to develop an overall assessment standard for evacuation models.

Although PEDFLOW was not specifically designed for fire evacuation, applying these recommended test cases to PEDFLOW will serve four main purposes. First, the test cases provide a basic set of simple geometries and pedestrian populations which allows those unfamiliar with PEDFLOW to get used to setting up scenarios and running simulations. Second, the comprehensive nature of the tests will identify capability shortfalls within PEDFLOW and prompt the addition of capabilities that did not exist before. Similarly, the quantitative and qualitative expectation associated with each test case easily highlights anomalous behaviors and identifies the need for code modifications to remove these unexplained behaviors. Lastly, once run, the results obtained from the test cases provide a benchmark for future post-development versions.

7.2 Existing Capabilities

Of the seventeen verification tests listed in Table 5, PEDFLOW had the capability to complete seven of the tests with little-to-no modifications. PEDFLOW successfully accomplished four of the ten verification tests associated with movement and navigation, the second core component of evacuation models: 1) speed in a corridor; 2) movement

around a corner; 3) elevator usage (although not available for evacuation scenarios); and 4) group behaviors. PEDFLOW also had the capability to complete three other verification tests outside the movement and navigation core component: 1) exit route allocation from the exit choice/usage core component, 2) dynamic availability of exit from the route available core component, and 3) congestion from the flow constraint core component.

7.2.1 NIST Verification Test 2.1: Speed in a Corridor

Speed in a corridor is a quantitative verification test in which PEDFLOW simply confirms that a pedestrian walks the length of a corridor at his/her assigned speed. Given a corridor 2 meters wide by 40 meters long and one pedestrian with a horizontal walking speed of 1 m/s, PEDFLOW confirmed that the pedestrian traverses the entire length of the corridor in 40 seconds. A recommended additional test would be to also test this scenario with an input flux of 1 ped/sec, assigning each pedestrian a walking speed of 1 m/s. The expected result would be a line of pedestrians spaced approximately 1 meter apart walking along the entire length of the corridor with an average velocity of 1 m/s.



Figure 40 Geometric Definition and Initial Pedestrian Placement for Verification Test 2.1

7.2.2 NIST Verification Test 2.3: Movement around a Corner

Movement around a corner is a qualitative verification test where PEDFLOW demonstrates that twenty uniformly distributed pedestrians can successfully navigate a

corner. For the purposes of this verification test, "uniformly distributed" meant evenly distributed and an input file was used to initialize the pedestrians at specific locations rather than randomly distributed uniform locations. Post-processing the data using Paraview as the visualization tool, provided visual confirmation that all twenty pedestrians navigate the corner without penetrating any barriers (Figure 41). This verification test is an excellent tool to use in order to illustrate the differing methods of defining paths in PEDFLOW.

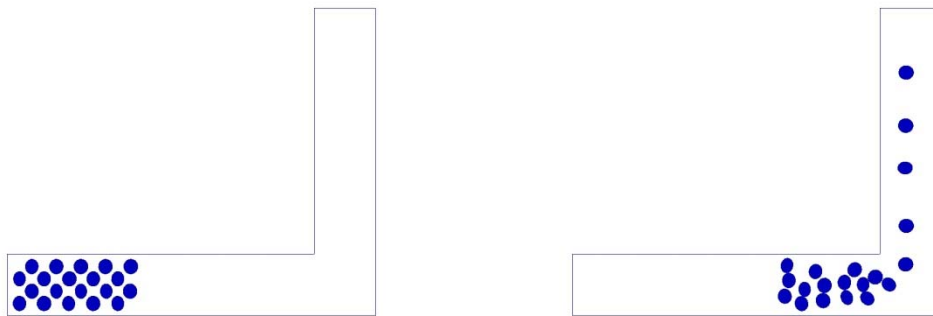


Figure 41 Geometric Definition, Pedestrian Initialization, and Qualitative Verification for Verification Test 2.3

7.2.3 NIST Verification Test 2.7: Elevator Usage

Although PEDFLOW previously included an elevator sub-model, the elevator is currently not a viable egress component within PEDFLOW. As currently coded, in evacuation situations everyone heads towards the nearest exits (defined as an in/out boundary condition) following a 'time-to-exit' gradient direction that is applied to the geometric mesh. The elevator is excluded from this mesh (the assumption was that people are not supposed to use elevators in an evacuation/fire situation) and therefore is not

available in evacuation simulations. However, in a non-evacuation simulation, elevator usage was quantitatively and qualitatively verified as outlined in the NIST paper (Figure 42). In the simulation, the pedestrian begins on the second floor, walks to the elevator and waits on the elevator to arrive. Once the elevator arrives, the pedestrian enters the elevator and rides the elevator to the first floor where the pedestrian then exits the elevator and leaves the building in a total time of 64 seconds. Including the elevator as a viable means of evacuation within PEDFLOW is an area requiring further development.

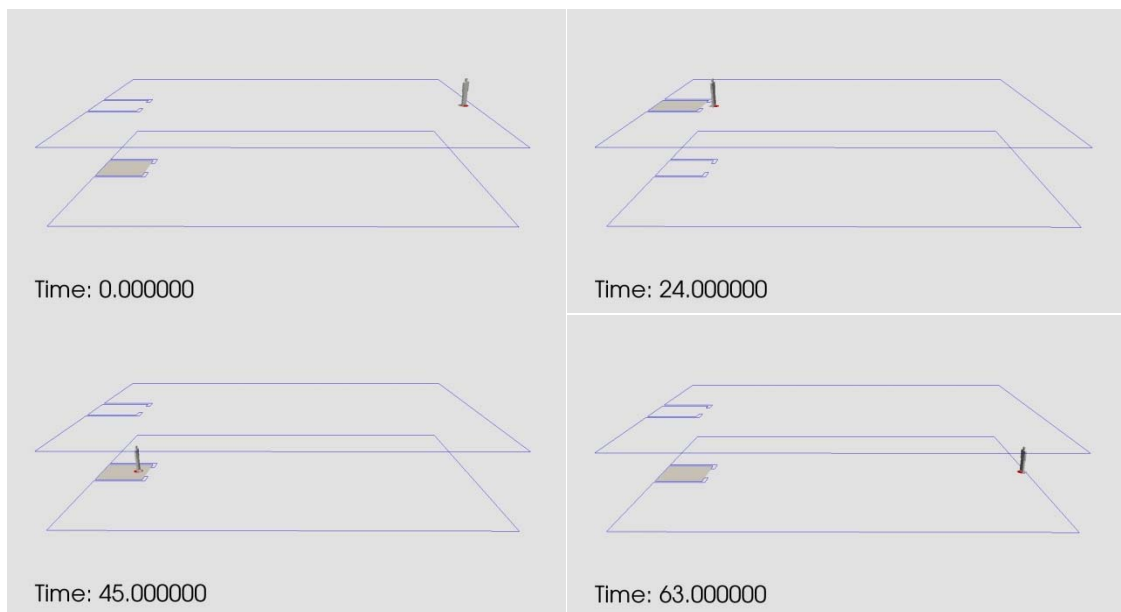


Figure 42 Verification of Elevator Usage in PEDFLOW (Verification Test 2.7)

7.2.4 NIST Verification Test 2.9: Group Behaviors

Group behaviors is a qualitative test of PEDFLOW's ability to replicate group dynamics, namely the ability of a group of individuals to stay together while exiting a room. PEDFLOW provides the user an opportunity to define many group types with

various behaviors. Some of the choices for groups behaviors include: 1) try to go to leader; 2) try to go parallel to leader; 3) try to go behind the leader (sophistic group, see Plato's "Protagoras"); 4) try to form a row (loose connection) behind the leader; 5) try to form a chain (strong connection) behind the leader; and 6) amoeba, force based group association. In addition, the user is able to set the maximum separation distance allowed before leaders begin to slow, as well as the maximum separation distance allowed before a group is split and/or separated for both low and high densities. For the purposes of the NIST verification test, a maximum separation distance of 3 meters before the leader slows was used and a group split distance threshold of 15 meters for low densities and 14 meters for high densities was applied. These values ensured the group stayed together and all members of the group exited the room within 8 seconds of each other (Figure 43).

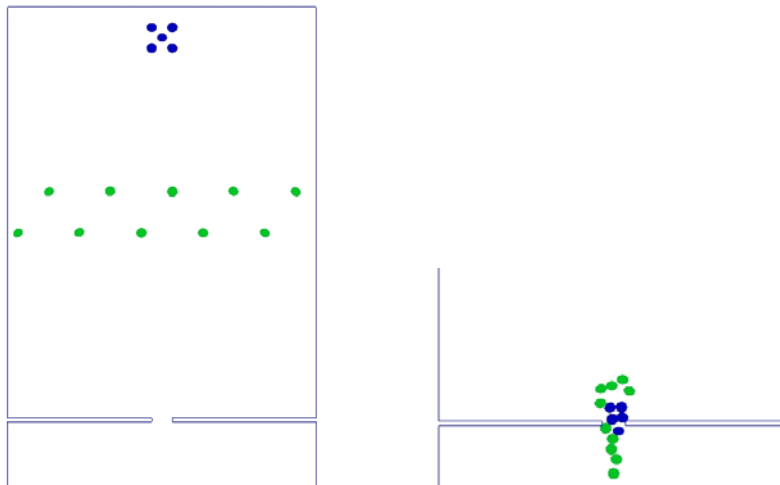


Figure 43 Geometric Definition, Pedestrian Initialization, and Group Cohesion through Exit for Verification Test 2.9

7.2.5 NIST Verification Test 3.1: Exit Route Allocation

In the exit route allocation verification test, PEDFLOW successfully demonstrated that, in evacuation mode, all pedestrians exit the building via the nearest exit (exit route is dynamically selected based upon shortest time to exit). The pedestrians were distributed among the twelve rooms as shown in Figure 44 in accordance with Figure 8 from Ronchi et al. [86]. The pedestrians were randomly assigned horizontal walking speeds of $1.25 \text{ m/s} \pm 10\%$, with a relaxation time of 0.5 m/s . Pedestrian size was assigned with a radius of $0.25 \text{ m} \pm 2\%$ and an ellipticity range between 0.0 and 0.5 . The minimum exit time was 3.05 seconds and the maximum exit time was, on average, around 17 seconds.

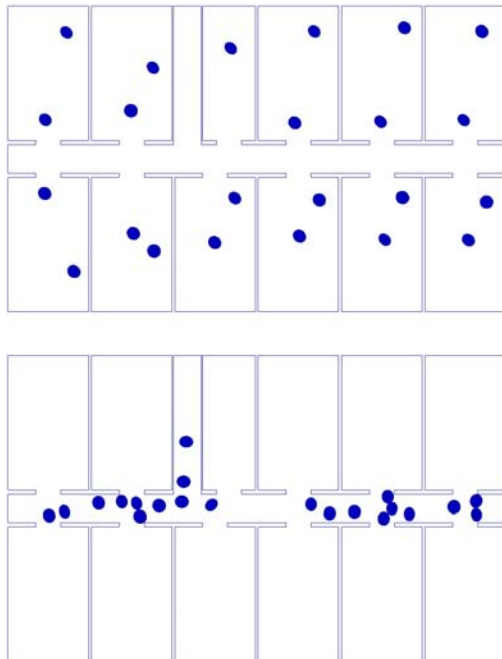


Figure 44 Geometric Definition, Initial Pedestrian Locations, and Qualitative Verification of Exit Selection for Verification Test 3.1

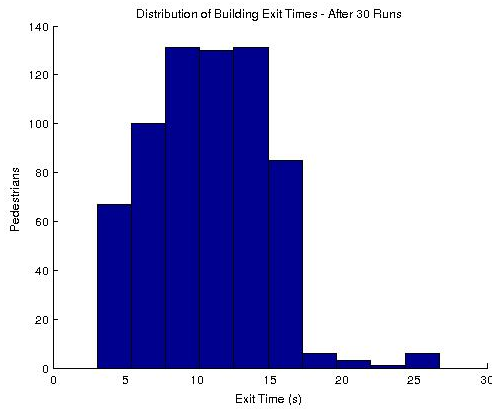


Figure 45 Building Exit Time Distribution after 30 Simulation Runs

7.2.6 NIST Verification Test 4.1: Dynamic Availability of Exit

Dynamic availability of exit is a qualitative verification test which demonstrates PEDFLOW's ability to close an exit and have the pedestrian(s) dynamically find an alternate exit. The user has the ability to define a scenario-dependent file in PEDFLOW which limits outflow fluxes. Setting an outflow flux to zero effectively closes off the exit and the evacuee will dynamically find an alternate exit. In addition, PEDFLOW has the ability to define paths that are modified in time, making it possible to not only close an exit, but cut-off an entire exit route within a building. When a path is interrupted PEDFLOW dynamically finds an alternate path to an exit.

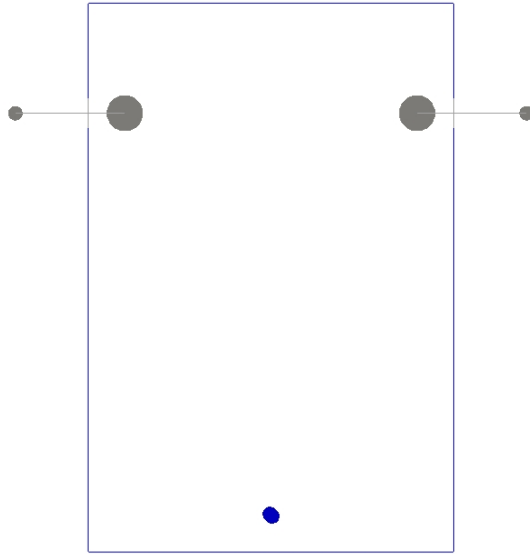


Figure 46 Geometric Definition and Initial Pedestrian Placement for Verification Test 4.1

7.2.7 NIST Verification Test 5.1: Congestion

The congestion verification test is a qualitative verification test intended to verify how well the simulation tool simulates congestion. In this case, this verification test intends to verify flow constraints in a staircase. The capability to simulate congestion previously existed in PEDFLOW; however, the specifications of this test failed to form congestion at the base of the stairs as intended (Figure 47). As can be seen from Figure 44, congestion does form at the exit of the room, but the flow limitation through the opening from the room simply prevents congestion on the stairs. Although the test specified in [86] was intended to test movement in the downward direction, it was beneficial to perform the test in both directions.

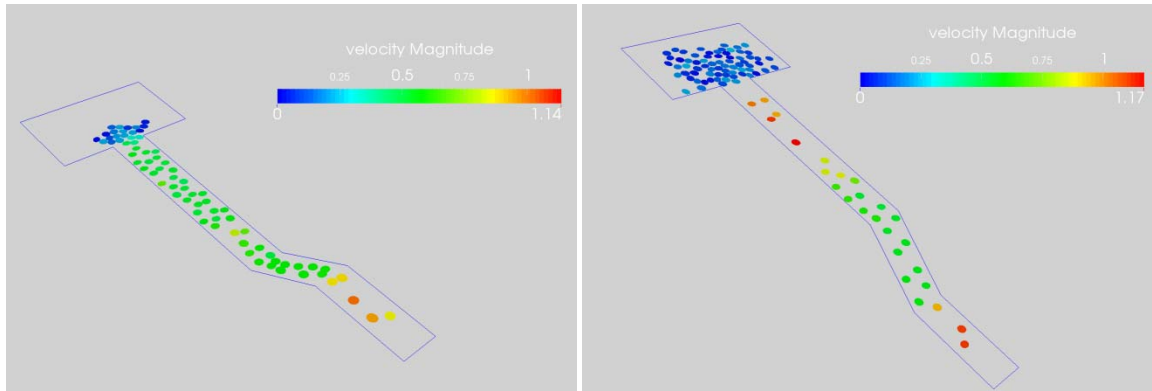


Figure 47 Comparison of Velocity in both the Upward (left) and Downward (right) Directions for Verification Test 5.1 (notice lack of congestion at the top of the stairs)

7.3 Modified Capabilities

In addition to the seven pre-existing PEDFLOW capabilities, there were five capabilities which existed but needed improvement. Four of these capabilities were from the movement and navigation core component, namely speed on stairs, assigned occupant demographics, horizontal counterflows, and people with movement disabilities. The fifth capability came from the flow constraint core component where anomalous behaviors were discovered.

7.3.1 NIST Verification Test 2.2: Speed on Stairs

The speed on stairs verification test quantitatively confirms a pedestrian's ability to travel up or down a flight of stairs at his/her assigned speed. Since each pedestrian is assigned only a horizontal (desired) velocity in PEDFLOW, the code makes appropriate velocity corrections for travel up/down both ramps and stairs.

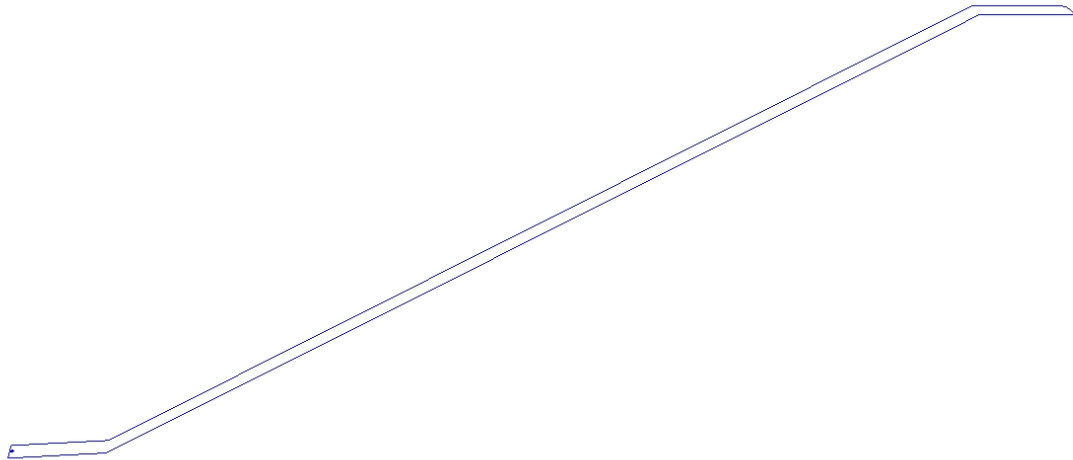


Figure 48 Geometric Definition and Initial Pedestrian Placement for Verification Test 2.2

While not explicitly specified by the NIST verification requirements for this test case, it is desirable to first conduct two additional tests which compute pedestrian adjusted velocities on ramps in the upward and downward directions (Figure 49). In fact, by doing these tests an anomaly was found for pedestrians traveling down the ramp and PEDFLOW's subroutine was modified to ensure accurate quantitative results.

Geometry: a ramp 2 meters wide with a length of 100 meters measured along a 30° incline.
Scenario: one pedestrian with an assigned horizontal walking speed of 1 m/s traverses the ramp in the (a) upward and (b) downward directions.
Expected Result: the pedestrian is expected to cover the distance in 100 seconds when traveling upward and 70 seconds when traveling downwards.

Figure 49 Recommended Additional Verification Test (Speed on Ramps)

Once convinced that the pedestrians were traveling with appropriate velocities up and down the ramp, the actual verification requirement to verify the speed on stairs was undertaken. In order for PEDFLOW to properly compute the speed on stairs, the step height and tread depth must be provided (both of which were not given in the NIST paper). A typical riser height used is 7 inches (0.18 m) and tread depth is 11 inches (0.28 m), which results in a stair gradient of approximately 32.7°. To maintain the 30° gradient already established in the ramp verification test, a step height of 0.154 meters and a tread length of 0.267 meters was used. Choosing these values allowed the use of the same geometric definition already established for the ramp with the inclusion of the stair steps. Two anomalies were immediately recognized. First, the velocity of the pedestrian was the same when traveling up or down the stairs and secondly, the speed of the pedestrian was significantly reduced (by more than 60%) when traversing the staircase. A pedestrian with an unimpeded horizontal velocity of 1.0 m/s was restricted to a velocity of 0.289 m/s when traveling the stairs in either direction.

In 2004 at the 10th International Conference on Mobility and Transport for Elderly and Disabled People, Fujiyama and Tyler [90] presented a rather complete set of empirical stair data (Figure 50). Their study consisted of two subject groups: a group of 6 healthy men and 12 healthy women between the ages of 60 and 81 (Group 1), and a second group consisting of 7 healthy men and 8 healthy women between the ages of 25 and 60 (Group 2). They measured the normal walking speeds and fast walking speeds of each participant on a horizontal surface and when ascending/descending four individual flights of stairs. The stairs had differing step riser heights and tread lengths, resulting in

stair gradients ranging from 24.6° to 38.8°. Fujiyama and Tyler noted that the participants in their study showed a high correlation between horizontal walking speed and speed on stairs and hypothesized that this is somehow related to the individual's step frequency.

Patterns of speeds	Stairs		Group1	Group2	Significance of Difference
	Stair No	Degree			
Normally ascending	Stair 1	38.8	0.44 ± 0.12	0.48 ± 0.10	NS
	Stair 2	35	0.52 ± 0.12	0.56 ± 0.13	NS
	Stair 3	30.5	0.59 ± 0.13	0.63 ± 0.14	NS
	Stair 4	24.6	0.73 ± 0.17	0.76 ± 0.17	NS
Normally descending	Stair 1	38.8	0.47 ± 0.13	0.59 ± 0.14	<0.05
	Stair 2	35	0.58 ± 0.16	0.65 ± 0.14	NS
	Stair 3	30.5	0.64 ± 0.15	0.74 ± 0.17	NS
	Stair 4	24.6	0.80 ± 0.23	0.87 ± 0.19	NS
Fast ascending	Stair 1	38.8	0.61 ± 0.18	0.78 ± 0.24	<0.05
	Stair 2	35	0.69 ± 0.20	0.91 ± 0.31	<0.05
	Stair 3	30.5	0.79 ± 0.20	0.97 ± 0.28	<0.05
	Stair 4	24.6	1.00 ± 0.23	1.16 ± 0.31	NS
Fast descending	Stair 1	38.8	0.62 ± 0.17	0.87 ± 0.20	<0.001
	Stair 2	35	0.70 ± 0.18	0.92 ± 0.19	<0.01
	Stair 3	30.5	0.84 ± 0.18	1.08 ± 0.23	<0.01
	Stair 4	24.6	1.01 ± 0.26	1.18 ± 0.20	<0.05
Normal walking on a flat surface			1.31 ± 0.23	1.40 ± 0.17	NS
Fast walking on a flat surface			1.71 ± 0.29	1.84 ± 0.15	NS

Results are given as mean ± SD.

Significance of difference tested using unpaired *t* tests.

NS = not significant

Figure 50 Empirical Stair Data (extracted from [90])

Exploring this theory, a new formula based on parametric values obtained from Fujiyama and Tyler's empirical data was devised (see Chapter 8). In general, a pedestrian's step frequency is simply the product of a person's desired velocity and the inverse of their step size. On a horizontal surface, the often assumed step size value is 0.8 meters which equates to a step frequency of 1.25 steps per second for a person with a desired horizontal velocity of 1.0 m/s. Using the data provided by Fujiyama and Tyler,

the corrected step size for a person traveling up a flight of stairs was found to be approximately 0.5 meters and the corrected step size for a person descending a flight of stairs is approximately 0.66 meters. Using these values and the modified PEDFLOW subroutine in equates to the observed simulation values of 0.463 m/s when the pedestrian is ascending the stairs and 0.502 m/s when descending (Figure 51).

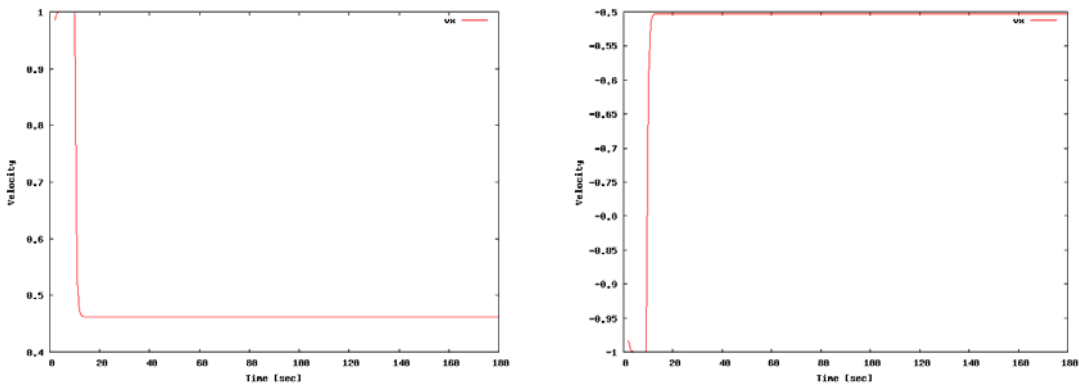


Figure 51 Improved PEDFLOW Velocity Curves when Traveling Up (left) and Down (right) a 30° Staircase

7.3.2 NIST Verification Test 2.4: Assigned Occupant Demographics

The next modified verification test, assigned occupant demographics, is a quantitative verification of the simulation tool's ability to properly assign pedestrian characteristics. To provide maximum flexibility, numerous pedestrian demographic options exist within PEDFLOW (Figure 52). Occupant types can be defined as either (1) pedestrians or (2) wheelchairs with user-specified averages and variations (defined as a percentage) available for the following characteristics: 1) velocity, 2) relaxation time, and 3) pedestrian size (radius). In addition, the user may also specify limits (max/min) for the following additional characteristics: 1) ellipticity, 2) pushiness, and 3) desired comfort

zone. In order to verify the assignment process within PEDFLOW, the characteristic data was output to a file and the assigned values were compared with the distribution desired. By completing this verification test, it was discovered that PEDFLOW was assigning all pedestrian characteristics using a uniform distribution when, in fact, a Gaussian distribution was desired for the velocity assignments. Without the benefit of these verification tests, this anomaly may have remained undiscovered.

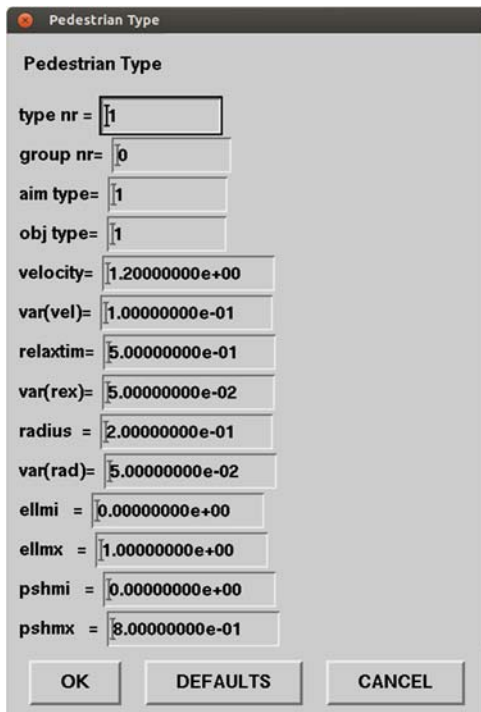


Figure 52 Assignment of Pedestrian Characteristics within PEDFLOW

7.3.3 NIST Verification Test 2.8: Horizontal Counterflows

Horizontal counter-flows, tests PEDFLOW's ability to simulate and reproduce emergent behaviors in uni-directional and bi-directional flows in a corridor. Upon initial

testing of the uni-directional verification test, some of the pedestrians displayed anomalous behaviors (such as moving to a random corner of the room prior to exiting the room). The problem was traced to one of the object collision algorithms, which was subsequently improved. While testing the bi-directional flows using opposing paths, the simulation would typically display what Helbing et al. [19] called "freezing-by-heating", or a complete stalemate, whereby none of the pedestrians could move. To solve this problem, the path input instructions were modified, requiring paths to be defined on half the corridor for pedestrians moving in each direction. Defining the paths this way does not prevent the pedestrians from using the entire corridor, but gives each group of pedestrians a tendency to stay to a particular side of the corridor. This may also be seen as a 'cultural behavior' (preferring the right side) that requires demographic information.

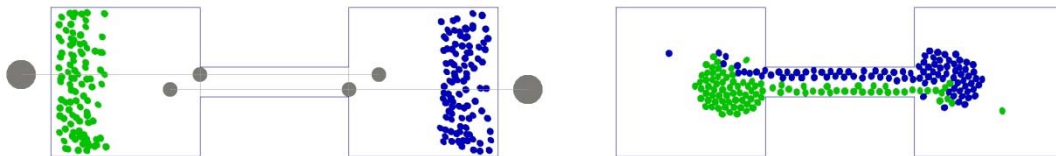


Figure 53 Geometric Definition, Initial Pedestrian Positions, and Horizontal Counterflow with “Cultural Behavior”

Table 6 Room 1 to Room 2 Traversal Time Statistics after 30 PEDFLOW Simulation Runs

Direction	Minimum (s)	Maximum (s)	Average (s)
Uni-directional (100 peds)	90	173	114.8
Bi-directional (100 vs 10)	96	142	108.6
Bi-directional (100 vs 50)	122	156	134.5
Bi-directional (100 vs 100)	120	271	176.9

7.3.4 NIST Verification Test 2.10: People with Movement Disabilities

The final verification test in the movement and navigation core component is the people with movement disabilities verification test. This test is intended to verify the simulation tool's ability to simulate a pedestrian with reduced mobility and increased space requirements (such as a wheelchair).

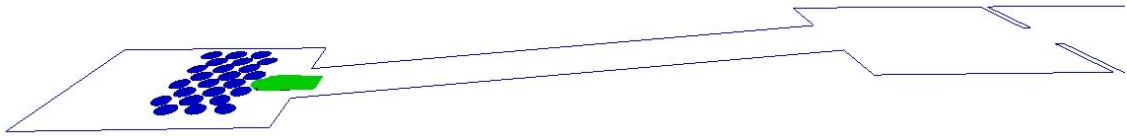


Figure 54 Geometric Definition and Initial Pedestrian Placement for Verification Test 2.10

The ability to define pedestrians as wheelchair occupants was pre-existing in PEDFLOW. In order to perform the test as outlined in the paper by Ronchi et al. [86], the geometry must be modified first since, as published, the ramp was too steep for a wheelchair. According to Fruin [3], the ramp should not exceed a 8.33% grade. Since the change in height between the two rooms was prescribed as 1 meter, the geometry shown in Figure 7 of [86] was modified to a ramp 12 meters long (rather than 2 meters). As can be seen from Table 7, the pedestrians took, on average, approximately five seconds longer to exit the room when following the wheelchair up or down the ramp.

Table 7 Room Exit Time Statistics after 30 PEDFLOW Simulation Runs

Lead Occupant	Ramp Direction	Minimum (s)	Maximum (s)	Average (s)
Wheelchair	Up	46	52	48.83
Pedestrian	Up	43	46	44.23
Wheelchair	Down	45	50	47.97
Pedestrian	Down	41	45	43.37

7.3.5 NIST Verification Test 5.2: Maximum Flow Rates

The maximum flow rate verification test confirms the simulation tool's ability to set flow rates. The user must place 100 occupants in the room, assign a specific maximum flow rate for the exit and ensure that the flow rate never exceeds the established threshold. During the initial attempt at this verification test, an anomalous behavior in the pedestrian initialization subroutine was discovered and the code was corrected. Once corrected, PEDFLOW confirmed that, with a limiting exit flux of 1 person per second, it takes 100 seconds for 100 pedestrians to exit the room (versus just 55 seconds when no limiting flux is present).

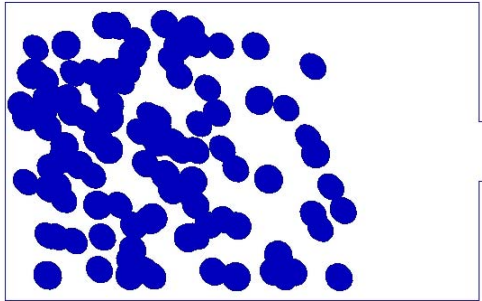


Figure 55 Geometric Definition and Initial Pedestrian Placement for Verification Test 5.2

7.4 Added Capabilities

Completion of the seventeen verification tests led to the addition of five capabilities which did not previously exist in PEDFLOW. The ability to assign pre-evacuation time delays did not exist nor did the ability to slow/incapacitate pedestrians due to reduced visibility or the inhalation of toxic materials. Exit route/choice was also severely limited by PEDFLOW's singular ability to force a pedestrian to select the nearest exit without consideration for social influence or route familiarity (affiliation). In addition, PEDFLOW uses a lot of random number generation. By specifying a different identifier in an initialization file, the initialization of the random numbers is changed, so that statistical data can be obtained from many PEDFLOW runs that use the same deterministic data but use different random data. The addition of these capabilities has significantly improved the robustness of PEDFLOW.

7.4.1 NIST Verification Test 1.1: Pre-evacuation Delay Times

The first core component of evacuation modeling concerns pre-evacuation time. In an evacuation scenario, pre-evacuation time is often categorized as the time an

individual needs for recognition and response, or in other words, the time elapsed from the initial sounding of an alarm to the time when the individual decides to act (evacuate, shelter-in-place, seek additional information, etc.). The verification test for this component confirms the simulation tool's ability to distribute a set of pre-evacuation time delays among the population. Prior to the application of this particular test, the capability to assign evacuation delay times did not exist in PEDFLOW. With the capability now added, users may now choose one of three delay options during an evacuation run: 1) no delay, 2) a delay based on a Gaussian random number, or 3) a delay based on a table of user-defined probabilities.

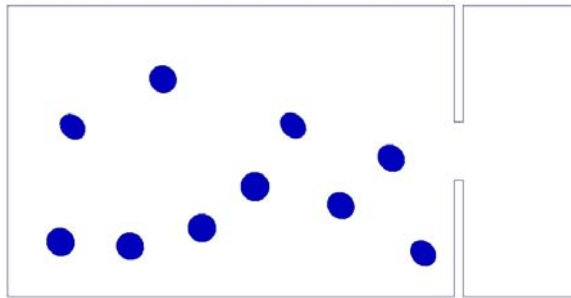


Figure 56 Geometric Definition, Initial Pedestrian Placement for Verification Test 1.1

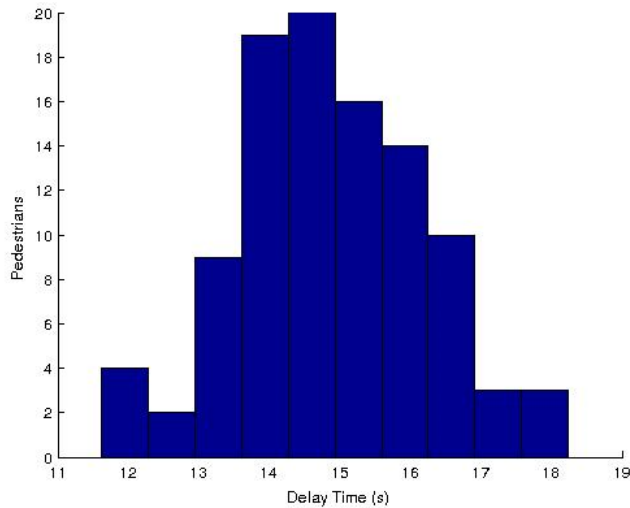


Figure 57 Pre-evacuation Delay Distribution after 10 runs (Verification Test 1.1)

7.4.2 NIST Verification Tests 2.5 & 2.6: Reduced Visibility vs. Walking Speed & Occupant Incapacitation

Prior to completing these verification tests, PEDFLOW had limited abilities to account for the physical impacts of smoke and other toxic materials on the pedestrian (smokeinhale previously existed). The user is now able to input a maximum smoke concentration level which leads to zero movement, or total impedance, as well as a value for toxic material inhalation which leads to incapacitation for each pedestrian type.

Given these values, PEDFLOW reads in smoke and toxicity data from an input file, interpolates concentrations across the domain, and then updates pedestrian health. The inhalation of toxic material is still monitored, but the pedestrian now becomes incapacitated if the levels exceed the established threshold. Using an established respiration rate of 15 liters per minute, PEDFLOW accumulates the total amount of toxic material inhaled based upon the pedestrian's current position in the domain and the interpolated toxicity levels at that location. After each update, PEDFLOW checks the

pedestrian's current toxic inhalation levels and marks the pedestrian incapacitated if the level exceeds the established threshold.

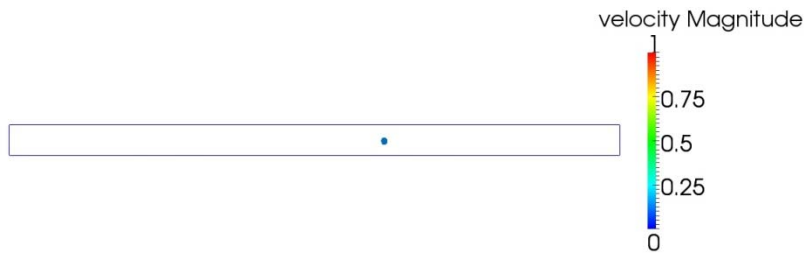


Figure 58 Geometric Definition and Initial Pedestrian Placement for Verification Test 2.5

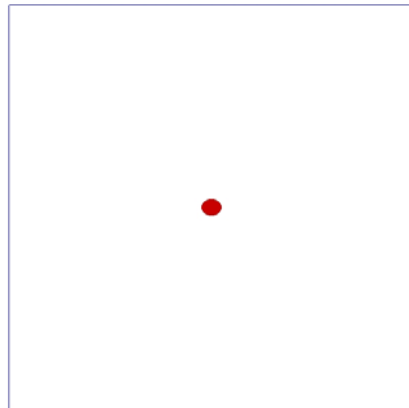


Figure 59 Geometric Definition and Initial Pedestrian Placement for Verification Test 2.6

In order to limit the pedestrian's walking speed in conditions where visibility is limited, a new subroutine was created which corrects the pedestrian's desired velocity for conditions of dense smoke. When smoke is present in the domain, the velocity reduction coefficient is computed as the maximum of two values as shown in Equation 62.

Equation 62 Velocity Reduction Coefficient for Conditions of Limited Visibility

$$c_{redu} = \max(c_{min}, 1 - \frac{\rho_{smoke}}{\rho_{max}})$$

For these purposes, assume that even in the most dense smoke (as long as the pedestrian doesn't succumb to an inhalation injury), the pedestrian is still able to crawl; therefore, $c_{min} = 0.1$. The variable ρ_{smoke} is the smoke concentration level at the pedestrian's current location in the domain and ρ_{max} is the user-defined value for the maximum smoke concentration level leading to zero movement. Given the velocity reduction coefficient, the pedestrian's corrected velocity adjusted for smoke density is then the minimum of the pedestrian's current velocity or the pedestrian's desired velocity reduced by the velocity reduction coefficient as shown in Equation 63.

Equation 63 Corrected Velocity for Conditions of Limited Visibility

$$v_{corr} = \min(v_{curr}, c_{redu} * v_{desured})$$

7.4.3 NIST Verification Tests 3.2 & 3.3: Social Influence & Affiliation

The completion of these verification tests led to numerous additions to the scenario-specific simulation inputs. Prior to the completion of these tests, the only exit-choice behavior available during evacuation scenarios was exit selection based on shortest time to exit. PEDFLOW now has the ability to include social influence, computed as an average motion of neighbors, and affiliation, modeled as a pedestrian's

desired to choose his/her usual path, to evacuation scenarios, both capabilities which simply did not exist before. In the case of social influence, the pedestrian follows the direction of pedestrians that "know" where they are going; however, if there are no "knowing" neighbors around, the pedestrians continue to the nearest available exit. For the affiliation case, the pedestrian always follows his/or her assigned (affiliated) path to the exit. The evacuation subroutine also includes the ability to define a mixture of these exit-choice behaviors for each pedestrian type.

7.5 Suggested Improvements to Recommended Test Cases

During the 2014 PED conference, Isenhour and Löhner presented the application of these recommended test cases to PEDFLOW [91], highlighting the lessons learned and modifications made to PEDFLOW and proposing the following recommendations for improvement: (1) for verification test 2.1, create a new test with an input flux of 1 ped/sec, assigning each pedestrian a walking speed of 1 m/s; the expected result would be a line of pedestrians spaced 1 meter apart along the entire length of the corridor; (2) for verification test 2.2, movement on stairs should be distinguishable from movement on ramps; therefore, recommend adding a test for movement on ramps (both directions) in addition to the recommended speed on stairs verification test; specify a ramp angle as well as a step height and tread length for consistency among the verification tests; (3) for verification test 2.3, define uniformly distributed; (4) for verification test 2.10, in order to assure nothing more than an 8.33% grade, modify the geometry shown in Figure 7 of [86] and make the ramp 12 meters long (rather than 2 meters); also, perform the verification

tests on the ramp in both the upward and downward directions; and (5) for verification test 5.1, perform the test in both directions; modify the test to ensure congestion on stairs.

Additionally, at the 2014 PED conference, Lubaś et al. [92] also analyzed the proposed NIST test cases and recommended a modification to the methodology suggested by NIST. Essentially, Lubaś et al. postulate that some of the tests proposed by NIST could be omitted in models that are designed for a particular or specific use. Therefore, they recommend that the tests break down into a basic set of verification tests (i.e., those tests that are applicable to all types of models) and an advanced set of tests that are dependent on model type, special features, and model applications. Moreover, Lubaś et al. proposed additional tests: (1) a test which measures velocity-density relationships for comparison with the fundamental diagram; (2) a test which verifies the model's ability to maintain group cohesion; (3) a test which checks for discretization errors; and (4) a test (or series of tests) which verify the qualitative phenomena often seen in pedestrian science such as stop-and-go waves, oscillations in counter-flow situations, freezing-by-heating effect, jamming, and lane formation.

7.6 Conclusion

The application of the seventeen verification tests recommended by NIST to the PEDFLOW simulation tool allowed the identification of several errors and anomalies. This led to rather significant improvements for approximately half of the recommended tests. Several cases led to new capabilities that did not exist before. And in other cases, anomalous behaviors were found, which led to an adjustment and corrections of the

existing code. Overall, this was a very valuable exercise. It is recommended that similar codes be also tested against this set of problems.

In addition, the performance of these verification tests revised PEDFLOW's evaluation against the categories as described by Kuligowski et al. [55]. Specifically, the additional capabilities that were added to PEDFLOW changed PEDFLOW's modeling method from a movement (M) only model to a partial-behavior (PB) model, improved the occupant's perspective of the building from a global (G) view to an individual (I) view, and incorporated some implicitly (I) defined, as well as some probabilistic (P), behaviors that were not available in PEDFLOW before (Table 8). Additionally, with the inclusion of pre-evacuation delay times, occupant incapacitation due to toxicity, and occupant response to reduced visibility conditions, PEDFLOW now contains all of the special features that were described by Kuligowski et al. (Table 9).

Table 8 Post-verification Evaluation of PEDFLOW According to Main Features [55]

Category	Remarks	Label
Available to Public	Yes, for a fee	Y
Modeling Method	Partial-behavior model	PB
Purpose	Any type of building	1
Grid/Structure	Continuous	Co
Perspective of Model/Occupant	Individual/Individual	I/I
Behavior	Implicit & Probabilistic	I & P
Movement	Inter-person distance	ID
Fire Data	Import	Y1
CAD	Import	Y
Visualization	In Paraview	Y
Validation	Past experiments	PE

Table 9 Post-verification Evaluation of PEDFLOW According to Special Features [55]

Category	Label
Counterflow	Y
Exit block/obstacles	Y
Fire conditions	Y
Toxicity	Y
Defining groups	Y
Disabilities/slow occupant groups	Y
Delays/pre-evacuation times	Y
Elevator use	Y
Route choice of the occupants	Optimal

8 PEDESTRIAN SPEED ON STAIRS: A MATHEMATICAL MODEL BASED ON EMPIRICAL ANALYSIS FOR USE IN COMPUTER SIMULATIONS

Recall from the previous chapter that while performing NIST Verification Test 2.2 – Speed on Stairs, an anomaly was discovered for pedestrians traveling on the stairs and the subroutines were modified in PEDFLOW to ensure accurate quantitative results. This chapter describes the mathematical model used within PEDFLOW and was presented during the 2016 Joint Mathematics Meeting [93].

A critical component of building evacuation simulations is pedestrian ascent and descent on stairs. Several researchers have conducted controlled laboratory experiments and performed observational studies in an effort to obtain empirical data and develop models that can be used to accurately predict the walking speed of pedestrians on stairs. Most recently, in 2014, Qu et al. [94] compiled an extremely thorough “state-of-the-art” summary of past experimental and observational data collection efforts, highlighting the studies of flow characteristics and evacuation processes. The availability and use of empirical data is essential to the calibration and validation of mathematical models used in computer simulations of pedestrian movement. This chapter will describe the mathematical model used in the PEDFLOW subroutine which adjusts a simulated pedestrian’s velocity to account for movement on stairs. In addition, this chapter will demonstrate how empirical data was used to determine individual step frequency on

stairs, how the model was verified (using NIST Verification Test 2.2) within PEDFLOW, and how the model performed against a newly collected set of empirical data.

8.1 Mathematical Model

In the absence of other pedestrians, it seems logical that an individual's speed on stairs is primarily dependent on two factors: the individual's normal walking speed or typical velocity on flat surfaces and the geometry of the stairs (i.e., riser height and tread depth). The assumption is that if an individual walks slow (or fast) on an unimpeded flat surface, then that same person will most likely also walk slow (or fast) when ascending or descending stairs. Therefore, it seems reasonable that a pedestrian's velocity on stairs could be computed by accounting for the slope of the stairs, the individual's horizontal step limitation as defined by the geometry of the stair (i.e., tread depth), and the frequency at which a person is able to physically step given the stair constraint as shown by Equation 64, where c_{slope} represents a speed adjustment coefficient based on the stair geometry (i.e., slope of the stair), d_{horz} limits the horizontal step to the size of the stair tread depth, and $freq$ denotes the number of steps per second a pedestrian takes while traveling on stairs.

Equation 64 Basic Velocity Correction Formula Used for Travel on Stairs

$$v_{corr} = (c_{slope})(d_{horz})(freq)$$

Since each pedestrian is assigned only a horizontal (desired) walking velocity in PEDFLOW, the code must make appropriate velocity corrections for travel up or down

stairs. In the case where the pedestrian travels up the stairs, one would expect velocity to decrease; therefore the velocity adjustment coefficient, c_{slope} , used in Equation 64 should have a value less than 1 and is modeled simply as the cosine of the stair angle (Equation 65). The blue line in Figure 60 illustrates the effect of the velocity adjustment coefficient (reduction factor) for travel up stairs; as the stair angle increases, the pedestrian's velocity will also decrease when ascending the stairs.

Equation 65 Velocity Reduction Coefficient for Stair Ascension

$$c_{slope} = \cos(\theta)$$

where

$$\theta = \text{atan}\left(\frac{d_{vert}}{d_{horz}}\right)$$

Similarly, if the pedestrian desires to descend the stairs, the computed velocity adjustment coefficient for the pedestrian should be greater than 1 which represents an increase factor due to gravity; however, this value should also be slightly higher for stairs with small gradients and then relatively smaller for stairs with steep gradients as it takes more physical effort counter gravity and carefully descend the stairs. The use of the formula shown in Equation 66 allows the pedestrian to walk slightly faster down stairs with small gradients, but walk relatively slower down stairs with steeper gradients (see the red line in Figure 60).

Equation 66 Velocity Reduction Coefficient for Stair Decent

$$c_{slope} = \cos(\theta) (1 - \sin(\theta) \cos(\theta))$$

where

$$\theta = \text{atan}\left(\frac{d_{vert}}{d_{horz}}\right)$$

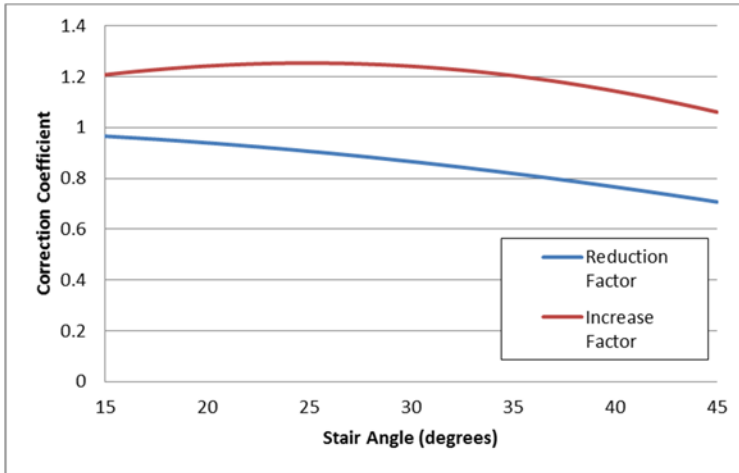


Figure 60 Ascent and Descent Velocity as a Function of Stair Angle

The first two components in Equation 64, c_{slope} and d_{horz} , adjust velocity based upon the given geometry of the stairs. Therefore, the third component, $freq$, must account for the pedestrian's desired walking speed on flat surfaces and adjust accordingly for travel on stairs. If an individual's step frequency is simply the number of steps a person takes per second, then this value can be computed by taking an individual's desired velocity and dividing by his/her normal step size as shown in Equation 67.

Equation 67 Individual Step Frequency

$$freq = (v_{desi}) \left(\frac{1}{s_{step}} \right)$$

For example, if an individual's desired velocity is 1.0 meters per second and their normal step size is 0.8 meters, then Equation 67 can be used to find that the step frequency for that individual is 1.25 steps per second. Perhaps a survey of available empirical data will help find a value which represents an individual's corrected step size when ascending or descending stairs.

8.2 Empirical Analysis

To find an appropriate value for step size on stairs, the empirical stair data presented by Fujiyama and Tyler [90] at the 10th International Conference on Mobility and Transport for Elderly and Disabled People was used (Figure 50). Recall from section 7.3.1 that Fujiyama and Tyler conjectured that the high correlation found between horizontal walking speed and speed on stairs is somehow related to an individual's step frequency.

Exploring this theory, it was possible to determine the individual's stair step frequency based on calculated values obtained from Fujiyama and Tyler's empirical data. To begin, the ascending and descending velocity adjustment coefficient, c_{slope} , was computed for each set of stairs using the formulas shown in Equation 65 (ascending) and Equation 66 (descending). By rearranging Equation 64 as shown in Equation 68, the number of steps per second displayed by each of the experimental groups while travelling on the stairs was calculated (labeled as "Steps Per Second" in Table 10 and Table 11).

Equation 68 Step Frequency Formula Used for Travel on Stairs to Find Steps Per Second

$$freq = \frac{v_{meas}}{(c_{slope})(d_{horz})}$$

With empirically determined frequency values, the appropriate corrected step size was determined by rearranging Equation 67 as shown in Equation 69 and computing the step size for each experimental group.

Equation 69 Corrected Step Size for Travel on Stairs

$$s_{corr} = (v_{meas}) \left(\frac{1}{freq} \right)$$

Using the data provided by Fujiyama and Tyler, it was found that, on average, the corrected step size for a person traveling up a flight of stairs is approximately 0.5 meters (Table 10) and the (average) corrected step size for a person descending a flight of stairs is approximately 0.66 meters (Table 11).

Table 10 Frequency and Step Size Correction Factors for Pedestrians Ascending a Flight of Stairs

	Stair No	Stair Gradient	Horizontal Velocity	Measured Velocity	Reduction Factor	Steps Per Second	Stepsize Correction Factor
Normal Pace	1	38.8	1.31	0.44	0.779337965	2.45470331	0.533669384
	2	35	1.31	0.52	0.819152044	2.53921114	0.515908259
	3	30.5	1.31	0.59	0.86162916	2.56460427	0.510800053
	4	24.6	1.31	0.73	0.909236109	2.41828845	0.541705436
	1	38.8	1.4	0.48	0.779337965	2.67785815	0.522805885
	2	35	1.4	0.56	0.819152044	2.73453508	0.511970028
	3	30.5	1.4	0.63	0.86162916	2.73847575	0.511233302
	4	24.6	1.4	0.76	0.909236109	2.51767017	0.556069662
Fast Pace	1	38.8	1.71	0.61	0.779337965	3.4031114	0.502481347
	2	35	1.71	0.69	0.819152044	3.36933786	0.507518114
	3	30.5	1.71	0.79	0.86162916	3.43396166	0.497967121
	4	24.6	1.71	1	0.909236109	3.3127239	0.516191524
	1	38.8	1.84	0.78	0.779337965	4.3515195	0.422840804
	2	35	1.84	0.91	0.819152044	4.4436195	0.414076858
	3	30.5	1.84	0.97	0.86162916	4.2163833	0.436392963
	4	24.6	1.84	1.16	0.909236109	3.84275973	0.478822547

Averages	
Stair 1	0.4954494
Stair 2	0.4873683
Stair 3	0.4890984
Stair 4	0.5231973
Overall	0.4987783

Table 11 Frequency and Step Size Correction Factors for Pedestrians Descending a Flight of Stairs

	Stair No	Stair Gradient	Horizontal Velocity	Measured Velocity	Increase Factor	Steps Per Second	Stepsize Correction Factor
Normal Pace	1	38.8	1.31	0.47	1.159916858	1.76174546	0.743580743
	2	35	1.31	0.58	1.20402761	1.92686611	0.679860418
	3	30.5	1.31	0.64	1.238428082	1.93552115	0.676820297
	4	24.6	1.31	0.8	1.253379729	1.92251279	0.681399889
	1	38.8	1.4	0.59	1.159916858	2.21155281	0.63303937
	2	35	1.4	0.65	1.20402761	2.15941892	0.648322559
	3	30.5	1.4	0.74	1.238428082	2.23794633	0.625573537
	4	24.6	1.4	0.87	1.253379729	2.09073266	0.669621722
Fast Pace	1	38.8	1.71	0.62	1.159916858	2.32400465	0.735798871
	2	35	1.71	0.7	1.20402761	2.32552807	0.735316862
	3	30.5	1.71	0.84	1.238428082	2.54037151	0.673129892
	4	24.6	1.71	1.01	1.253379729	2.42717239	0.704523504
	1	38.8	1.84	0.87	1.159916858	3.2611033	0.564226223
	2	35	1.84	0.92	1.20402761	3.05640832	0.602013805
	3	30.5	1.84	1.08	1.238428082	3.26619194	0.563347174
	4	24.6	1.84	1.18	1.253379729	2.83570636	0.648868312

Averages	
Stair 1	0.6691613
Stair 2	0.6663784
Stair 3	0.6347177
Stair 4	0.6761034
Overall	0.6615902

Using these values in the PEDFLOW subroutine provides an analytically derived method to microscopically adjust individual pedestrian velocities during the simulation runs. A summary of the model, where $\theta = \text{atan}\left(\frac{d_{vert}}{d_{horz}}\right)$ represents the stair angle, is shown in Equation 70.

Equation 70 Velocity Correction Formula Used for Travel on Stairs

$$v_{corr} = (c_{slope})(d_{horz})(freq)$$

where

$$c_{slope} = \begin{cases} \cos(\theta) & \theta > 0 \\ \cos(\theta)(1 - \sin(\theta)\cos(\theta)) & \theta < 0 \end{cases}$$

d_{horz} : stair tread length

$$freq = (v_{desi})\left(\frac{1}{s_{corr}}\right), \quad s_{corr} = \begin{cases} 0.5 & \theta > 0 \\ 0.66 & \theta < 0 \end{cases}$$

8.3 Verification of Model

According to Oberkampf and Roy [95], verification is defined as “the process of assessing software correctness and numerical accuracy of the solution to the given mathematical model.” In practice, this means that the programmer ensures that the model is implemented correctly from a computational standpoint within the code, without regard to the relationship between the model and real world data. To verify PEDFLOW’s use of the speed on stairs formula developed in the preceding section, a specific verification test published by Ronchi et al. [86] from the United States’ National Institute of Standards and Technology (NIST) was used. The particular test used was Verification Test 2.2: Speed on Stairs which quantitatively confirms a simulated pedestrian’s ability to travel up or down a flight of stairs at his or her assigned speed. Assuming that a simulated

pedestrian's assigned horizontal (desired) velocity is 1.0 meters per second and using a typical riser height of 7 inches (0.18m) and tread depth of 11 inches (0.28m), Equation 70 can be used to analytically determine that the simulated pedestrian should travel at a speed of 0.471 meters per second when ascending the stairs and 0.519 meters per second when descending. Using the scenario proposed by Ronchi et al. and the parametric inputs in PEDFLOW confirmed that the subroutine correctly modifies the pedestrian's velocity when travelling up or down stairs (Figure 61).

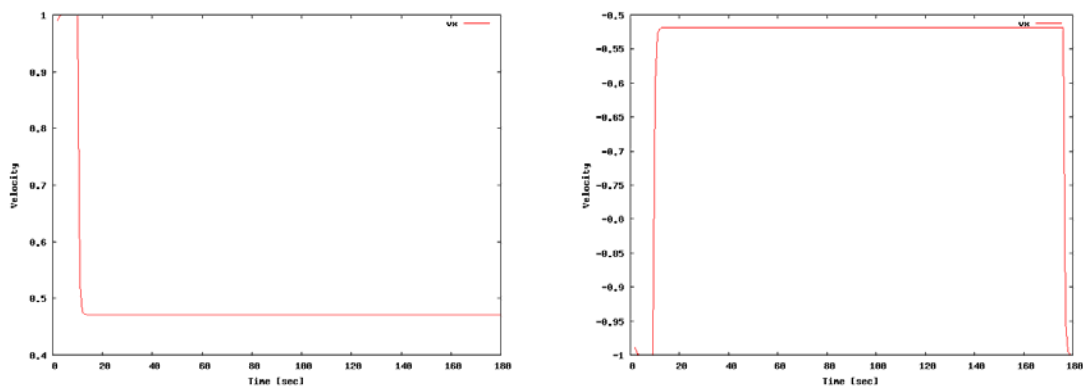


Figure 61 PEDFLOW Velocity Curves when Traveling Up (left) and Down (right) a 32.7° Staircase

8.4 Johnson Center Validation

Once convinced that the model was implemented correctly within PEDFLOW, the next objective was to determine if the model correctly simulates real world (experimental data) through validation. As defined by Oberkamp and Roy [94], validation is “the process of assessing the physical accuracy of a mathematical model based on comparisons between computational results and experimental data.” To validate the speed on stairs model, empirical data was collected during a routine fire drill at

GMU's Johnson Center, a four-story Student Center located on the Fairfax Campus in Northern Virginia, USA. In total, the Johnson Center has eleven stairs; however, only eight of these stairs can be used for evacuation purposes (Figure 62).

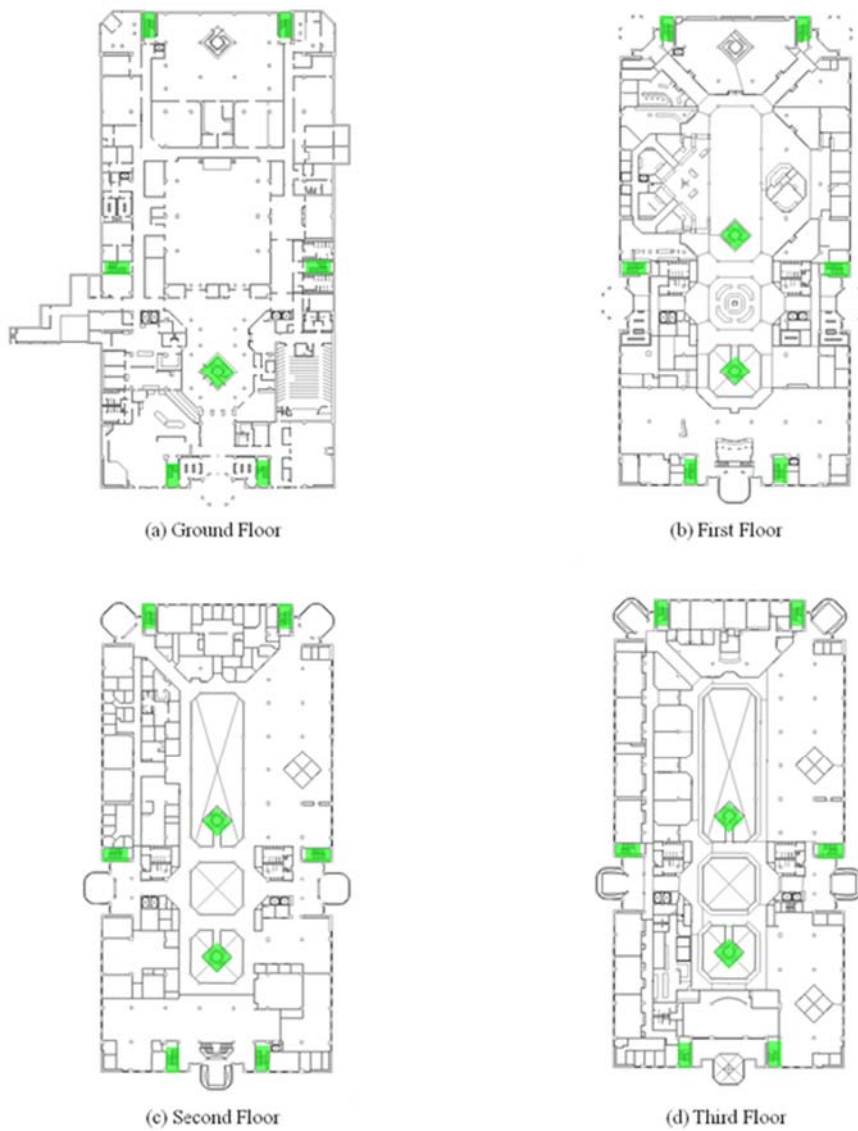


Figure 62 Johnson Center Floor Plans (Stairs Highlighted in Green)

For pedestrian egress, the Johnson Center has two centrally-located large “open” staircases and six “enclosed” stairwells which are located on the perimeter of the building. The South Central staircase runs from the ground floor to the third floor, as do the six perimeter stairwells. The Central Stairwell runs from the first floor to the third floor and, routinely, is the most traveled staircase for ingress and egress.

The fire drill occurred at 0800 hours on the morning of March 16, 2015 and lasted approximately 10 minutes. The footage from the interior security cameras was used to determine occupant initial locations and activities, as well as occupant evacuation routes and behaviors during the drill. As shown in Figure 63, a total of 83 occupants used the stairs to evacuate the building, with most of the pedestrians choosing to use the central and south central stairs.

Occupant Route Selection Stair Choice: Initial Location	Exit Choice:					Grand Total
	South Exit	East Exit	North East Exit	North West Exit	West Exit	
East Stair						
2nd Floor		6				6
North East Stair						
2nd Floor			1			1
3rd Floor			1			1
North West Stair						
3rd Floor				2		2
West Stair						
3rd Floor					2	2
Central Stair						
2nd Floor		10	8			18
3rd Floor		9	7	2	2	20
South Central Stair						
1st Floor	3		1			4
2nd Floor	3	14				17
3rd Floor	1	8				9
Ground Floor			1	2		3
Grand Total	7	47	19	6	4	83

Figure 63 Occupant Evacuation Route Described by Initial Location, Stair, and Exit Choice

Turning the data collection efforts to the central and south central stairs, video was used to ascertain the amount of time each individual took to descend the stairs by simply noting the time (on video) he/she entered the stairs and the time (on video) that he/she exited the stairs. The number of pedestrians who traveled the central or south central stairs as well as the minimum, maximum, and average descent times can be seen in Table 12.

Table 12 Stair Descent Statistics as Recorded from Security Camera Footage

	Peds	Video		
		Min	Max	Average
South Central Stair				
2F to 1F	26	14	20	17.15
1F to GF	7	19	32	26.71
Central Stair				
3F to 2F	20	14	24	19.15
2F to 1F	37	14	27	18.97

Using the occupant demographics, initial locations, route selection, and exit choices, a PEDFLOW simulation was built to recreate the Johnson Center fire drill. During the simulation, the times that each simulated pedestrian entered or exited the stairs was recorded so that simulated descent times could be computed for comparison with the empirical data. Figure 64 demonstrates that (on average) the PEDFLOW computed stair descent times nicely represent the occupant stair descent times observed on video. The average stair descent times for each pedestrian was computed for each of 20 simulation runs. Shown on the graphs in Figure 64 are the average descent times with the error bars representing two standard deviations from the mean.

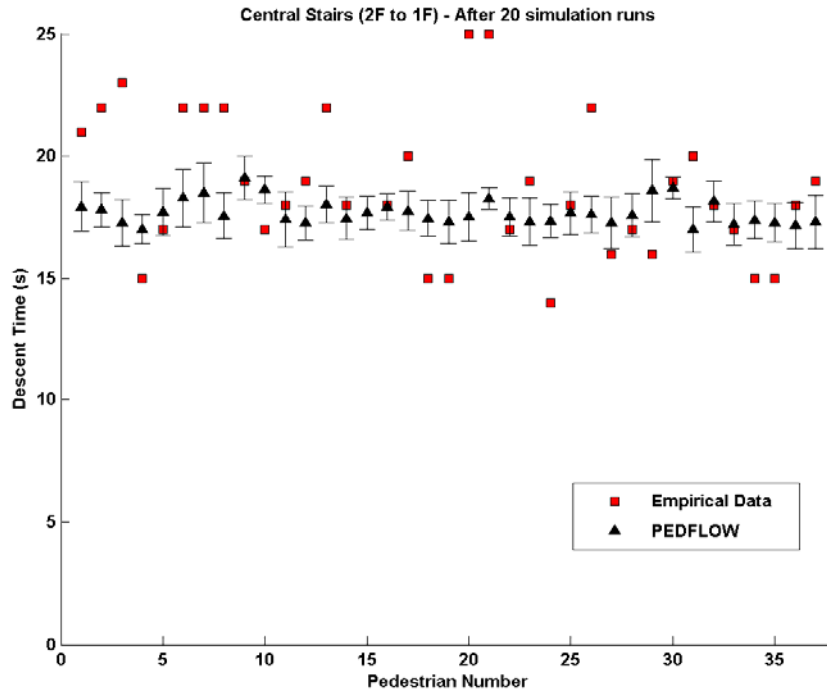


Figure 64 Example Comparison of PEDFLOW Stair Descent Times with Empirical Data Obtained from Video

Table 13 Average Stair Descent Times after 20 PEDFLOW Simulation Runs

	Peds	Video			PEDFLOW		
		Min	Max	Average	Min	Max	Average
South Central Stair							
2F to 1F	26	14	20	17.15	16.2	20.4	18.24
1F to GF	7	19	32	26.71	27.4	51.6	33.95
Central Stair							
3F to 2F	20	14	24	19.15	16.3	21.5	19.49
2F to 1F	37	14	27	18.97	15.3	21.4	17.70

8.5 Conclusion

This chapter introduces a speed on stairs velocity correction model for use in computer-based pedestrian simulations. Pedestrian ascent and descent on stairs is a critical component of building evacuation simulations and the model proposed here was

developed using data from controlled laboratory experiments and observational studies. The model was then verified using a specific “speed on stairs” verification test from NIST and tested against a newly collected set of empirical data. It was shown that for three out of the four sets of stairs, the model performed exceptionally well and the average descent times after 20 simulation runs were within two seconds of the empirical results.

The empirical data used to validate this model was from a building evacuation study of a routine fire drill where the majority of pedestrians were descending the stairs. Therefore, as of publication, the model is only validated for computer simulated pedestrian descent scenarios; further research is needed to obtain data and validate the model for pedestrian ascent on stairs. In addition, further research is necessary to determine why the pedestrians descending the south central stairs from the first floor to the ground floor travel significantly slower in the simulation than they did on video.

9 VALIDATION OF PEDFLOW

In order to properly assess the behavioral components of an evacuation simulation tool, researchers require accessible and adequate experimental data for both qualitative and quantitative model validation. One such potential data set on high-rise building evacuations was recently reported on by Peacock et al. [96] and is available from the United States' National Institute of Standards and Technology (NIST). Researchers from the Engineering Laboratory at NIST collected occupant egress data in the stairwells of several high-rise buildings during fire drill evacuations making data from five of the buildings readily available to the public [97]. After downloading this data, it was found suitable for establishing occupant initial locations, pre-evacuation time distributions, and other parametric inputs for the PEDFLOW simulation code. Several core behavioral components of PEDFLOW (such as pre-evacuation time distributions and speed on stairs) were validated by running multiple simulations and directly comparing the predicted values with the actual values collected by NIST. This chapter summarizes the work on the stairwell data sets, highlighting the methodology behind the extraction of values from the data for the parametric inputs, and demonstrating the results obtained for a 10-story high-rise building.

9.1 Description of NIST Stairwell Data

In an attempt to develop a verification and validation standard for building fire evacuation models, Ronchi et al. [86] highlighted several available data-sets which potentially could be used to validate core behavioral components of building evacuation models. This chapter will focus specifically on the application of the stairwell evacuation data-set referenced by Ronchi et al. [86] and provided on-line by Kuligowski and Peacock [97]. Although Peacock et al. provide a consolidated report [96] containing potential parametric inputs, it was deemed valuable to manually process the raw data-sets provided by NIST and determine if the data-sets would allow the extraction of values for parametric input.

Although the NIST researchers collected stairwell evacuation data from a total of nine buildings ranging in height from 6 to 62 stories, the on-line NIST repository of stairwell evacuation data currently contains stairwell data from five of the buildings (only those data-sets approved for release are available). The stairwell data described in this paper comes from the two stairwells of Building 5, a 10-story office building on the West Coast of the United States. According to Peacock et al. [96], Building 5 consists of two identical stairwells (A and B) with a full stair width of 1.27 meters, stair riser height of 0.178 meters, stair tread depth of 0.279 meters, and an exit width of 0.91 meters. To collect the data, the NIST researchers placed cameras in each of the stairwells and recorded the evacuation drill. From the video, the NIST researchers transcribed pedestrian identification information and evacuation data into a spreadsheet. The spreadsheet contains the following identification information for each occupant:

1. gender

2. items carried (yes/no)
3. body size (relative to stair width)
4. alone or in a group
5. assisting others
6. floor on which first seen
7. occupant description

Using this identifying information, evacuation specific data was recorded for each pedestrian as he/she traveled down the stairwell and entered each of the camera views:

1. location in stairwell (relative to handrail)
2. handrail usage (yes/no)
3. time individual entered camera view
4. time individual exited camera view

Using the data from both stairwells (stairwell A and stairwell B), the total evacuation time was extracted for each pedestrian and consolidated the two sets of data into a single data-set (Figure 65). Total evacuation time was computed by subtracting the time the individual exited the first floor camera view from the camera's recorded alarm initiation time.

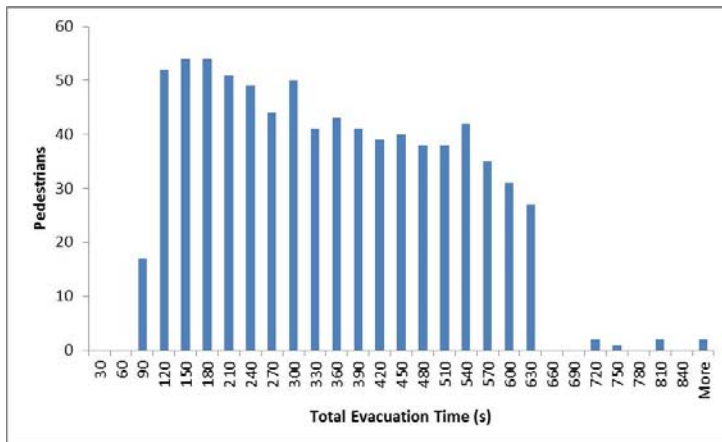


Figure 65 Evacuee Total Evacuation Times from a 10-story Building [97]

In addition to total evacuation time, a starting floor for each pedestrian was also extracted from the database. According to the notes in the spreadsheet, the “Floor First Seen” column is the highest floor in the stairwell where the evacuee was first seen and if the column is blank, then the occupant entered from a floor above the camera position. Since the cameras were placed on each of the odd numbered floors, it was assumed that if the evacuee was not first seen on the odd numbered floor, then the evacuee entered from the even numbered floor immediately above the highest floor where pedestrian was recorded in the camera view. For example, evacuee number 1 from Stairwell A of Building 5 has a blank in the “Floor First Seen” column. Since the only record of evacuee number 1 on video is on the first floor camera, it was assumed that evacuee number 1 started on the second floor. Similarly, evacuee number 3 from stairwell A also has a blank “First Floor Seen” value, but has a video record for the cameras on the first and third floors. Therefore, it is assumed that evacuee number 3 started on the fourth floor.

Continuing in this manner starting floor positions were developed for each of the pedestrians (Figure 66).

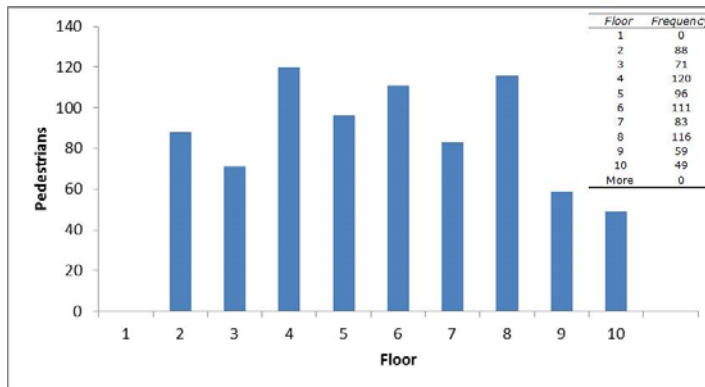


Figure 66 Evacuee Initial Floor Locations in a 10-story Building [97]

According to the description in Peacock et al. [96] the “Floor First Seen” column was also used to compute a “pre-observation” delay value for a subset of the evacuees . Those evacuees who entered the stairwell from even numbered floors (between camera locations) were not included in the computation of these values. The authors called this value a “pre-observation” delay rather than the typical pre-evacuation delay to distinguish the fact that this value not only includes all activities prior to starting evacuation, but also includes the time it took to walk to the stairwell while evacuating. To compute the distribution of pre-observation delay times from the data-set, the value in the “Floor First Seen” column was taken and the alarm initiation time (for that particular camera) was simply subtracted from the time the individual initially entered the camera view (Figure 67).

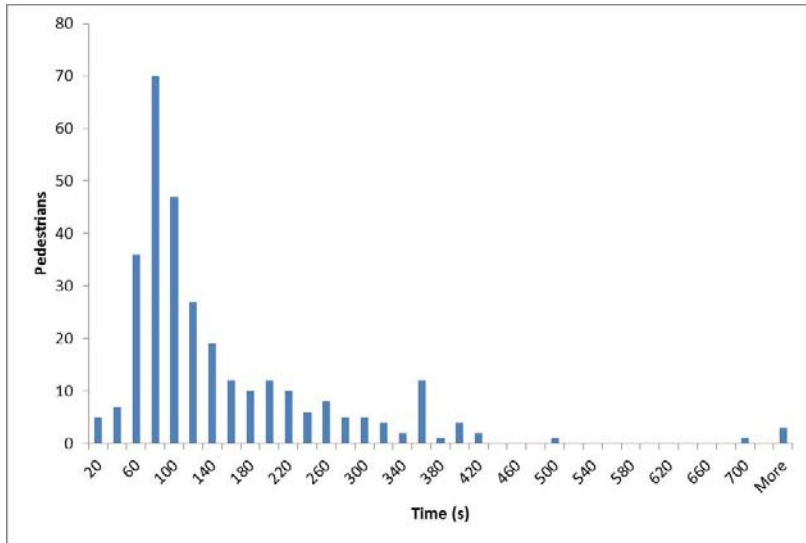


Figure 67 Evacuee Pre-observation Delay Times in a 10-story Building [97]

9.2 Geometric and Pedestrian Definitions

Using the geometric description of the stairwells provided by Peacock et al. [96], a simple 10-story building was created within PEDFLOW with two stairwells, each with an exit at the base of the stairs (Figure 68).

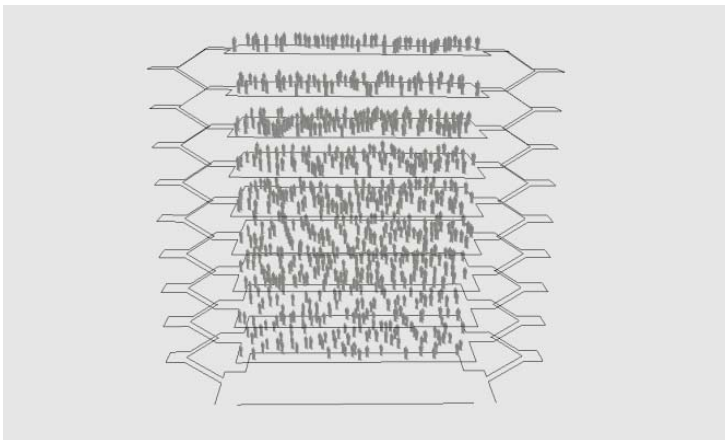


Figure 68 Evacuee Initial Positions and Geometric Description of a 10-story Building with 2 Stairwells

The pedestrians were distributed throughout the building in accordance with the distribution given in Figure 66. In order to represent a wide set of pedestrian demographics within the building, the pedestrians were initialized with a velocity distribution of 1.00 +/- 0.5% meters per second, a relaxation time of 0.50 meters per second, a radius of 0.25 +/- 0.02% meters, an ellipticity value in the range of 0.0 to 1.0, a pushiness value in the range of 0.0 to 0.80, and a desired comfort zone of 0.25 meters. To set up the evacuation run, the pre-observation delay time was used as the pre-evacuation delay since the travel-to-stairwell time difference between the two values is well within the statistical uncertainty. Two pre-observation delay time distributions were used. First, a Gaussian distribution with parametric values as reported by Peacock et al. [96] in Table 3 which provided an average pre-observation delay time of 171 +/- 124 seconds for the 10-story building. Second, the distribution extracted from Kuligowski and Peacock [97] and shown in Figure 67.

9.3 Comparison of Actual and Simulated Values

Prior to running the full simulation, it is desirable to confirm that, when unimpeded, the pedestrians' average stair descent speeds were somewhat near to the value reported in Table 3 from Peacock et al. [96]. Therefore, a single pedestrian was initiated on the tenth floor and recorded his velocity throughout the descent. Figure 69 clearly shows that this pedestrian's velocity when descending the stairs is within the 0.44 +/- 0.19 meters per second range provided by Peacock et al. [96].

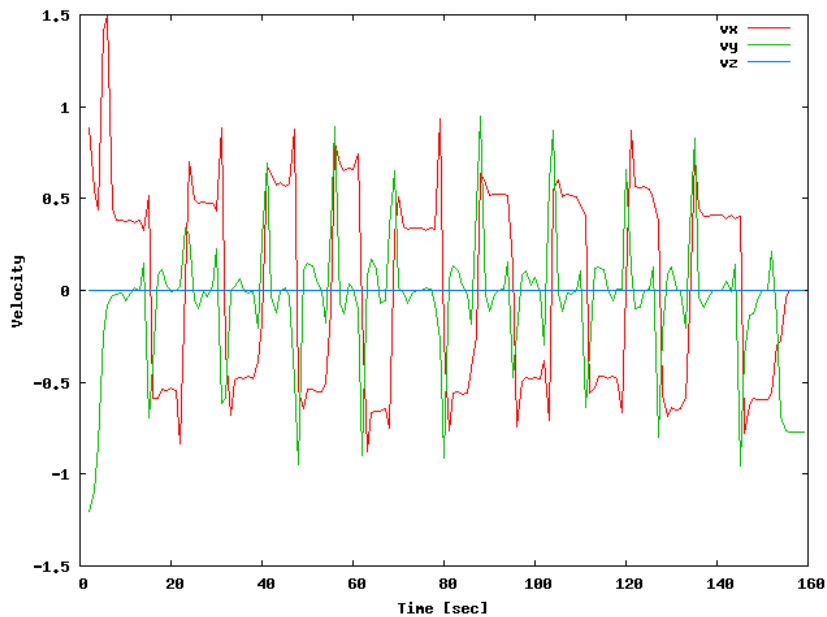


Figure 69 Average Velocity during Descent from 10th Floor

When using a Gaussian distribution with a mean of 171 seconds and standard deviation of 124 seconds for the pre-evacuation delay, the PEDFLOW simulation evacuated the 10-story building in 742 seconds, 4 minutes and 40 seconds faster than the actual total evacuation time of 1022 seconds recorded by Peacock et al. [96]. As can be seen from Figure 70, this type of distribution does not seem to properly fit the pre-observation data (left), nor does it provide a fit for the observed building exit times (right).

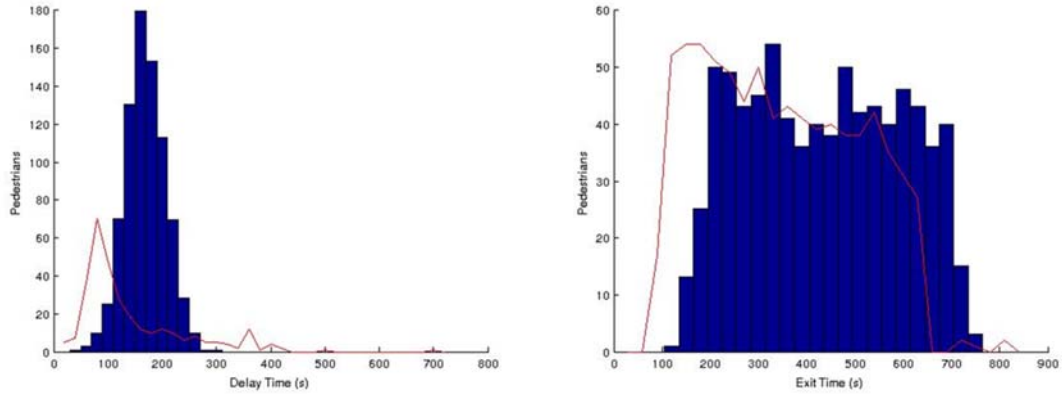


Figure 70 Comparison of Experimental (red line) versus Simulation-obtained Values for Pre-Evacuation Delay (left) and Building Exit Times (right) for Gaussian Distribution of Pre-evacuation Delay

However, when using the distribution of pre-observation times shown in Figure 67, the results are much more satisfactory. The 10-story building is now evacuated in 872 seconds, only 2 minutes and 30 seconds faster than the actual evacuation time. As shown in Figure 71, the user-defined table of pre-evacuation times (left) seems to match the pre-observation times obtained during the evacuation drill. Similarly, notice in Figure 71 that the simulated building exit times (right) also better match the evacuation exit times recorded by Peacock et al. [96].

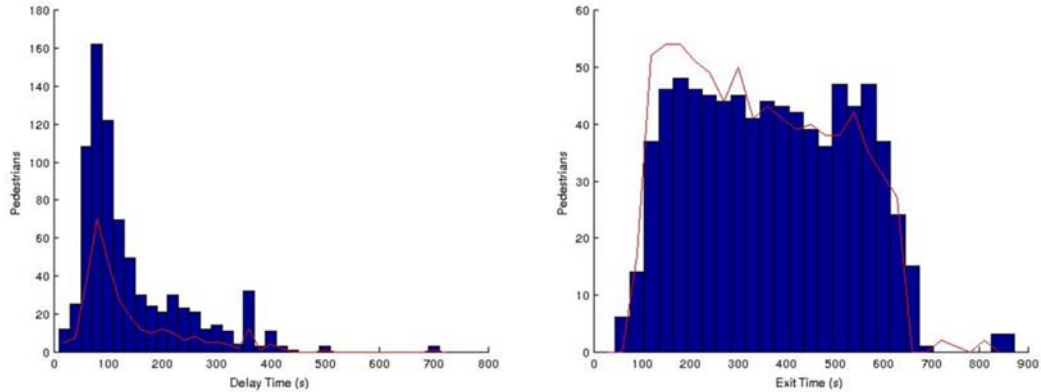


Figure 71 Comparison of Experimental (red line) versus Simulation-obtained Values for Pre-evacuation Delay (left) and Building Exit Times (right) with Video-extracted Pre-evacuation Delay

It is important to note that during the actual evacuation drill, six firefighters entered one of the stairwells and traveled against the floor of traffic up to the seventh floor. The simulation results described in this section do not account for the effects from this type of counterflow. Methods to implement the movement of emergency responders into evacuation scenarios has begun, but further research is necessary. In addition, some of the individuals with lengthy pre-observation delay values (identifiable outliers in Figure 67) were individuals with responsibilities to sweep the floor and ensure all occupants evacuate prior to evacuating themselves. Typically, these individuals wore yellow safety vests during the evacuation and although they are treated in this analysis as regular evacuees, a better solution currently under development is to assign them pedestrian characteristics consistent with their responsibilities within the simulation.

9.4 Conclusion

The NIST stairwell data readily available and is suitable for use in validation of a pedestrian simulation tool. With a relatively small amount of pre-processing, the data can

be used to establish parametric inputs such as occupant initial locations and pre-evacuation time distributions. This validation study demonstrated the importance of selecting the correct pre-evacuation distribution and confirms that pre-movement times affect the movement phase and should not be neglected nor modeled as a simple addition to total evacuation time. In addition, the data can be used to validate several core behavioral components of the simulation tool such as the assignment of the pre-evacuation time distributions and speed on stairs. Although this paper focuses specifically on the evacuation drill of the 10-story building, further research and attempted validation tests are on-going for the other four buildings available from NIST.

10 BUILDING EVACUATION STUDY – SPRING 2015

This study was designed to capture the activities of building occupants prior to and immediately after a routine fire drill in a student center on the campus of GMU. Video from the exterior security cameras positioned at each exit allowed for the extraction of evacuation times for each occupant. The analysis of interior security camera footage allowed the capture of occupant initial locations and activities, as well as occupant evacuation routes and behaviors during the drill. In addition, the footage provided reliable pre-evacuation behaviors and times for almost all of the building's occupants at the time of the alarm.

10.1 Johnson Center

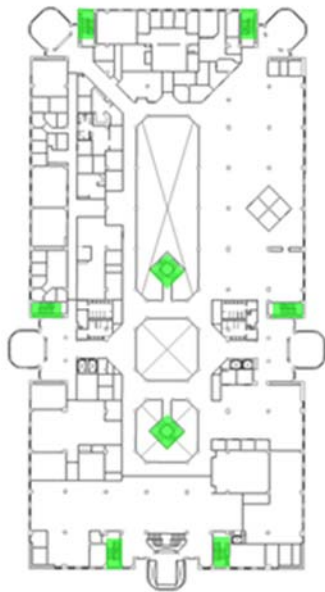
The Johnson Center is a four-story Student Center located on the Fairfax Campus of GMU. The ground floor houses a coffee shop (Starbucks), bistro, cinema, and ballroom. Located on the first floor are the bank, bookstore, computer store, library, another coffee shop (Panera Bread), and a food court with a large seating area. The second floor contains administrative office space, the admissions office, and numerous locations for individual and group study, while the third floor houses the computer lab, collaborative learning lab, quiet meditation corner, and more individual and group study locations. In total, the Johnson Center has approximately 30,000 square meters of space available to the university's students, staff, and faculty (Figure 72).



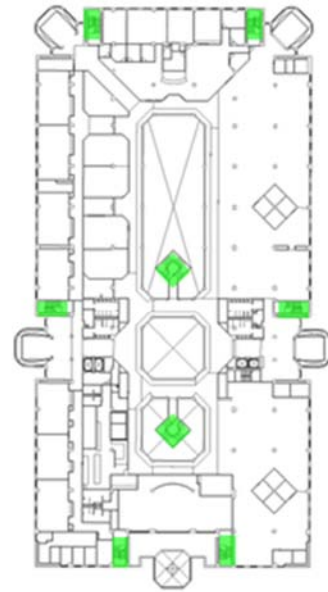
(a) Ground Floor



(b) First Floor



(c) Second Floor



(d) Third Floor

Figure 72 Johnson Center Floor Plans (Stairs Highlighted in Green)

In total, the Johnson Center has eleven stairs; however, only eight of these stairs can be used for evacuation purposes. For pedestrian egress, the Johnson Center has two centrally-located large “open” staircases and six “enclosed” stairwells which are located on the perimeter of the building (highlighted in green in Figure 72 and Figure 73). The South Central staircase runs from the ground floor to the third floor, as do the six perimeter stairwells. The Central Stairwell runs from the first floor to the third floor and, routinely, is the most traveled staircase for ingress and egress.



Figure 73 Johnson Center Exits (Stairs Highlighted in Green)

The Johnson Center has five primary exits; for ease of identification, each exit is named according to its cardinal direction: South, East, West, North East, and North

West. The South exit is located on the ground floor while the other four exits are located on the first floor (Figure 73). There are no exterior exits on the second and third floors of the Johnson Center.

All exits consist of two sets of double-leaf swing doors, and are constructed in a similar manner (Figure 74). Each door is approximately 0.9 meters wide, yielding a total opening width of 1.8 meters for each door pair.

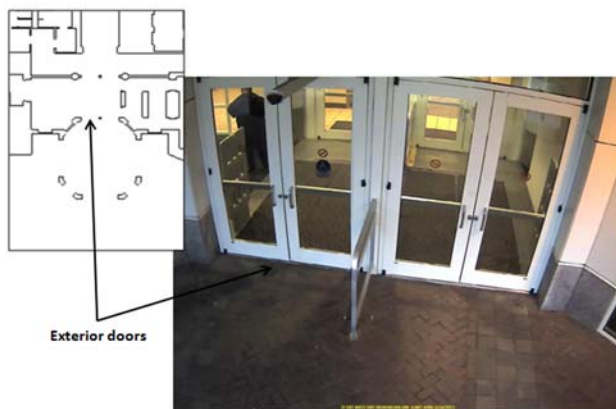


Figure 74 Johnson Center Exterior Doors

10.2 Video Analysis

Occupant evacuation times were extracted using video from the exterior security cameras positioned at each exit. The analysis of interior security camera footage provided occupant initial locations and activities, as well as occupant evacuation routes and behaviors during the drill. In addition, the video footage allowed the collection of pre-alarm activities, post-alarm behaviors and evacuation delay times for almost all of the building's occupants.

10.2.1 Overall Evacuation Times

The fire alarm sounded promptly at 0800 hours the morning of March 16, 2015 and lasted approximately 9 minutes. In total, 190 occupants evacuated the building with 22 occupants leaving through the South Exit, 15 leaving through the West Exit, 29 leaving through the North West Exit, 53 leaving through the North East Exit and 71 leaving through the East Exit. Using video footage obtained from the exterior security cameras (Figure 75), evacuation times were manually ascertained for each individual measured as the pedestrian crossed the threshold of the respective doorway. Each security camera includes a time/date stamp allowing for extraction of the exact evacuation time. Figure 75 shows representative still images for three of the five exit doors.



Figure 75 Representative Images from Exterior Security Cameras (Left: West Door, Center: Northwest Door, Right: East Door)

As the pedestrians exited each door, occupants were numbered and evacuation times were recorded in a sequential manner, beginning with the South doors and continuing with the West, North West, North East, and East doors, respectively (Figure 76). The minimum evacuation time was 9 seconds while the maximum evacuation time was 521 seconds, with an average evacuation time of 177 seconds.

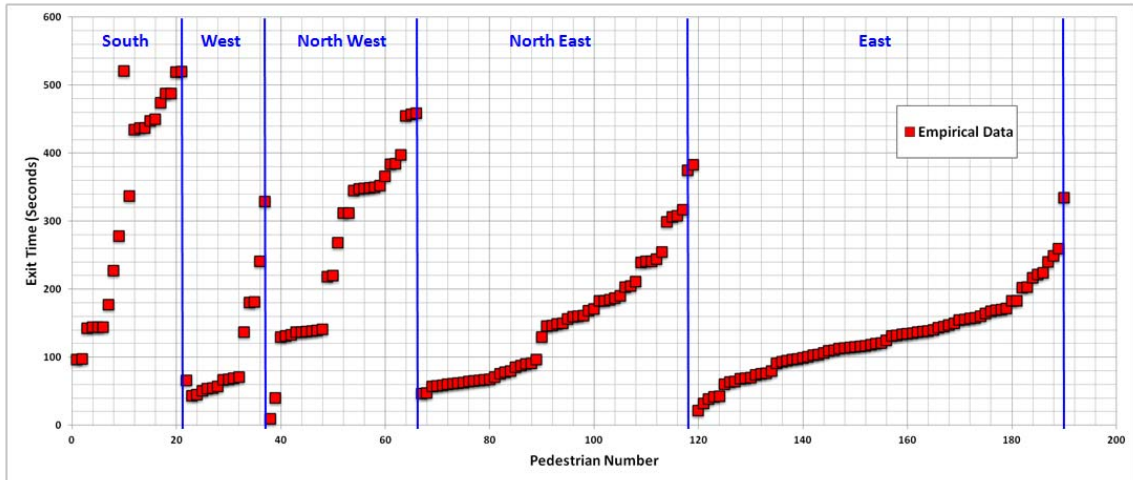


Figure 76 Johnson Center Occupant Evacuation Time (Grouped by Exit Door)

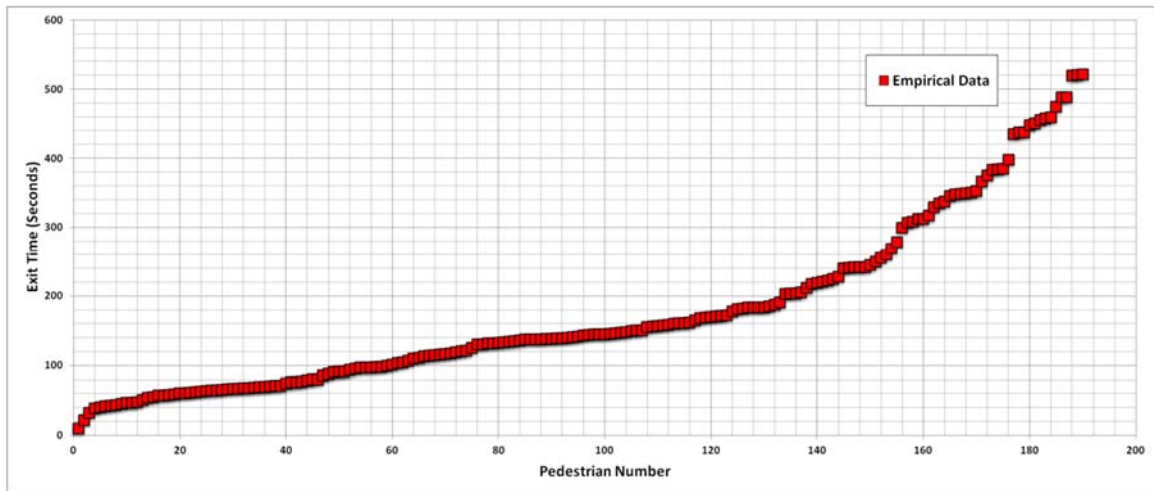


Figure 77 Johnson Center Occupant Evacuation Times (Aggregate)

10.2.2 Occupant Initial Locations and Activities

Footage from 120 of the building’s security cameras permitted the collection of occupant initial locations and activities at the time of the fire drill, as well as individual pre-evacuation times. The initial locations for each of the occupants seen on the security

cameras were plotted using true-to-scale floor plans for the Johnson Center and a plot digitizing program (Figure 78). Pedestrians were identified using the sequential numbering assigned upon exit such that occupants 1-22 were those who exited via the south exit; occupants 23-37 exited via the west exit; occupants 38-66 exited via the northwest exit; occupants 67-119 exited via the northeast exit; and occupants 120-191 were those who exited via the east exit. This method of identification allowed cross-referencing between camera views, ensured the accuracy of each individual's initial location, and confirmed the initial occupant count.

However, not all areas of the Johnson Center are covered by the security cameras. Therefore, initial locations were coded as directly observed or indirectly observed. A directly observed initial position was one where the location of the occupant at the start of the fire drill was visible on the security footage. An indirectly observed initial position was one where the initial location was not visible; however, the location of the camera and the subsequent appearance of the individual on the video allowed the initial location to be estimated with a high degree of confidence. Figure 78 demonstrates a portion of the method that was used to determine the initial locations for occupants on the second floor. The top figure shows three camera views where direct observation of the initial locations was possible. The bottom figure provides an example of a case where no initial positions were seen on the second floor's east stairwell exit camera; however, watching the video allowed for the indirect observation and estimation of initial positions for eight occupants. Additionally, cross-referencing with another camera allowed for the direct observation of three other occupants.

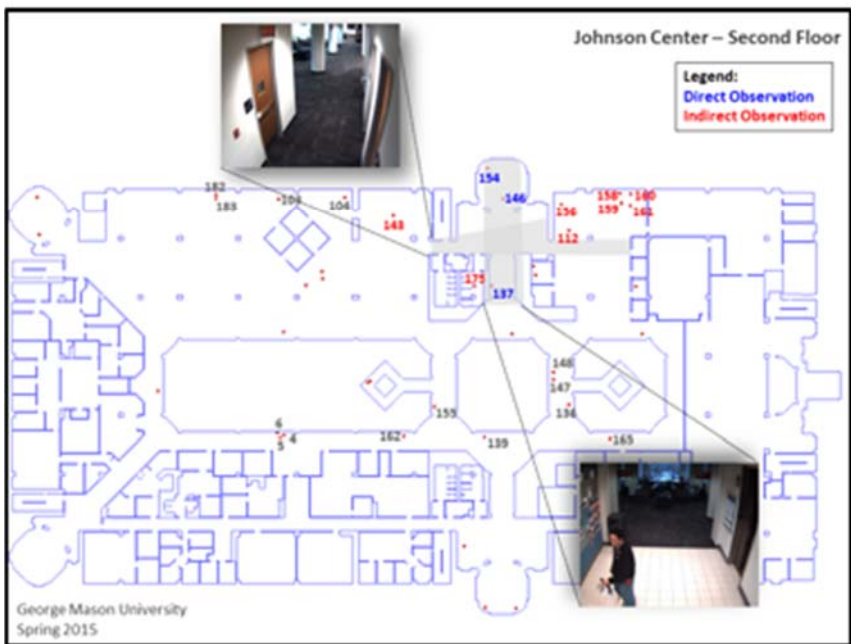
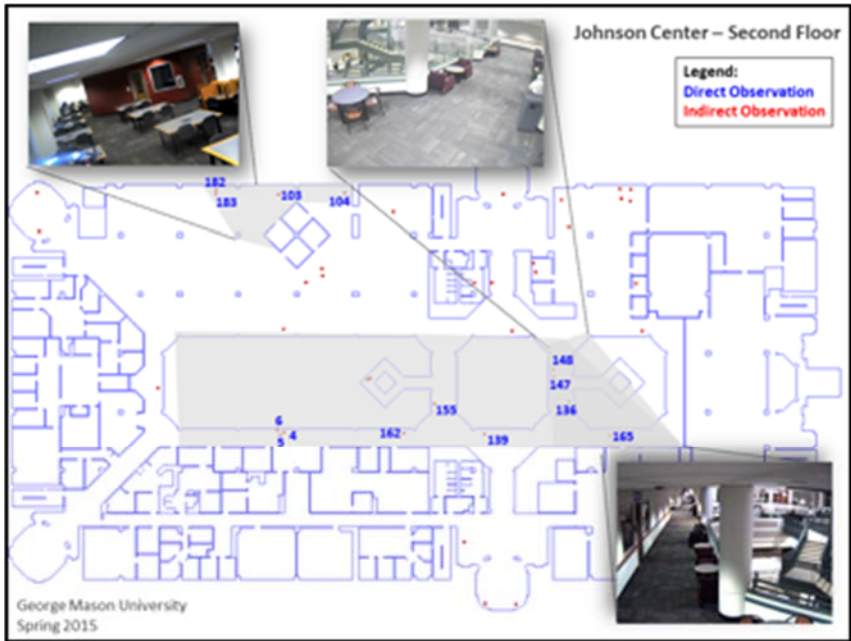


Figure 78 Representative Images from Interior Security Cameras Demonstrating Progressive Identification of Initial Locations

Continuing in this manner, accurate initial locations were obtained for 174 of the 190 occupants (91%). Eighteen occupants were on the ground floor, most of which included food service workers, maintenance personnel, and students in the coffee shop. After analyzing the video, this number was increased to 20 to account for the two individuals who entered the building through the south exit approximately 80 seconds after the alarm sounded (Figure 79). It is also important to note that if an individual performed a pre-evacuation activity (such as returning to an office to retrieve a coat or stopping at the restroom prior to evacuating), then that occupant's initial location was adjusted to the location where movement towards the exit began.

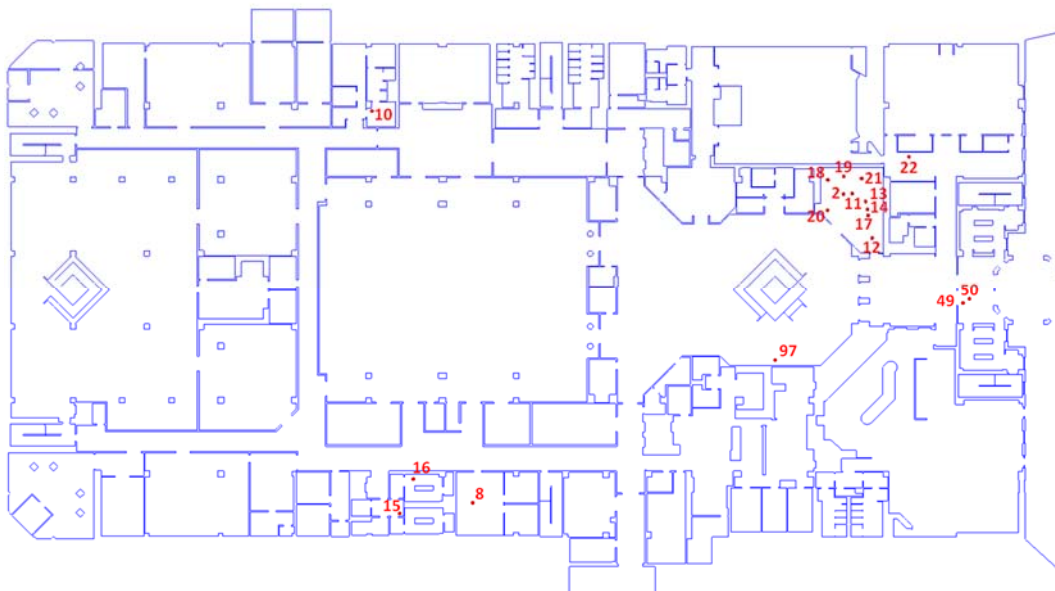


Figure 79 Initial Occupant Locations – Johnson Center Ground Floor

The first floor food court, stores, and study areas had a total of 94 occupants at the time of the alarm (Figure 80). Once again, these numbers were adjusted to 18 and 96,

respectively, to account for the two non-compliant individuals who started on the ground floor and delivered white message boards to specific locations on the first floor prior to evacuating the building. Additionally, several customer-based locations on the first floor, such as the bookstore, library, convenience store, and Panera Bread, did not have security cameras inside the business but did have security cameras on the exit doors. Therefore initial positions were again indirectly observed and estimated based on the customer's observed exit from the customer-based location.

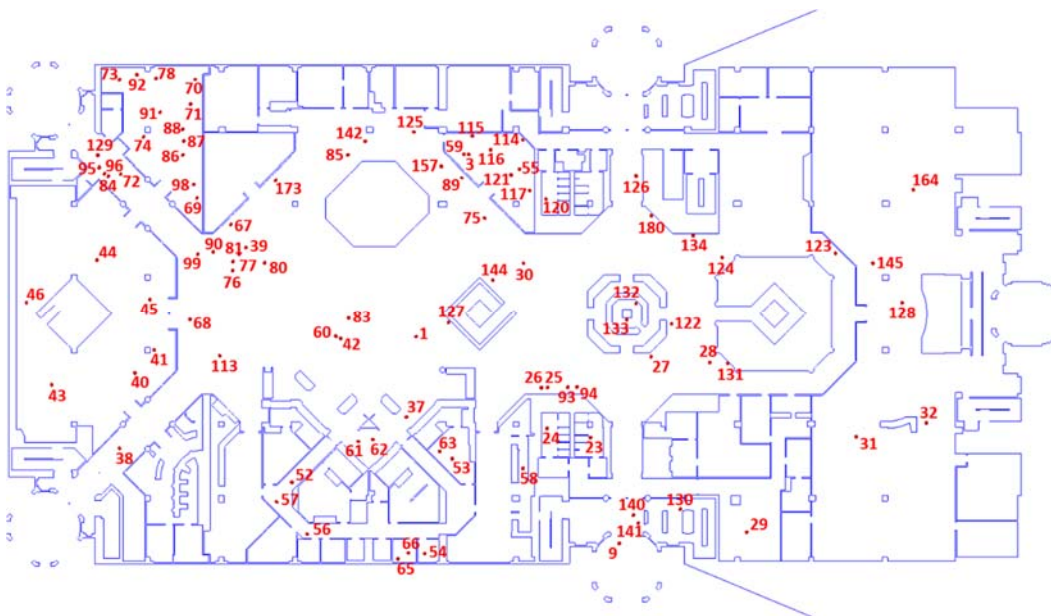


Figure 80 Initial Occupant Locations – Johnson Center 1st Floor

The upper two floors, consisting of administrative offices and study areas, had 42 and 34 occupants, respectively (Figure 81). Initial locations on the third floor in the admissions office as well as the computer lab were indirectly observed and estimated.

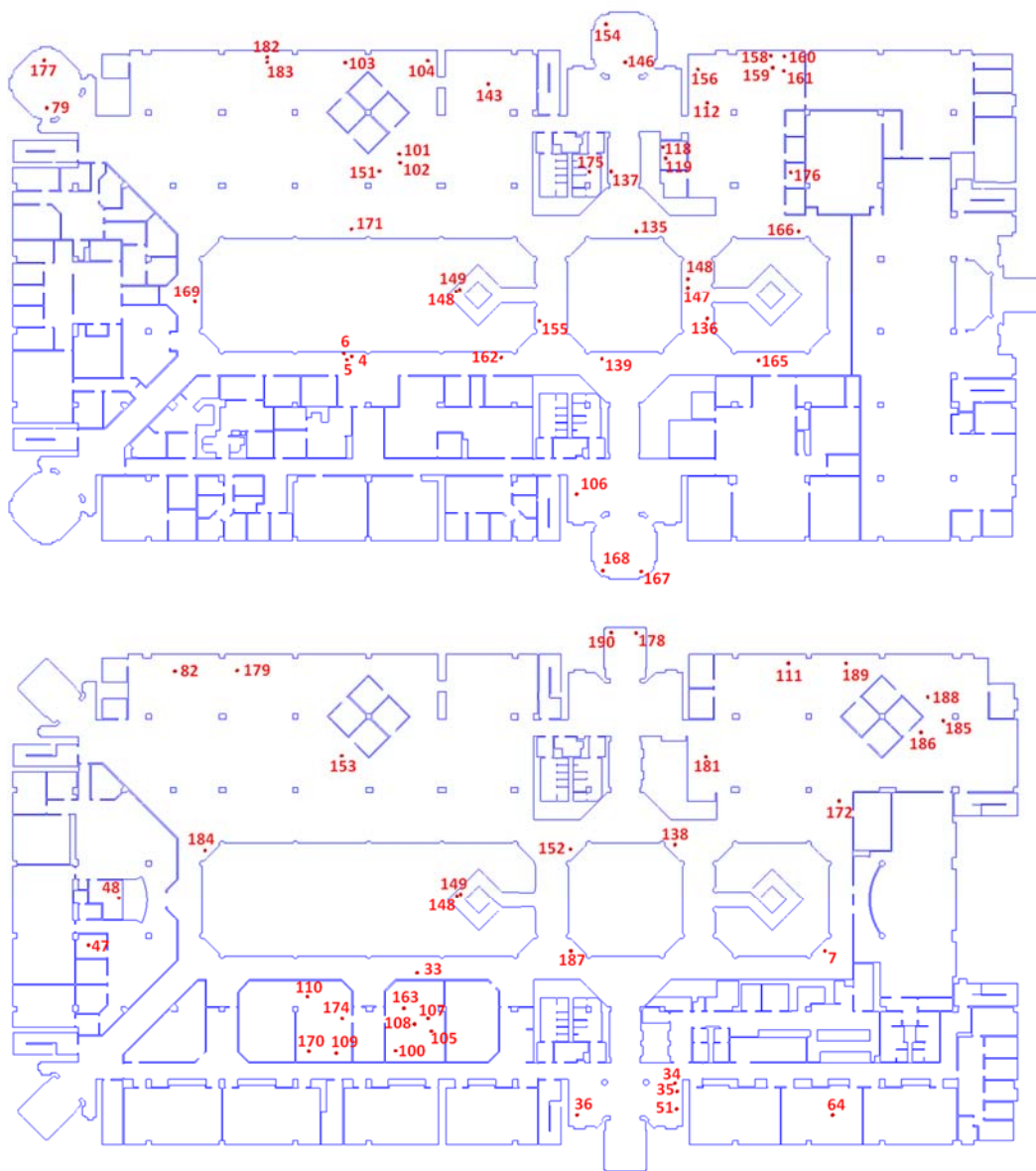


Figure 81 Initial Occupant Locations – Johnson Center 2nd (top) and 3rd (bottom) Floors

At the time of the alarm 47 of the occupants were employees, 25 were customers, and 118 were students (Table 14). For the purposes of this study an employee includes those members of the food service industry, library workers, book store employees, and administrative office staff who were in the Johnson Center at the time of the drill. A

customer is categorized as a student or staff member who, at the time of the alarm, was engaged in the purchase or consumption of goods (coffee, food, etc.) and/or services (locker, restroom, etc.). The remainder of the occupants were students, who were studying or relaxing (sleeping) at various locations throughout the building, or in transit between locations.

Table 14 Initial Occupant Activities

Occupant	Initial Activity														Grand Total
Category	Eating	Food Service	Locker	Office	Purchasing Coffee	Restroom	Shopping	Sleeping	Standing	Studying	Unknown	Walking	Walking up Stairs	Working	Grand Total
Employee		31		4										12	47
Customer	6		1		10	4	4								25
Student								1	2	95	2	16	2		118
Grand Total	6	31	1	4	10	4	4	1	2	95	2	16	2	12	190

10.2.3 Evacuation Delay

For the purposes of this study, evacuation delay is defined as the amount of time between the initiation of an alarm and an occupant’s initiation of movement to an exit.

Recall from Section 3.2 and Section 5.2 that this measurement is sometimes referred to as “pre-evacuation delay” or “pre-evacuation time”; Gwynne, et al. [74] define pre-evacuation time as the “time taken by an individual to purposefully initiate evacuation.”

For these purposes, evacuation delay, pre-evacuation delay, and pre-evacuation time refer to the same time measurement. Each individual’s evacuation delay time was determined during the initial location analysis of the video footage. If the initial location was directly observed, then the evacuation delay time was also directly observed. For a directly observed occupant, evacuation delay time was recorded as the time the individual initiated his or her movement towards the exit. However, for the indirectly observed

occupants, a pre-observation time was recorded based on the location the individual was first seen on video (similar to the methods used by Peacock et al. in their collection of stairwell data [96]) and then adjusted accordingly based on the distance to the estimated initial position. The minimum evacuation delay was 0 seconds (a pedestrian was on his/her way out of the building when the alarm sounded) while the maximum evacuation delay was 469 seconds, with an average evacuation time of 113 seconds (Figure 82 and Figure 83).

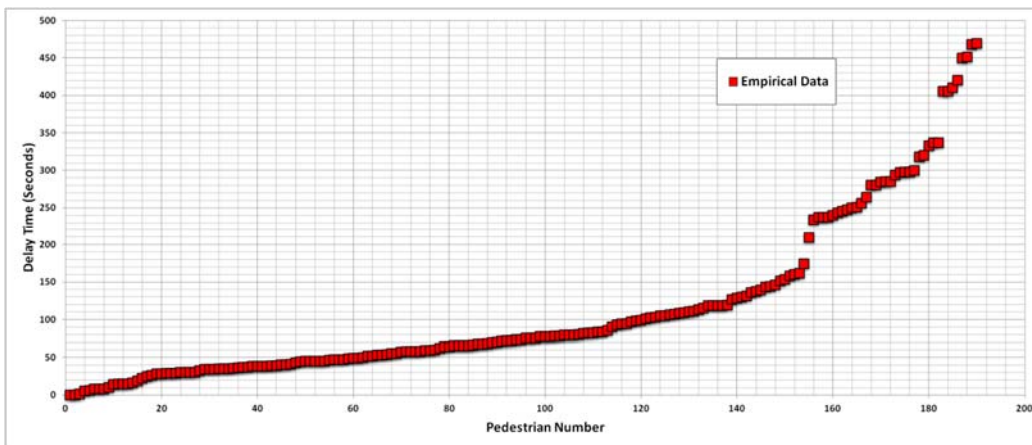


Figure 82 Johnson Center Occupant Evacuation Delay (Aggregate)

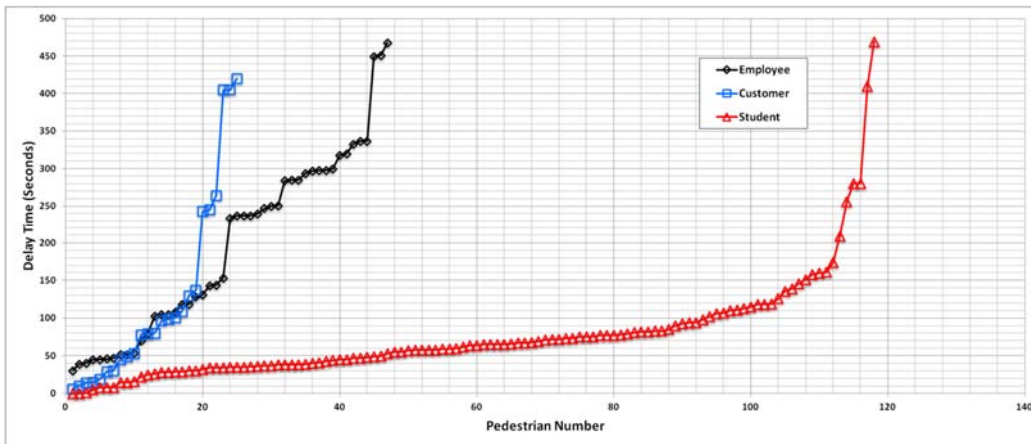


Figure 83 Johnson Center Occupant Evacuation Delay (Grouped by Occupant Type)

10.2.4 Occupant Route-to-Exit Selection

Thorough analysis of the security camera footage also allowed the extraction of building occupant route-to-exit choices. Once each occupant finished all pre-evacuation activities and made the decision to evacuate, he or she was followed on the security camera footage from the initial location to the exit. The specific route-to-exit traveled by each occupant was noted.

Of the 16 occupants who started to evacuate from the ground floor, 15 used the south exit. One occupant chose to ascend the south central stairs, traverse the entire building and exit through the north east exit. Interestingly, two non-compliant pedestrians entered the south exit approximately 80 seconds after the alarm sounded, climbed the south central stairs, traversed the entire building and exited through the northwest exit. Figure 84 shows the route and exit choices for all of the occupants who began on the ground floor. Those who ascended the south central stairs are highlighted in yellow. Direct observation of the South Central Stair on security camera video was possible.

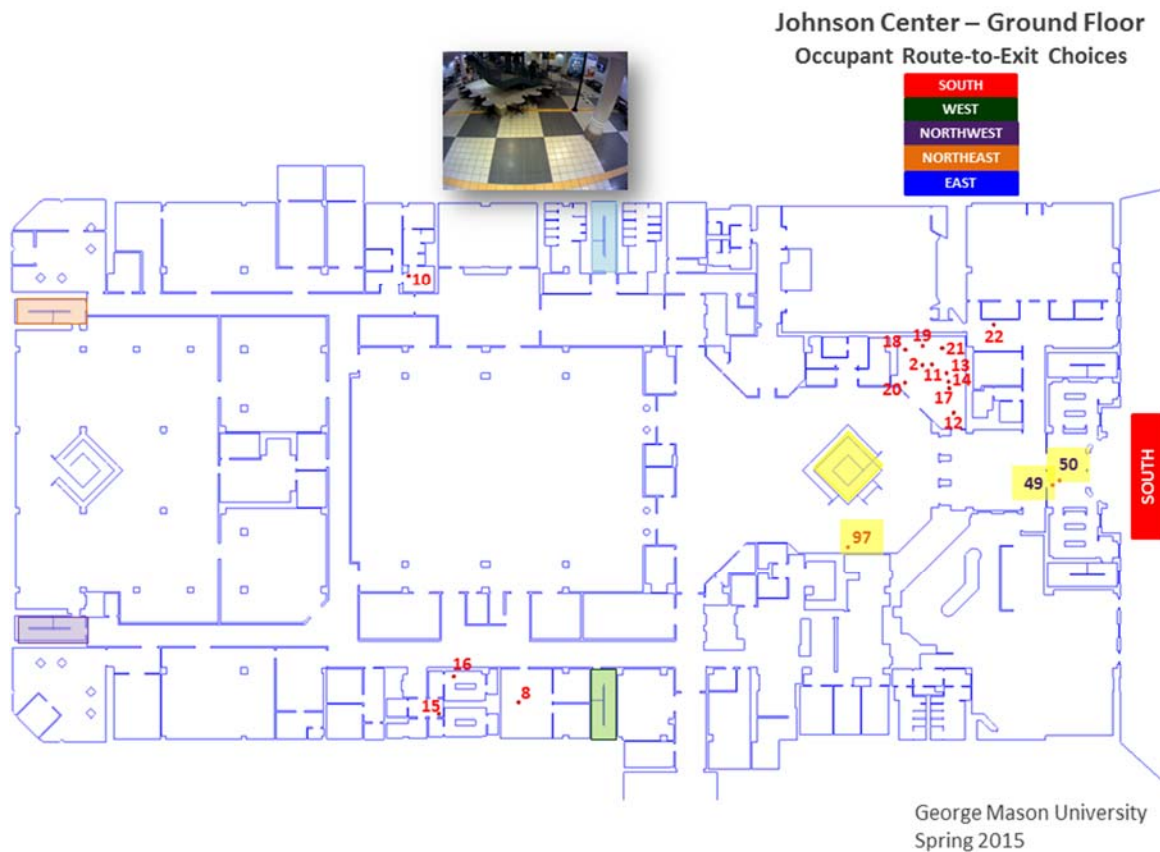


Figure 84 Occupant Route-to-Exit Choices (Ground Floor)

Of the 96 occupants who started to evacuate from the first floor, 93 used exits available on the first floor; however, 3 occupants (highlighted in yellow) elected to use the south central stairs and exit on the ground floor through the south exit (Figure 85). None of the security cameras on the first floor allowed for direct observation of occupants on the stairs; however, alternate video footage on either side of the Central and south central stairs allowed observation of the occupants once they had descended the stairs and moved towards their respective exits.

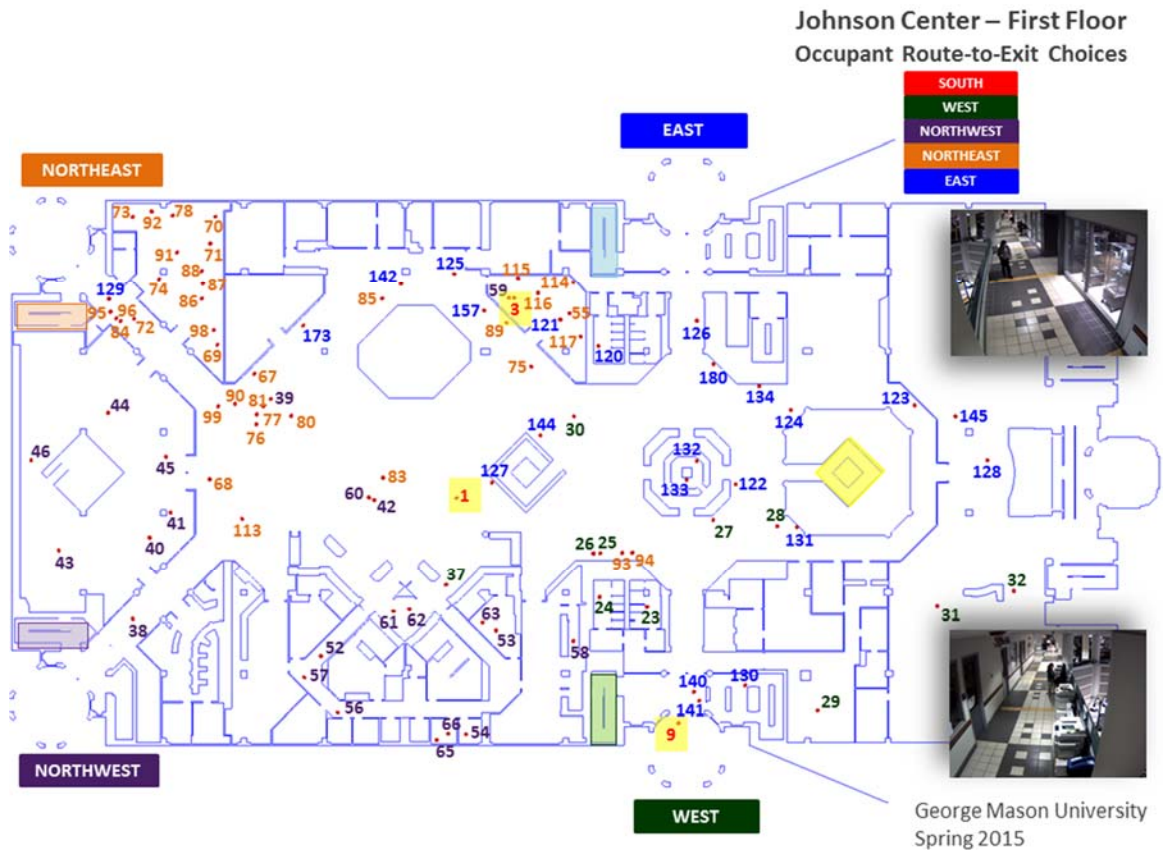


Figure 85 Occupant Route-to-Exit Choices (First Floor)

Figure 86 illustrates the route-to-exit choices for the 42 occupants who started to evacuate from the second floor. Eighteen of the occupants used the Central Stair with 10 opting to use the east exit and the other 8 using the north east exit. Seventeen occupants used the South Central Stair (highlighted in yellow) with 14 exiting the staircase on the first floor and using the east exit while the other three continued to the ground floor and exited via the south exit. Six occupants chose to use the east stairwell (highlighted in

blue) and exit through the east doors while one other occupant chose the northeast stairwell and northeast exit (highlighted in orange).

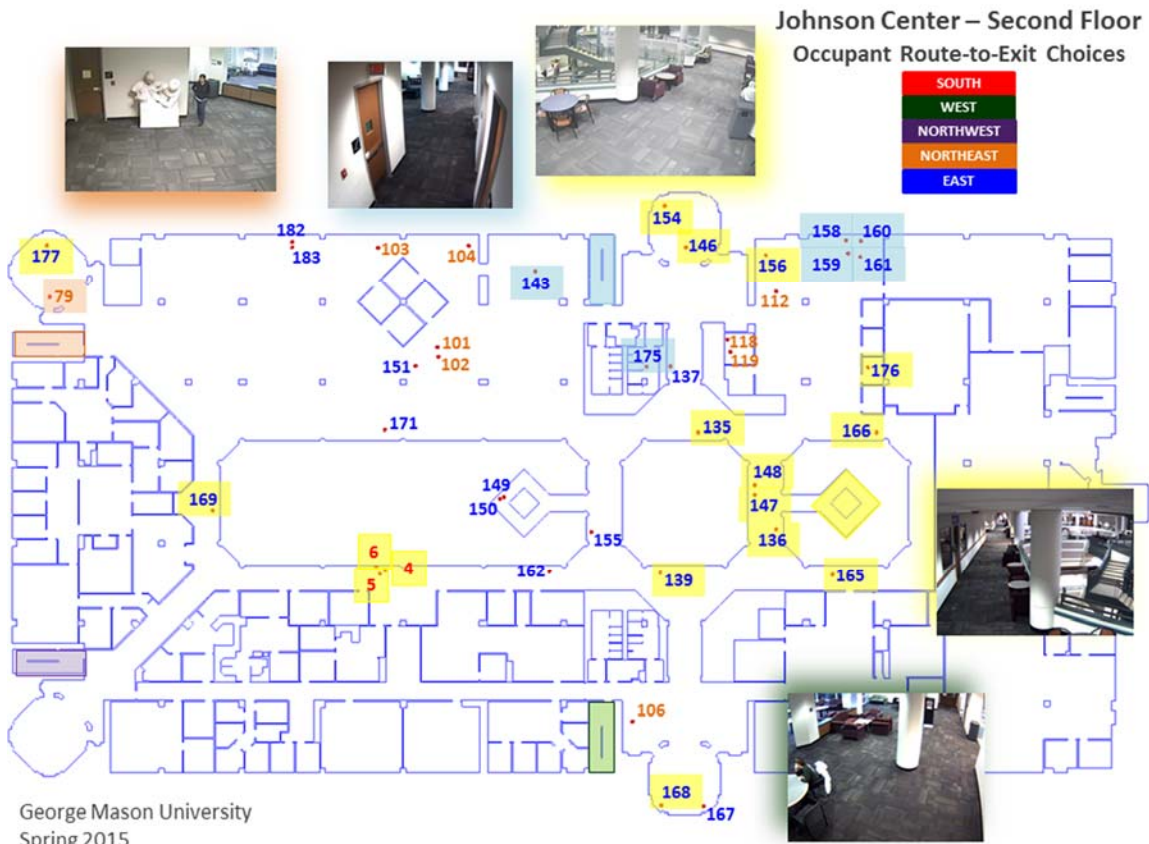


Figure 86 Occupant Route-to-Exit Choices (Second Floor)

Similarly, Figure 87 describes the route-to-exit choices for the 34 occupants who started to evacuate from the third floor. Twenty of the occupant chose the central stairs with 9 exiting via the east exit, 7 via the northeast exit, 2 via the northwest exit, and 2 via the west exit. Nine occupants used the South Central Stair (highlighted in yellow) with 8 exiting the staircase on the first floor and using the east exit while 1 occupant continued

to the ground floor and exited via the south exit. One occupant used the northeast stairwell (highlighted in orange) and exited through the northeast doors, two occupants used the northwest stairwell (highlighted in purple) and exited through the northwest doors, and two occupants used the west stairwell (highlighted in green) and exited through the west doors.

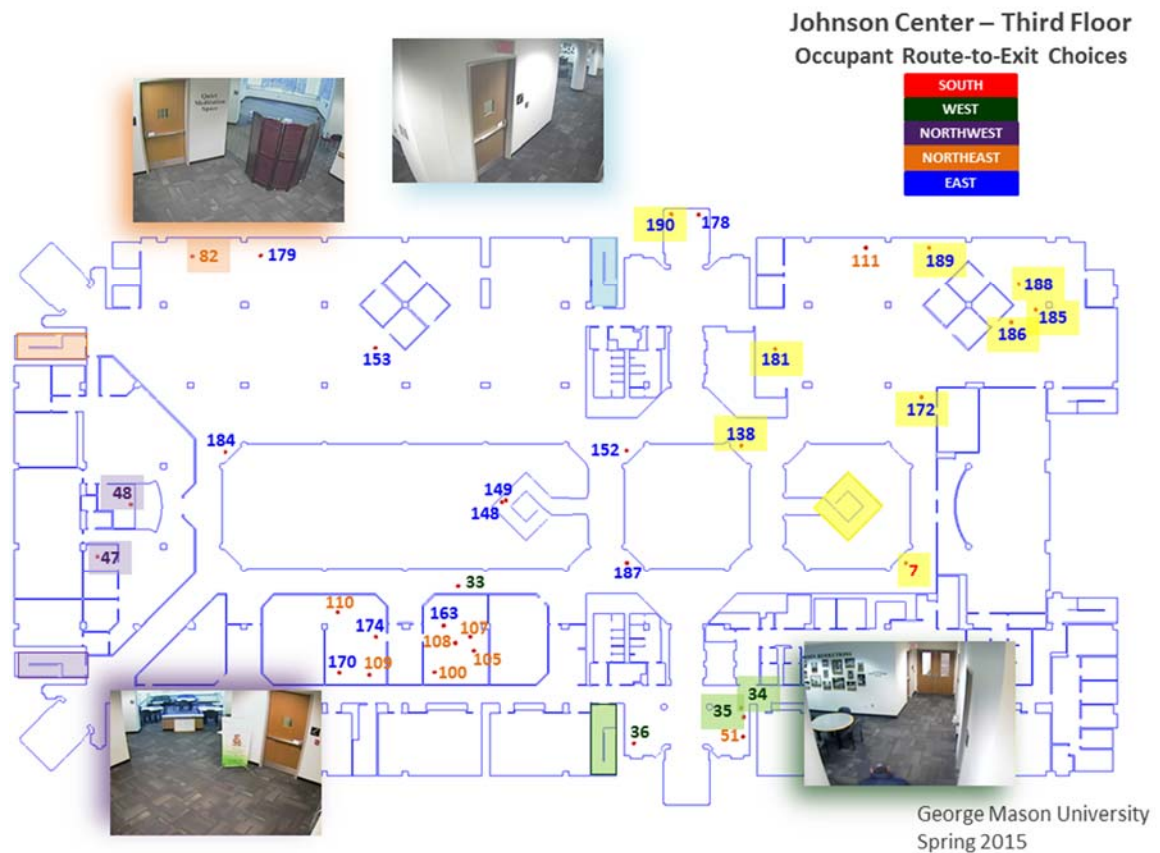


Figure 87 Occupant Route-to-Exit Choices (Third Floor)

Table 15 summarizes the route-to-exit for the 83 occupants who either ascended or descended the stairs during the evacuation of the building. The table describes the

occupant's evacuation route by initial floor location, choice of stair, and ultimate exit choice.

Table 15 Occupant Evacuation Route Described by Initial Location, Stair, and Exit Choice

Occupant Route Selection Stair Choice: Initial Location	Exit Choice:					Grand Total
	South Exit	East Exit	North East Exit	North West Exit	West Exit	
East Stair						
2nd Floor		6				6
North East Stair						
2nd Floor			1			1
3rd Floor			1			1
North West Stair						
3rd Floor				2		2
West Stair						
3rd Floor					2	2
Central Stair						
2nd Floor		10	8			18
3rd Floor		9	7	2	2	20
South Central Stair						
1st Floor	3		1			4
2nd Floor	3	14				17
3rd Floor	1	8				9
Ground Floor			1	2		3
Grand Total	7	47	19	6	4	83

Table 15 illustrates that less than 16% (12 of 76) of the occupants located initially on the second or third floor opted to take the most expeditious route out of the Johnson Center. Rather than using the stairwells located nearest the exterior walls of the building, most occupants moved to the interior of the building and descended the central or south central stairs. It is most likely that path affiliation (previously described in Section 5.3) impacted the route-to-exit selection as the occupants chose to evacuate by their more familiar regularly used routes.

10.3 PEDFLOW Simulation

Using the data extracted from the video analysis, the evacuation drill was recreated using PEDFLOW. Specifically, input files were created that assigned initial positions and evacuation delay times as recorded from the video. Routes from initial locations to the exit (path/stair selection and exit choice) were also created for each individual. For the initial study, occupants were assigned desired velocities in the range of $1.20 \pm 10\%$ meters per second. Using these values, it was found that 130 (68.5%) of the pedestrians had exit times within 10 seconds of their actual exit time as seen on video and 151 (79.5%) of the pedestrians had exit times within 10% of their actual exit time as seen on video (Figure 88).

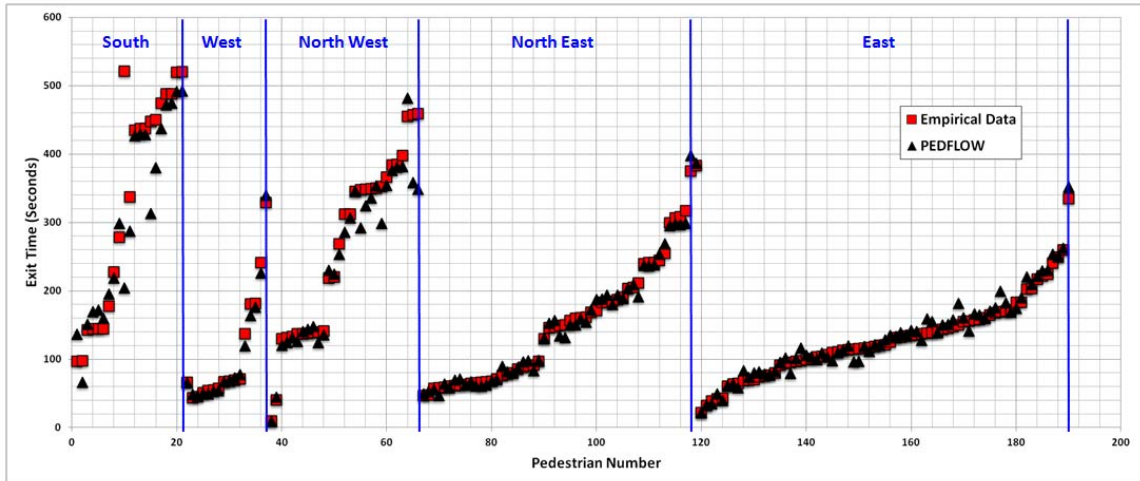


Figure 88 Occupant Evacuation Times (Empirical Data vs PEDFLOW)

For comparison purposes, five randomized Johnson Center simulations were created in PEDFLOW using inputs derived from the Spring 2015 fire drill (Figure 89). These simulations also contained 190 occupants who were given randomized initial

locations and path assignments that corresponded to the initial locations and paths collected from the video analysis. For example, fourteen occupants were assigned random initial positions on the second floor and told to exit the building via path 10, which requires the simulated pedestrians to use the south central stairs and east exit. In addition, the pre-evacuation delay times were randomly distributed using a table of probabilities based on the data collected from the actual fire drill.

• INPUTS*

– Occupant Demographics (190 Occupants Total)

- VELOCITY: 1.20 +/- 10% m/s
- RELAXATION TIME: 0.50 m/s
- RADIUS: 0.25 +/- 2% m
- ELLIPTICITY: [0,0.5]
- PUSHINESS: [0,0.8]
- COMFORT ZONE: 0

– Occupant Initial Locations (by Floor) & Path Assignments

Path:	1	2	3	4	5	6	7	8	9	10
Ground Floor	15		2		1					
First Floor	3	11	23		35		24			
Second Floor	3				1	8	6	10	14	
Third Floor	1	2	2	2	2	1	7		9	8

- Path 1 – Exit via South Exit using fastest time to exit path
- Path 2 – Exit via West Exit using fastest time to exit path
- Path 3 – Exit via West Exit using the central stairs (familiarity)
- Path 4 – Exit via North West Exit using fastest time to exit path
- Path 5 – Exit via North West Exit using the central stairs
- Path 6 – Exit via North East Exit using fastest time to exit path
- Path 7 – Exit via North East Exit using the central stairs
- Path 8 – Exit via East Exit using fastest time to exit path
- Path 9 – Exit via East Exit using the central stairs
- Path 10 – Exit via East Exit using the south central stairs

– Occupant Pre-Evacuation Delay Times (Type 2 – Table of Probabilities)

Time (s)	Percentage
10	0.079
30	0.153
50	0.174
70	0.153
90	0.074
110	0.095
130	0.037
150	0.032
170	0.016
190	0.000
210	0.005
230	0.026
250	0.032
270	0.005
290	0.047
310	0.011
330	0.021
350	0.000
370	0.000
390	0.000
410	0.016
430	0.005
450	0.011
470	0.011

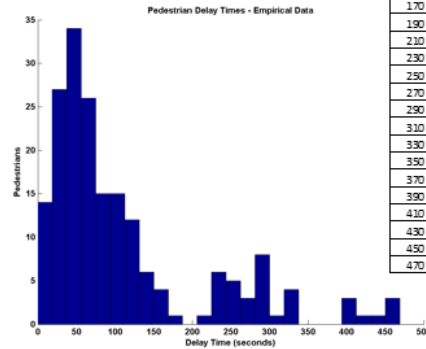


Figure 89 Johnson Center Simulation Inputs used with PEDFLOW (*Derived from Spring 2015 Fire Drill)

Each of these five simulation runs had different velocity assignments (Figure 90) and different pre-evacuation delay assignments (Figure 91); however, the overall evacuation times were very similar to the actual fire drill (Figure 92).

- RESULTS (Individual PEDFLOW Simulation Runs)
 - Occupant Desired Velocity (190 Occupants Total)

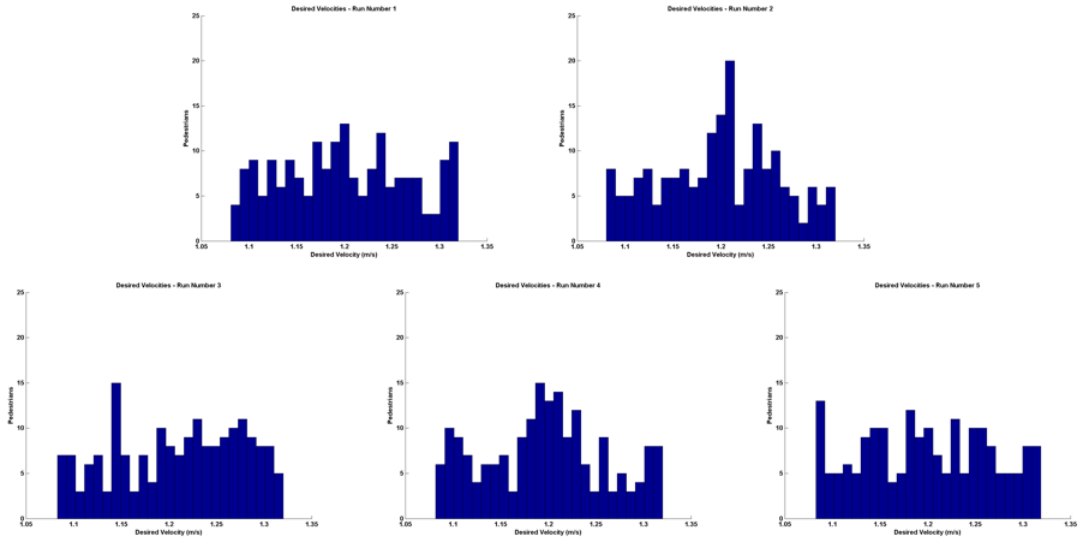


Figure 90 Occupant Desired Velocity Assignments for 5 Randomized PEDFLOW Trials

- RESULTS (Individual PEDFLOW Simulation Runs)
 - Occupant Delay Times (190 Occupants Total)

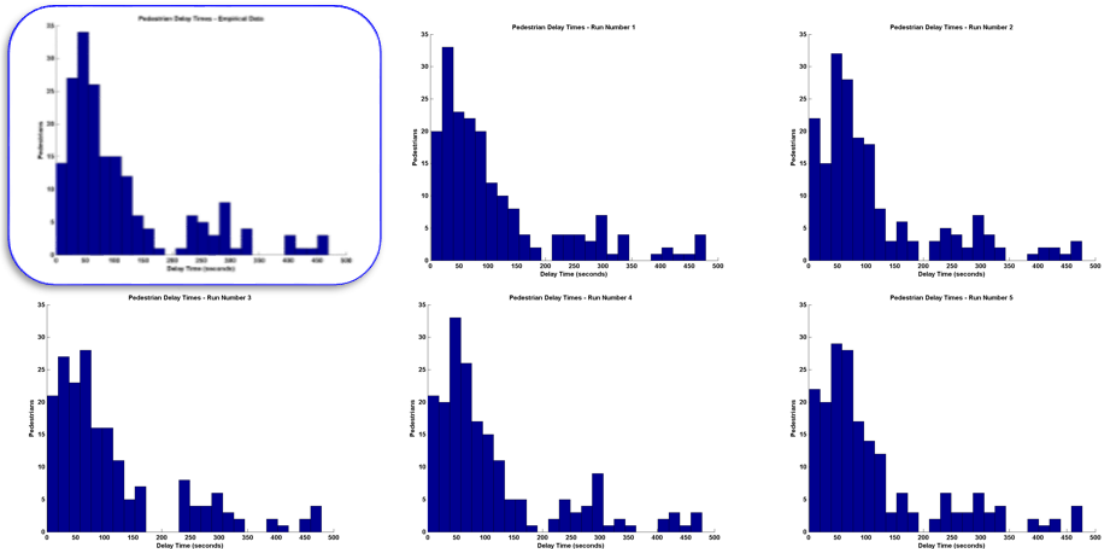


Figure 91 Occupant Evacuation Delay Time Assignments (based on a table of probabilities) for 5 PEDFLOW Trials

- RESULTS (Individual PEDFLOW Simulation Runs)
 - Occupant Exit Times (190 Occupants Total)

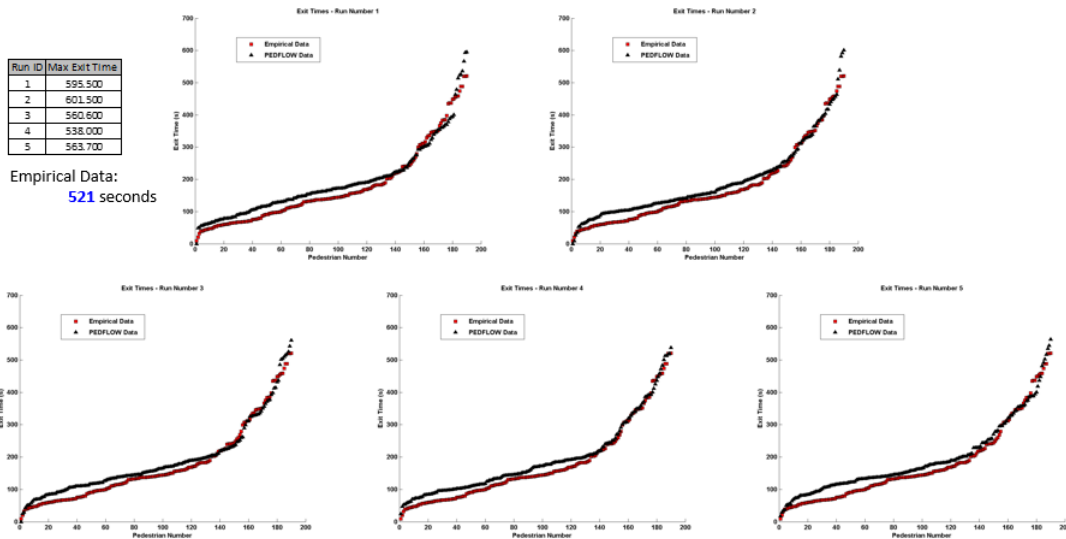


Figure 92 Overall Evacuation Exit Times for 5 Randomized PEDFLOW Trials

10.4 Conclusion

The study of the Johnson Center fire drill proved beneficial for a variety of reasons. First, this observational building evacuation study resulted in a very thorough newly collected set of empirical data which not only served to validate PEDFLOW, but can now also be used by other researchers to validate similar computer simulation codes. Secondly, since GMU’s director of emergency services typically conducts fire drills during times of low usage, the model can now be used to study and extrapolate what might happen if the drill were to occur during a period of higher usage. Additionally, as a result of the study, the director of emergency services now knows that the majority of the building occupants use the central stairs to evacuate (rather than the exterior stair cases) and that the customers and employees in the coffee shops tend to delay evacuating.

Both of these deficiencies could be addressed through education, regulatory guidance, and/or policy updates.

11 CONCLUSION

The main purpose of this dissertation was to implement an evacuation model which goes beyond the standards established by engineering codes and employs a mathematical formulation which accounts for occupant behaviors during the pre-movement phase, which was defined as the period following activation of the alarm but prior to the initiation of evacuation movement. This dissertation demonstrates that the time needed for pre-movement activities impacts the overall evacuation and provides a methodology to adjust the typical deterministic design calculations used by civil engineers. Given the pre-existing pedestrian simulation tool, PEDFLOW, this work not only incorporated pre-movement behaviors described in literature into PEDFLOW, but also included behaviors observed during the pre-movement phase of routine fire drills on the campus of GMU.

The objectives of this research was 1) to implement a mathematical formulation which accounts for pre-movement behaviors and demonstrate the effects of these behaviors on subsequent movement patterns and processes during facility evacuations, and 2) to implement a computational model to account for the situation dependent dynamic processes which determine the selection of route and exit from a building and show the effect of these choices on overall evacuation. This work accomplished both of these objectives. Prior to the start of this project, PEDFLOW did not have any pre-

evacuation capabilities, nor did it contain modules to account for physiological, sociological, or psychological factors seen during evacuation. PEDFLOW now contains modules which account for pedestrian discomfort, exhaustion, social influence, and affiliative behaviors such as familiar route and exit choice.

11.1 Contributions

The application of the pre-movement behaviors to evacuation simulations allows emergency planners to adjust the more deterministic civil engineering predictions. As demonstrated in this dissertation, the use of this methodology leads to more accurate building clearance predictions and may also lead to adjusted building capacities and/or modified building design elements. Additionally, this dissertation furthers pedestrian science by providing an in-depth review of various mathematical models, evacuation dynamics, and data collection efforts. Pertaining to evacuation dynamics, this dissertation is the first in the field to thoroughly analyze a single-alarm implementation of Reneke's Evacuation Decision Model, demonstrating how each component of the model potentially affects pre-evacuation time computations. Although more research and empirical data is needed to determine appropriate values and distributions for the EDM, Reneke's model does appear to incorporate many of the physical, social, and psychological factors previously identified by Kuligowski [62]. Secondly, this dissertation is the very first to provide a thorough description, evaluation, verification, and validation of the PEDFLOW simulation software. Although portions of the mathematical models used in PEDFLOW have been described elsewhere [85], this dissertation includes the first complete description of the various computations used to create the aggregate force vector, as well

as the subsequent steps necessary to advance the pedestrians within the PEDFLOW simulation. Additionally, this dissertation contains the first-ever review of PEDFLOW as evaluated against the methodologies and criteria used by Kuligowski et al. in their technical reports [54], [55]. The application of the NIST-recommended verification tests to PEDFLOW, as presented in this dissertation, led to some rather significant improvements to the software and was one of the first to demonstrate the utility in conducting the tests on comparable simulation codes. PEDFLOW now contains a pre-evacuation module which assigns delay times according to distributions; allows occupants to dynamically select routes and exits based on shortest time to exit, affiliation, or social influence criteria; and enables the assignment of a floor warden to clear the building. Lastly, an observational building evacuation study was completed which resulted in a very thorough newly collected set of empirical data for use by researchers in the validation of computer simulation models.

An incidental result of this research was presented in Chapter 8. This chapter presented a novel mathematical model to govern pedestrian speed on stairs which was based on empirical evidence, verified against a NIST-recommended test case, and partially validated using observational data. This model was then again validated in Chapter 9 using stairwell data collected by NIST. The verification and validation of PEDFLOW resulted in the following two publications:

M. L. Isenhour and R. Löhner, “Verification of a Pedestrian Simulation Tool Using the NIST Recommended Test Cases,” *Transportation Research Procedia*, vol. 2, pp. 237–245, 2014.

M. L. Isenhour and R. Löhner, “Validation of a Pedestrian Simulation Tool Using the NIST Stairwell Evacuation Data,” *Transportation Research Procedia*, vol. 2, pp. 739–744, 2014.

11.2 Future Work

Several opportunities exist to continue the research contained within this dissertation. First of all, although the NIST-recommended test cases serve as a starting point in establishing a standard for verification of simulation software, there is still more work to be done to create an industry-wide standard and solidify the proper set of benchmark tests for the various types of pedestrian simulation software. Secondly, this dissertation demonstrated a simple implementation of Reneke's EDM; it would be beneficial to not only implement a multiple alarm situation, but also attempt to utilize the Johnson Center data to determine appropriate values for the parameters needed in Reneke's EDM. Additionally, the social influence aspect of evacuation modules should be expanded to include "directed" influence; that is, what occurs when a floor warden or someone of authority not only directs occupants to leave, but also directs which route to take and which exit to use. An extension such as this would enable the modeling of active shooter "shelter in place" scenarios as well as other scenarios when people do not evacuate until told to do so by emergency responders. Researchers must continue to develop and improve evacuation simulation programs, such as PEDFLOW, which model various potentially dangerous scenarios and situations in the hopes of providing insight and predictive abilities to prevent a disaster, or in the case of a disaster, minimize the loss of life.

REFERENCES

REFERENCES

- [1] B. D. Hankin and R. A. Wright, "Passenger Flow in Subways," *OR*, vol. 9, no. 2, pp. 81–88, Jun. 1958.
- [2] V. M. Predtechenskii and A. I. Milinskii, *Planning for Foot Traffic Flow in Buildings*. New Delhi: Amerind Publishing Co., 1978.
- [3] J. J. Fruin, *Pedestrian planning and design*. New York: Metropolitan Association of Urban Designers and Environmental Planners, 1971.
- [4] M. Schreckenberg and S. D. Sharma, Eds., *Pedestrian and Evacuation Dynamics*. New York: Springer, 2001.
- [5] W. Daamen, D. C. Duives, and S. P. Hoogendoorn, Eds., *Transportation Research Procedia: The Conference on Pedestrian and Evacuation Dynamics 2014 (PED 2014), 22-24 October 2014, Delft, The Netherlands*, vol. 2. Elsevier Ltd, 2014.
- [6] E. R. Galea and University of Greenwich, Eds., *Pedestrian and Evacuation Dynamics 2003: proceedings of the 2nd International Conference on Pedestrian and Evacuation Dynamics, Greenwich, UK, 20-22 August 2003*. London: CMS Press, University of Greenwich, 2003.
- [7] N. Waldau, P. Gattermann, H. Knoflacher, and M. Schreckenberg, Eds., *Pedestrian and Evacuation Dynamics 2005*. New York: Springer, 2007.
- [8] W. W. F. Klingsch, C. Rogsch, A. Schadschneider, and M. Schreckenberg, Eds., *Pedestrian and Evacuation Dynamics 2008*. New York: Springer, 2010.
- [9] R. D. Peacock, E. D. Kuligowski, and J. D. Averill, Eds., *Pedestrian and Evacuation Dynamics*. New York: Springer, 2011.
- [10] U. Weidmann, U. Kirsch, and M. Schreckenberg, Eds., *Pedestrian and Evacuation Dynamics 2012*. New York: Springer, 2014.
- [11] A. Ripley, *The unthinkable: who survives when disaster strikes - and why*. New York: Three Rivers Press, 2009.
- [12] Z. Fang, J. P. Yuan, Y. C. Wang, and S. M. Lo, "Survey of pedestrian movement and development of a crowd dynamics model," *Fire Safety Journal*, vol. 43, no. 6, pp. 459–465, Aug. 2008.
- [13] H. Klüpfel, T. Meyer-König, J. Wahle, and M. Schreckenberg, "Microscopic Simulation of Evacuation Processes on Passenger Ships," in *Theory and Practical Issues on Cellular Automata*, S. Bandini and T. Worsch, Eds. London: Springer, 2001, pp. 63–71.
- [14] A. Schadschneider, W. Klingsch, H. Klüpfel, T. Kretz, C. Rogsch, and A. Seyfried, "Evacuation Dynamics: Empirical Results, Modeling and Applications," in *Encyclopedia of Complexity and Systems Science*, R. A. Meyers, Ed. New York: Springer, 2009, pp. 3142–3176.

- [15] N. Bellomo and C. Dogbe, “On the Modeling of Traffic and Crowds: A Survey of Models, Speculations, and Perspectives,” *SIAM Review*, vol. 53, no. 3, pp. 409–463, Jan. 2011.
- [16] D. Helbing and P. Molnár, “Social force model for pedestrian dynamics,” *Phys. Rev. E*, vol. 51, no. 5, pp. 4282–4286, May 1995.
- [17] D. Helbing, P. Molnár, I. J. Farkas, and K. Bolay, “Self-organizing pedestrian movement,” *Environment and Planning B: Planning and Design*, vol. 28, no. 3, pp. 361 – 383, 2001.
- [18] D. Helbing, I. Farkas, and T. Vicsek, “Simulating dynamical features of escape panic,” *Nature*, vol. 407, no. 6803, pp. 487–490, Sep. 2000.
- [19] D. Helbing, I. Farkas, P. Molnár, and T. Vicsek, “Simulation of pedestrian crowds in normal and evacuation situations,” presented at the Pedestrian and Evacuation Dynamics, 2002, pp. 21–58.
- [20] T. I. Lakoba, D. J. Kaup, and N. M. Finkelstein, “Modifications of the Helbing-Molnár-Farkas-Vicsek Social Force Model for Pedestrian Evolution,” *SIMULATION*, vol. 81, no. 5, pp. 339–352, May 2005.
- [21] U. Weidmann, *Transporttechnik der Fussgänger*. Zürich: Institut für Verkehrsplanung, 1993.
- [22] S. Seer, C. Rudloff, T. Matyus, and N. Brändle, “Validating Social Force based Models with Comprehensive Real World Motion Data,” *Transportation Research Procedia*, vol. 2, pp. 724–732, 2014.
- [23] V. Blue and J. Adler, “Emergent Fundamental Pedestrian Flows from Cellular Automata Microsimulation,” *Transportation Research Record: Journal of the Transportation Research Board*, vol. 1644, no. -1, pp. 29–36, Jan. 1998.
- [24] V. J. Blue and J. L. Adler, “Cellular automata microsimulation for modeling bi-directional pedestrian walkways,” *Transportation Research Part B: Methodological*, vol. 35, no. 3, pp. 293–312, Mar. 2001.
- [25] A. Schadschneider, “Cellular Automaton Approach to Pedestrian Dynamics - Theory,” arXiv e-print cond-mat/0112117, Dec. 2001.
- [26] C. Burstedde, K. Klauck, A. Schadschneider, and J. Zittartz, “Simulation of pedestrian dynamics using a two-dimensional cellular automaton,” *Physica A: Statistical Mechanics and its Applications*, vol. 295, no. 3–4, pp. 507–525, Jun. 2001.
- [27] C. Burstedde, A. Kirchner, K. Klauck, A. Schadschneider, and J. Zittartz, “Cellular Automaton Approach to Pedestrian Dynamics - Applications,” arXiv e-print cond-mat/0112119, Dec. 2001.
- [28] A. Kirchner and A. Schadschneider, “Simulation of evacuation processes using a bionics-inspired cellular automaton model for pedestrian dynamics,” *Physica A: Statistical Mechanics and its Applications*, vol. 312, no. 1–2, pp. 260–276, Sep. 2002.
- [29] T. Kretz and M. Schreckenberg, “F.A.S.T. - Floor field- and Agent-based Simulation Tool,” arXiv e-print physics/0609097, Sep. 2006.

- [30] T. Kretz and M. Schreckenberg, “The F.A.S.T.-Model,” in *Cellular Automata*, S. E. Yacoubi, B. Chopard, and S. Bandini, Eds. Springer Berlin Heidelberg, 2006, pp. 712–715.
- [31] T. Kretz, “Pedestrian Traffic-Simulation and Experiments,” Universität Duisburg-Essen, Fakultät für Physik» Theoretische Physik, 2007.
- [32] M. Batty, “Agent-Based Pedestrian Modeling,” *Environ Plann B Plann Des*, vol. 28, no. 3, pp. 321–326, Jun. 2001.
- [33] R. Kukla, J. Kerridge, A. Willis, and J. Hine, “PEDFLOW: Development of an Autonomous Agent Model of Pedestrian Flow,” *Transportation Research Record: Journal of the Transportation Research Board*, vol. 1774, no. -1, pp. 11–17, Jan. 2001.
- [34] M. Batty, B. Jiang, and M. Thurstain - Goodwin, “Local movement: agent-based models of pedestrian flows.” Centre for Advanced Spatial Analysis UCL, 1998.
- [35] T. Schelhorn, D. O’Sullivan, M. Haklay, and M. Thurstain - Goodwin, “STREETS: an agent-based pedestrian model.” Centre for Advanced Spatial Analysis UCL, 1999.
- [36] M. Batty, “Agent-based pedestrian modelling.” Centre for Advanced Spatial Analysis UCL, 2003.
- [37] M. Batty, J. Desyllas, and E. Duxbury, “Safety in Numbers? Modelling Crowds and Designing Control for the Notting Hill Carnival,” *Urban Stud*, vol. 40, no. 8, pp. 1573–1590, Jul. 2003.
- [38] S. J. Guy, J. Chhugani, S. Curtis, P. Dubey, M. Lin, and D. Manocha, “PLEdistrans: a least-effort approach to crowd simulation,” in *Proceedings of the 2010 ACM SIGGRAPH/Eurographics Symposium on Computer Animation*, Aire-la-Ville, Switzerland, Switzerland, 2010, pp. 119–128.
- [39] M. Whittle, *Gait analysis: an introduction*, Fourth Edition. Elsevier Ltd, 2007.
- [40] S. Curtis and D. Manocha, “Pedestrian Simulation Using Geometric Reasoning in Velocity Space,” in *Pedestrian and Evacuation Dynamics 2012*, U. Weidmann, U. Kirsch, and M. Schreckenberg, Eds. Springer International Publishing, 2014, pp. 875–890.
- [41] S. Curtis, S. J. Guy, B. Zafar, and D. Manocha, “Virtual Tawaf: A case study in simulating the behavior of dense, heterogeneous crowds,” in *2011 IEEE International Conference on Computer Vision Workshops (ICCV Workshops)*, 2011, pp. 128–135.
- [42] L. F. Henderson, “The Statistics of Crowd Fluids,” *Nature*, vol. 229, no. 5284, pp. 381–383, Feb. 1971.
- [43] L. F. Henderson, “On the fluid mechanics of human crowd motion,” *Transportation Research*, vol. 8, no. 6, pp. 509–515, Dec. 1974.
- [44] R. L. Hughes, “A continuum theory for the flow of pedestrians,” *Transportation Research Part B: Methodological*, vol. 36, no. 6, pp. 507–535, Jul. 2002.
- [45] R. L. Hughes, “The Flow of Human Crowds,” *Annual Review of Fluid Mechanics*, vol. 35, no. 1, pp. 169–182, 2003.
- [46] P. Kachroo, *Pedestrian dynamics*. Boca Raton: CRC Press, 2009.

- [47] D. Helbing and A. Johansson, "Pedestrian, Crowd, and Evacuation Dynamics," *arXiv:1309.1609 [physics]*, Sep. 2013.
- [48] D. Helbing, "A Fluid-Dynamic Model for the Movement of Pedestrians," *Complex Systems*, vol. 6, no. 5, pp. 391–415, 1992.
- [49] S. Hoogendoorn and P. Bovy, "Gas-Kinetic Modeling and Simulation of Pedestrian Flows," *Transportation Research Record: Journal of the Transportation Research Board*, vol. 1710, no. -1, pp. 28–36, Jan. 2000.
- [50] B. Zhan, D. N. Monekosso, P. Remagnino, S. A. Velastin, and L.-Q. Xu, "Crowd analysis: a survey," *Machine Vision and Applications*, vol. 19, no. 5–6, pp. 345–357, Apr. 2008.
- [51] A. Treuille, S. Cooper, and Z. Popović, "Continuum crowds," *ACM Trans. Graph.*, vol. 25, no. 3, pp. 1160–1168, Jul. 2006.
- [52] P. M. Torrens, "Moving Agent Pedestrians Through Space and Time," *Annals of the Association of American Geographers*, vol. 102, no. 1, pp. 35–66, 2012.
- [53] S. Gwynne, E. R. Galea, M. Owen, P. J. Lawrence, and L. Filippidis, "A review of the methodologies used in the computer simulation of evacuation from the built environment," *Building and Environment*, vol. 34, no. 6, pp. 741–749, Nov. 1999.
- [54] E. D. Kuligowski and R. D. Peacock, "A Review of Building Evacuation Models," National Institute of Standards and Technology, Technical Note (NIST TN) 1471, Jul. 2005.
- [55] E. D. Kuligowski, R. D. Peacock, and B. L. Hoskins, "A Review of Building Evacuation Models, 2nd Edition," National Institute of Standards and Technology, Technical Note (NIST TN) 1680, Nov. 2010.
- [56] "Evacmod.net - Evacuation Modelling Portal | Evacmod.net." [Online]. Available: <http://www.evacmod.net/>. [Accessed: 15-Nov-2015].
- [57] H. A. MacLennan, M. A. Regan, and R. Ware, "An engineering model for the estimation of occupant pre-movement and or response times and the probability of their occurrence," *Fire and Materials*, vol. 23, no. 6, pp. 255–263, 1999.
- [58] S. Gwynne, E. Kuligowski, and D. Nilsson, "Representing evacuation behavior in engineering terms," *Journal of Fire Protection Engineering*, vol. 22, no. 2, pp. 133–150, May 2012.
- [59] J. Lord, B. Meacham, A. Moore, R. Fahy, and G. Proulx, "Guide for Evaluating the Predictive Capabilities of Computer Egress Models," National Institute of Standards and Technology, Gaithersburg, MD, NIST CGR 06-886, Dec. 2005.
- [60] M. Spearpoint, "The Effect of Pre-evacuation on Evacuation Times in the Simulex Model," *Journal of Fire Protection Engineering*, vol. 14, no. 1, pp. 33–53, Feb. 2004.
- [61] P. Reneke, "Evacuation Decision Model," National Institute of Standards and Technology, NIST IR 7914, Feb. 2013.
- [62] E. D. Kuligowski, "Terror Defeated: Occupant Sensemaking, Decision-Making And Protective Action In The 2001 World Trade Center Disaster," University of Colorado, 2011.
- [63] J. D. Sime, "Crowd psychology and engineering," *Safety Science*, vol. 21, no. 1, pp. 1–14, Nov. 1995.

- [64] J. L. Bryan, "A Selected Historical Review of Human Behavior in Fire," *FPE*, no. 16, pp. 4–10, Oct. 2002.
- [65] S. Horiuchi, "An Overview Of Research On 'People-Fire Interactions,'" *Fire Safety Science*, vol. 2, pp. 501–510, 1989.
- [66] P. Whiting, "A review of international research efforts related to occupant pre-movement behaviour and response times in fire," BRANZ, Judgeford, New Zealand, SR143, 2005.
- [67] S. M. V. Gwynne, "Conventions in the Collection and Use of Human Performance Data," 2010. [Online]. Available: <http://www.evacmod.net/videos/papers/NISTGCR10-928.pdf>.
- [68] L. Shi, Q. Xie, X. Cheng, L. Chen, Y. Zhou, and R. Zhang, "Developing a database for emergency evacuation model," *Building and Environment*, vol. 44, no. 8, pp. 1724–1729, Aug. 2009.
- [69] S. Horiuchi, Y. Murozaki, and A. Hukugo, "A Case Study Of Fire And Evacuation In A Multi-purpose Office Building, Osaka, Japan," *Fire Safety Science*, vol. 1, pp. 523–532, 1986.
- [70] P. Brennan, "Timing Human Response In Real Fires," *Fire Safety Science*, vol. 5, pp. 807–818, 1997.
- [71] G. Proulx and R. Fahy, "The Time Delay To Start Evacuation: Review Of Five Case Studies," *Fire Safety Science*, vol. 5, pp. 783–794, 1997.
- [72] E. D. Kuligowski and D. S. Mileti, "Modeling pre-evacuation delay by occupants in World Trade Center Towers 1 and 2 on September 11, 2001," *Fire Safety Journal*, vol. 44, no. 4, pp. 487–496, May 2009.
- [73] G. Proulx, "The Time Delay to Start Evacuating upon Hearing a Fire Alarm," *Proceedings of the Human Factors and Ergonomics Society Annual Meeting*, vol. 38, no. 14, pp. 811–815, Oct. 1994.
- [74] S. Gwynne, E. R. Galea, J. Parke, and J. Hickson, "The Collection and Analysis of Pre-evacuation Times Derived from Evacuation Trials and Their Application to Evacuation Modelling," *Fire Technology*, vol. 39, no. 2, pp. 173–195, Apr. 2003.
- [75] M. Kimura and J. Sime, "Exit Choice Behaviour During The Evacuation Of Two Lecture Theatres," *Fire Safety Science*, vol. 2, pp. 541–550, 1989.
- [76] J. Sime, "Human Behaviour in Fires," Fire and Emergency Planning Department, London, Publication (Reports and summaries) 45, 1992.
- [77] S. Y. Ko, "Comparison of Evacuation Times Using Simulex and EvacuationNZ Based on Trial Evacuations," Fire Engineering Research Report, Department of Civil Engineering, University of Canterbury, Christchurch, New Zealand, 2003.
- [78] H. Weckman, S. Lehtimäki, and S. Männikkö, "Evacuation of a theatre: exercise vs calculations," *Fire and Materials*, vol. 23, no. 6, pp. 357–361, 1999.
- [79] J. D. Sime, "Affiliative behaviour during escape to building exits," *Journal of Environmental Psychology*, vol. 3, no. 1, pp. 21–41, Mar. 1983.
- [80] J. D. Sime, "Movement toward the Familiar Person and Place Affiliation in a Fire Entrapment Setting," *Environment and Behavior*, vol. 17, no. 6, pp. 697–724, Nov. 1985.

- [81] G. Proulx, A. Kaufman, and J. Pineau, “Evacuation Time and Movement in Office Buildings,” Institute for Research in Construction, National Research Council Canada, Ottawa, Canada, Internal Report IRC-IR-711, 1996.
- [82] S. Gwynne, E. R. Galea, M. Owen, P. J. Lawrence, and L. Filippidis, “A systematic comparison of building EXODUS predictions with experimental data from the Stapelfeldt trials and the Milburn House evacuation,” *Applied Mathematical Modelling*, vol. 29, no. 9, pp. 818–851, Sep. 2005.
- [83] G. Proulx, “Evacuation time and movement in apartment buildings,” *Fire Safety Journal*, vol. 24, no. 3, pp. 229–246, 1995.
- [84] K. M. Crawford, “Effect of Safety Factors on Timed Human Egress Simulations,” Research Project Report, School of Engineering, University of Canterbury, Christchurch, New Zealand, 1999.
- [85] R. Löhner, “On the modeling of pedestrian motion,” *Applied Mathematical Modelling*, vol. 34, no. 2, pp. 366–382, Feb. 2010.
- [86] E. Ronchi, E. D. Kuligowski, P. A. Reneke, R. D. Peacock, and D. Nilsson, “The Process of Verification and Validation of Building Fire Evacuation Models,” National Institute of Standards and Technology, NIST TN 1822, Nov. 2013.
- [87] IMO, “Guidelines for evacuation analysis for new and existing passenger ships,” International Maritime Organization, MSC Circ 1238, 2007.
- [88] RiMEA, “Richtlinie für Mikroskopische Entfluchtungsanalysen,” Richtlinie für Mikroskopische Entfluchtungs-Analysen, Version 2.2.1, 2009.
- [89] C. Rogsch, H. Klüpfel, R. Könnecke, and A. Winkens, “RiMEA: A Way to Define a Standard for Evacuation Calculations,” in *Pedestrian and Evacuation Dynamics 2012*, U. Weidmann, U. Kirsch, and M. Schreckenberg, Eds. Springer International Publishing, 2014, pp. 455–467.
- [90] T. Fujiyama and N. Tyler, “An explicit study on walking speeds of pedestrians on stairs,” in *Proceedings of the 10th International Conference on Mobility and Transport for Elderly and Disabled People*, Hamamatsu, Japan, 2004, pp. 643–652.
- [91] M. L. Isenhour and R. Löhner, “Verification of a Pedestrian Simulation Tool Using the NIST Recommended Test Cases,” *Transportation Research Procedia*, vol. 2, pp. 237–245, 2014.
- [92] R. Lubaś, M. Mycek, J. Porzycki, and J. Wąs, “Verification and Validation of Evacuation Models – Methodology Expansion Proposition,” *Transportation Research Procedia*, vol. 2, pp. 715–723, 2014.
- [93] M. L. Isenhour, “Pedestrian Speed on Stairs: A Mathematical Model Based on Empirical Analysis for use in Computer Simulations,” presented at the Joint Mathematics Meeting, Seattle, Washington, 2016.
- [94] Y. Qu, Z. Gao, Y. Xiao, and X. Li, “Modeling the pedestrian’s movement and simulating evacuation dynamics on stairs,” *Safety Science*, vol. 70, pp. 189–201, Dec. 2014.
- [95] W. L. Oberkampf and C. J. Roy, *Verification and Validation in Scientific Computing*. Cambridge University Press, 2010.

- [96] R. D. Peacock, B. L. Hoskins, and E. D. Kuligowski, "Overall and local movement speeds during fire drill evacuations in buildings up to 31 stories," *Safety Science*, vol. 50, no. 8, pp. 1655–1664, Oct. 2012.
- [97] E. D. Kuligowski and R. D. Peacock, "Building Occupant Egress Data," National Institute of Standards and Technology, Gaithersburg, MD, Report of Test 4024, 2010.

BIOGRAPHY

Michelle Lynn Isenhour graduated from East Jackson High School, Jackson, Michigan in 1990. She graduated from the United States Military Academy as a Distinguished Cadet in 1994 with a Bachelor of Science degree in Applied Mathematics and was subsequently commissioned as a Second Lieutenant in the United States Army. Throughout her tenure in the Army, Michelle served in various positions of increasing responsibility including a 12-month combat tour during Operation Iraqi Freedom. She received her Master of Science degree in Applied Mathematics from Western Michigan University in 2004 and served as an assistant professor in the Department of Mathematical Sciences, United States Military Academy from July 2004 to June 2006 and July 2014 to present.